

AD-A153 980

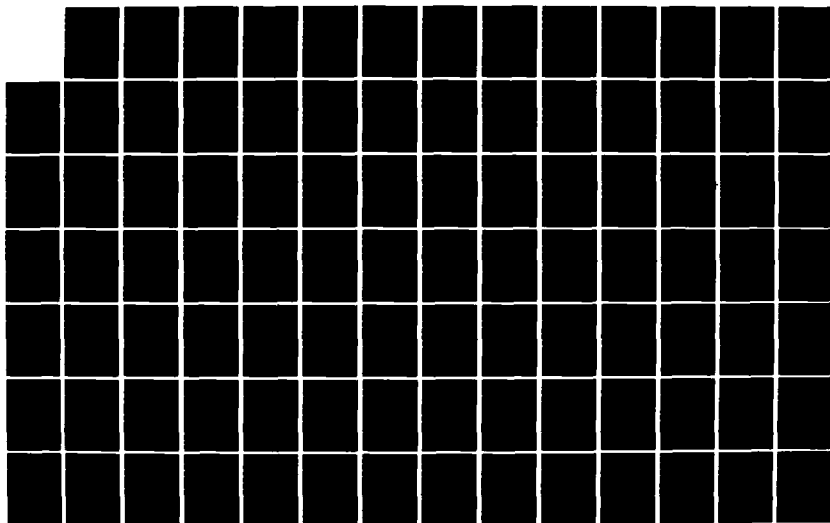
MILLIMETER WAVE GENERATION BY RELATIVISTIC ELECTRON
BEAMS(U) POLYTECHNIC INST OF NEW YORK FARMINGDALE DEPT
OF ELECTRICAL E. S P KUO ET AL. 01 DEC 84 POLY-84-007
AFOSR-TR-85-0342 AFOSR-83-0001

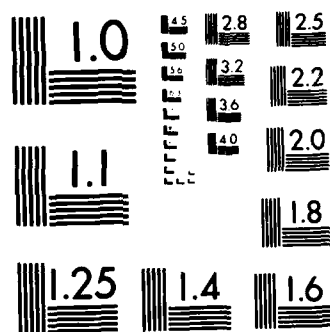
1/2

UNCLASSIFIED

F/G 20/9

NL





MICROCOPY RESOLUTION TEST CHART
NATIONAL BUREAU OF STANDARDS-1963 A

PROGRESS REPORT

Millimeter Wave Generation by Relativistic Electron Beams
Oct. 1, 1983-Sept. 30, 1984

for

Air Force Office of Scientific Research
Arlington, Virginia

under

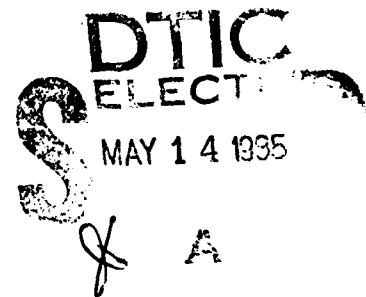
Grant No. AFOSR-83-0001

submitted by

Principal Investigator: Spencer S-P Kuo

Co-principal Investigator: Bernard R-S Cheo

Polytechnic Institute of New York



Approved for public release;
distribution unlimited.

AD-A153 980

DTIC FILE COPY

REPORT DOCUMENTATION PAGE

1a. REPORT SECURITY CLASSIFICATION Unclassified		1b. RESTRICTIVE MARKINGS	
2a. SECURITY CLASSIFICATION AUTHORITY		3. DISTRIBUTION/AVAILABILITY OF REPORT Approved for public release; distribution unlimited	
2b. DECLASSIFICATION/DOWNGRADING SCHEDULE			
4. PERFORMING ORGANIZATION REPORT NUMBER(S) POLY 84-007		5. MONITORING ORGANIZATION REPORT NUMBER(S) AFOSR-TR- 85 - 0342	
6a. NAME OF PERFORMING ORGANIZATION Polytechnic Institute of NY	6b. OFFICE SYMBOL (If applicable)	7a. NAME OF MONITORING ORGANIZATION AFOSR/NP	
6c. ADDRESS (City, State and ZIP Code) Dept. of Electrical Engineering Route 110, Farmingdale, NY 11735		7b. ADDRESS (City, State and ZIP Code) Building 410 Bolling AFB, DC 20332-6448	
8a. NAME OF FUNDING/SPONSORING ORGANIZATION AFOSR	8b. OFFICE SYMBOL (If applicable) NP	9. PROCUREMENT INSTRUMENT IDENTIFICATION NUMBER AFOSR-83-0001	
8c. ADDRESS (City, State and ZIP Code) Building 410 Bolling AFB DC 20332-6448		10. SOURCE OF FUNDING NOS.	
		PROGRAM ELEMENT NO. 61102F	PROJECT NO. 2301
		TASK NO. A 8	WORK UNIT NO. N/A
11. TITLE (Include Security Classification) Millimeter Wave Generation by Relativistic Electron Beams			
12. PERSONAL AUTHOR(S) Spencer P. Kuo and Bernard R. Cheo			
13a. TYPE OF REPORT Annual	13b. TIME COVERED FROM 10/1/83 TO 9/30/84	14. DATE OF REPORT (Yr., Mo., Day) 12/1/84	15. PAGE COUNT 16+appendix (5)
16. SUPPLEMENTARY NOTATION			
17. COSATI CODES		18. SUBJECT TERMS (Continue on reverse if necessary and identify by block number)	
FIELD	GROUP	SUB. GR.	
		millimeter wave generation, relativistic electron beams, wave-plasma interaction, electron cyclotron maser instability, ECRH, parametric instabilities.	
19. ABSTRACT (Continue on reverse if necessary and identify by block number)			
<p>We are studying various wave-plasma interaction processes towards the understanding of the collective physics of plasmas. The processes include the mechanisms leading to the generation of millimeter waves by relativistic electron beams (electron cyclotron maser instability) and the mechanisms providing channels for anomalous absorption of electromagnetic waves (electron cyclotron resonance heating and parametric instabilities). A single nonlinear equation which describes the temporal evolution of the field amplitude of the electron cyclotron maser instability has been derived self-consistently. Three adiabatic invariants of the electron motion under electron cyclotron resonance heating by three differently polarized heater: (1) ordinary mode; (2) extraordinary mode; and (3) electrostatic mode are derived. Wave plasma interaction leading to various parametric instabilities in the ionosphere has also been studied.</p>			
20. DISTRIBUTION/AVAILABILITY OF ABSTRACT UNCLASSIFIED/UNLIMITED <input checked="" type="checkbox"/> SAME AS RPT. <input checked="" type="checkbox"/> DTIC USERS <input type="checkbox"/>		21. ABSTRACT SECURITY CLASSIFICATION Unclassified	
22a. NAME OF RESPONSIBLE INDIVIDUAL Dr. Robert J. Barker		22b. TELEPHONE NUMBER (Include Area Code) (202) 767-5011	22c. OFFICE SYMBOL NP

I. Introduction

During the period between Oct. 1, 1983 and Sept. 30, 1984 a number of topics of investigation have been pursued, and several of these have yielded positive results. Basically, we are studying various wave-plasma interaction processes towards the understanding of the collective physics of plasmas. The processes include the mechanisms leading to the generation of millimeter waves by relativistic electron beams and the mechanisms providing channels for anomalous absorption of electromagnetic waves. The topics of investigation are divided into two general categories:

- A. wave-plasma interaction near the electron cyclotron (harmonic) resonance; and
- B. wave-plasma interaction not near the resonance.

Most of the significant results have been published or accepted for publication in several journal papers and preceding issued papers, and reported at APS meeting on plasma physics.

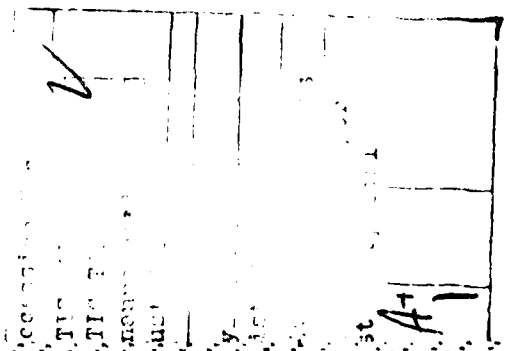
In Section II of this report, a description of the work on wave-plasma resonant interaction at cyclotron harmonics is included. Both processes which lead to generation of millimeter waves by relativistic electron beams (electron cyclotron Maser mechanism) or absorption of injected EM waves by relativistic plasmas are analyzed. Section II gives a brief description of the theoretical work in the general area of instabilities excited by wave-plasma interactions. Applications of the theoretical results to problems encountered in the laboratory plasmas and the space plasmas are also discussed.

Appendix 1 is a copy of a reprint entitled "Analysis of Electron Cyclotron Maser Instability" published in the physics Letters A. Appendix 2 is a copy of a reprint entitled "Oscillating Two Stream Instability of Ducted Whistler Pump" published in The Physics of Fluids. Appendix 3 is a copy of a reprint entitled "Excitation of Upper Hybrid Waves by a Thermal Parametric Instability" published in the Journal of Plasma Physics. Appendix 4 is a copy of a reprint entitled "Relativistic Adiabatic Trivariants of Electron Motion under ECRH" accepted for publication in Physics Letters A. Appendix 5 is a copy of a reprint entitled "Earth's Magnetic Field Perturbations as the Possible Environmental Impact of the Conceptualized Solar Power Satellite (SPS)" which will appear in the December issue of The Journal of Geophysical Research. Four proceedings issued papers:

- 1. "Modulational Instability of Lower Hybrid Waves";
 - 2. "Ionospheric and Magnetospheric Modifications Caused by the Injected ULF Waves";
 - 3. "Artificial Ionospheric Disturbances Caused by Powerful Radio Waves"; and
 - 4. "On the Spread F Echoes from the Ionospheric Heated Region".
- and a copy of each of the two manuscripts:

- 1. "A Theoretical Model of Artificial Spread F Echoes"; and
- 2. "Simultaneous Excitation of Earth Magnetic Field Fluctuations and Plasma Density Irregularities by Powerful Radio Waves from VLF to SHF Bands"

which have been submitted to Radio Science for publication are also attached at the end of this report.



List of Publications

The following publications include work supported by the present Grant, which was duly acknowledged.

(1) Journal Articles:

1. S.P. Kuo and B.R. Cheo, "Analysis of Electron Cyclotron Maser Instability," *Physics Letters A*, 103A(9), 427-432, 1984.
2. S.P. Kuo and M.C. Lee, "Oscillating Two Stream Instability of Ducted Whistler Pump," *Phys. Fluids*, 27(6), 1434-1438, 1984.
3. M.C. Lee and S.P. Kuo, "Excitation of Upper Hybrid Waves by a Thermal Parametric Instability," *J. Plasma Phys.*, 30, 463-478, 1983.
4. M.C. Lee and S.P. Kuo, "Earth's Magnetic Field Perturbations as the Possible Environmental Impact of the Conceptualized Solar Power Satellite (SPS)," *J. Geophys. Res.*, 89(A-12), 11043-11047, 1984.
5. S.P. Kuo and B.R. Cheo, "Relativistic Adiabatic Invariants of Electron Motion under ECRH", accepted for publication in *Phys. Lett. A*.
6. S.P. Kuo, M.C. Lee and S.C. Kuo, "A Theoretical Model of Artificial Spread F Echoes," accepted for publication in *Radio Science*.
7. M.C. Lee and S.P. Kuo, "Simultaneous Excitation of Earth's Magnetic Field Fluctuations and Plasma Density Irregularities by Powerful Radio Waves from VLF to SHF Bands," submitted to *Radio Science*.

(2) Proceedings Issued Papers:

1. S.P. Kuo and M.C. Lee, "On the Spread F Echoes from the Ionospheric Heated Region," *Symposium on the Effect of the Ionosphere on C³I Systems*, P56-3, p. 1-7, Virginia, May 1984.
2. M.C. Lee and S.P. Kuo, "Artificial Ionospheric Disturbances Caused by Powerful Radio Wave," *Symposium on the Effect of the Ionosphere on C³I Systems*, P56-1, p. 1-7, Virginia, May 1984.
3. S.P. Kuo and M.C. Lee, "Modulational Instability of Lower Hybrid Waves," *1984 International Conference on Plasma Physics*, June 1984, Switzerland, P17-4, p. 218.
4. M.C. Lee and S.P. Kuo, "Ionospheric and Magnetospheric Modifications caused by the Injected ULF Waves," *1984 International Conference on Plasma Physics*, June 1984, Switzerland, P11-11, p. 139.

(3) Conference Papers

1. S.P. Kuo, E. Levi and B.R. Cheo, "Saturation of Loss-cone Electron-Cyclotron Maser Instability by Quasi-Linear Diffusion Process," *Bull. Amer. Phys. Soc.*, 28(8), 1060, 1983.
2. B.R. Cheo, S.P. Kuo and E. Levi, "Nonlinear Evolution of Electron Cyclotron Maser Instability," *Bull. Amer. Phys. Soc.*, 28(8), 1060, 1983.
3. S.P. Kuo and M.C. Lee, "Thermal Oscillation Two Stream Instability of Whistler Pump," *Bull. Amer. Phys. Soc.*, 28(8), 1106, 1983.
4. S. Chi and S.P. Kuo, "Superadiabaticities of Electron Trajectory Under ECRH," *Bull. Amer. Phys. Soc.* 28(8), 1180, 1983.

II. Wave Plasma Interaction Near the Electron Cyclotron (Harmonic) Resonance

(1) Analysis of Electron Cyclotron Maser Instability

In this work a single nonlinear equation which describes the temporal evolution of the field amplitude of the electron cyclotron maser instability is derived self-consistently. Thus one can expect to directly derive the power gain, the conversion efficiency and also the dynamic properties of the collective response of the electron beam to the excited wave fields from this single equation without relying on particle simulation. Our approach is beginning with solving the equations of motion of a single electron moving in the wave fields and then following with averaging the results over the initial electron velocity distribution to obtain the collective response of electrons to the wave fields.

(1.1) Governing Rate Equations

The motion of electrons in a dc magnetic field and the waveguide mode fields is governed by a set of coupled nonlinear differential equations:

$$\frac{d}{dt} \vec{R} = \vec{P} / \gamma m_0 \quad (1)$$

$$\frac{d}{dt} \vec{P} = -e \left[\vec{E} + \frac{1}{c} \vec{v} \times (\vec{B} + z B_0) \right] \quad (2)$$

$$m_0 c^2 \frac{d}{dt} \gamma = -e \vec{E} \cdot \vec{v} \quad (3)$$

where $\gamma = (1 + P^2 / m_0^2 c^2)^{1/2}$, $\vec{P} = \gamma m_0 \vec{v}$ and the wave fields \vec{E} and \vec{B} inside a circular waveguide of radius R_w are given by

A. TE_{mn} mode

$$\begin{aligned} B_z &= B_{z0} J_m(\alpha_{mn} R) \cos(m\phi + k_z z - \omega t) \\ E_r &= (\omega / \alpha_{mn} c) B_{z0} (m / \alpha_{mn} R) J_m(\alpha_{mn} R) \cos(m\phi + k_z z - \omega t) \\ E_\phi &= (\omega / \alpha_{mn} c) B_{z0} J_m'(\alpha_{mn} R) \sin(m\phi + k_z z - \omega t) \\ B_r &= -(k_z c / \omega) E_\phi \text{ and } B_\phi = (k_z c / \omega) E_r \end{aligned} \quad (4)$$

where α_{mn} is the n th root of the equation $J_m'(\alpha_{mn} R_w) = 0$

B. TM_{mn} mode

$$\begin{aligned} E_z &= E_{z0} J_m(\alpha_{mn} R) \cos(m\phi + k_z z - \omega t) \\ E_r &= -(k_z E_{z0} / \alpha_{mn}) J_m'(\alpha_{mn} R) \sin(m\phi + k_z z - \omega t) \\ E_\phi &= -(k_z E_{z0} / \alpha_{mn}) (m / \alpha_{mn} R) J_m(\alpha_{mn} R) \cos(m\phi + k_z z - \omega t) \\ B_r &= (\omega / k_z c) E_\phi \text{ and } B_\phi = (\omega / k_z c) E_r \end{aligned} \quad (5)$$

where $\alpha_{mn} R_w$ is the n th root of the equation $J_m(\alpha_{mn} R_w) = 0$

In order to provide some physical insight into the mathematical procedure employed to study the problem, we first decompose Eq. (2) into transverse and parallel components and write the transverse equation in terms of a complex variable $P^- = P_x - iP_y$:

$$\left[\frac{d}{dt} + i(\Omega + \Omega_z) \right] P^- = -e \left[E^- - i(v_z/c) B^- \right] \quad (6)$$

$$\frac{d}{dt} P_z = -e \left[E_z + (P_x B_y - P_y B_x) / \gamma m_0 c \right] \quad (7)$$

where $E^- = E_x - iE_y = e^{-i\phi}(E_r - iE_\phi)$, $B^- = B_x - iB_y = e^{-i\phi}(B_r - iB_\phi)$, $\Omega = \Omega_0 / \gamma$,

$$\Omega_o = eB_o/m_o c \text{ and } \Omega_z = eB_z/\gamma m_o c.$$

We now express the transverse components of the electron momentum (P_x, P_y) in terms of the polar coordinates (P_\perp, θ). Thus, $P_x = P_\perp \cos \theta$, $P_y = P_\perp \sin \theta$ and $P^2 = P_\perp^2 e^{-i\theta}$. Let (R_o, ϕ_o) be the coordinates of the guiding center of the electron. As shown in Fig. 1, the spatial coordinates (R, ϕ) of the electron can be expressed in terms of its guiding center coordinates (R_o, ϕ_o) and its momentum space coordinates (P_\perp, θ) as follows

$$R^2 = R_o^2 + R_L^2 - 2R_o R_L \cos(\pi/2 - \phi_o + \theta)$$

and

$$\phi = \phi_o - \sin^{-1} \left[(R_L/R) \cos(\phi_o - \theta) \right] = \theta - \frac{\pi}{2} + \sin^{-1} \left[(R_o/R) \cos(\phi_o - \theta) \right] \quad (8)$$

where $R_L = v_\perp/\Omega = P_\perp/m_o \Omega_o$ is the Lamour radius of the electron.

With the aid of the addition theorem of Bessel function:

$$J_m(\bar{w}) \left\{ \frac{Z - ze^{i\phi_1}}{Z - ze^{-i\phi_1}} \right\}^{m/2} = \sum_{l=-\infty}^{+\infty} J_{m+l}(Z) J_l(z) e^{-il\phi_1} \quad (9)$$

where $\bar{w} = (Z^2 + z^2 - 2Zz \cos \phi_1)^{1/2}$, and $|Z| > |z|$ the following results are derived:

$$J_m(\alpha_{mn} R) = e^{im(\phi_o - \phi)} \sum_{l=-\infty}^{+\infty} J_{m+l}(\alpha_{mn} R_o) J_l(\alpha_{mn} R_L) e^{-il(\pi/2 - \phi_o + \theta)} \quad (10)$$

$$J_{m\pm 1}(\alpha_{mn} R) = e^{\pm i(m\pm 1)(\phi_o - \phi)} \sum_{l=-\infty}^{+\infty} J_{m\pm 1+l}(\alpha_{mn} R_o) J_l(\alpha_{mn} R_L) e^{\pm il(\pi/2 - \phi_o + \theta)}$$

In obtaining Eq. (10), we have substituted $\bar{w} = \alpha_{mn}$, $Z = \alpha_{mn} R_o$, $z = \alpha_{mn} R_L$ and $\phi_1 = \pi/2 - \phi_o + \theta$ into Eq. (9), and used the relation

$$(R_o - R_L e^{i\phi_1})/(R_o - R_L e^{-i\phi_1}) = e^{-2i(\phi_o - \phi)}$$

derived from Eq. (8). Although Eq. (10) is the result for $R_o > R_L$ case (since $|Z| > |z|$ is required for Eq. (9) to hold), it can be shown that Eq. (10) also holds for $R_L > R_o$ case, where $Z = \alpha_{mn} R_L$, $z = \alpha_{mn} R_o$, and

$$(R_L - R_o e^{i\phi_1})/(R_L R_o e^{-i\phi_1}) = e^{-2i(\pi/2 - \theta + \phi)}$$

should be employed in Eq. (9).

Although the wave fields (4) and (5) seen by a stationary observer are simple harmonic at frequency ω , the fields and hence the forces seen by the gyrating electrons consist of an infinite number of frequency components oscillating at $\omega - N'\Omega - k_z V_z$ ($N' = 1, 2, 3, \dots$). Thus, if the wave frequency ω is near one of the Doppler shifted harmonics, i.e., $\omega \simeq N\Omega + k_z v_z$, the $N' = N$ term becomes the slowest term and has the dominant influence on the orbit evolution. Including only this term in (6), we may first define a self-consistent trajectory, prior to express (6) explicitly, as $R_L = R_L(t)$ and

$$\theta = \theta_o + \Psi(t) + \int_0^t \Omega(t') dt'$$

where $R_L(t)$ and $\Psi(t)$, to be determined self-consistently, are the time dependent Larmour radius and phase varying slowly due to the presence of this slowly time varying force. We next substitute these relations and the fields (4) or (5) into (6), (7) and (3), and then drop all fast oscillating terms. With the aid of (10) and the relation

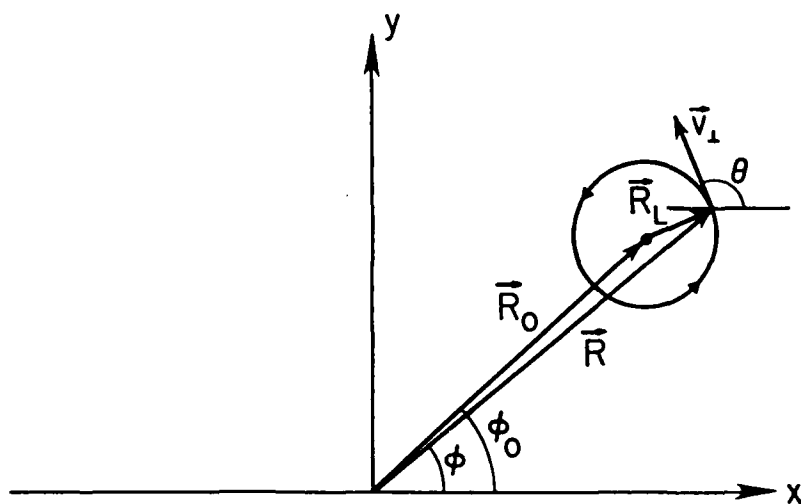


Fig. 1 Relationship between (R, ϕ) , (R_0, ϕ_0) and (R_L, θ) , which represents the transverse spatial coordinates, guiding center coordinates, and the momentum space coordinates of the electron, respectively.

$$\exp (i a \sin \phi) = \sum_{p=-\infty}^{+\infty} J_p(a) \exp (i p \phi)$$

Two sets of self-consistent governing equations for the slowly varying functions γ , R_L , Ψ and v_z are derived for wave fields of TE_{mn} mode and TM_{mn} mode, respectively, as follows:

A. TE_{mn} mode

$$\frac{d}{dt} \alpha = a_e (w - k_z v_z) J_N'(\alpha) \cos \Phi_e \quad (11)$$

$$\frac{d}{dt} \Phi_e = \Delta w \left[1 + a_e J_N(\alpha) \sin \Phi_e \right] - a_e (w - k_z v_z) \left[\frac{1}{\alpha} \frac{d}{d\alpha} [\alpha J_N'(\alpha)] \right] \sin \Phi_e \quad (12)$$

$$\frac{d}{dt} \gamma = a_e (\Omega_o^2 w / \gamma \alpha_{mn}^2 c^2) \left[\alpha J_N'(\alpha) \right] \cos \Phi_e \quad (13)$$

$$\frac{d}{dt} v_z = -a_e (\Omega_o^2 w / \gamma^2 k_z \alpha_{mn}^2 c^2) (k_z v_z - k_z^2 c^2 / w) \left[\alpha J_N'(\alpha) \right] \cos \Phi_e \quad (14)$$

where

$$\alpha = \alpha_{mn} R_L, \quad \Phi_e = (m - N) \theta_o - \int \Delta w dt + N(\Phi + \theta_o + \pi/2) + k_z z_o + \pi/2,$$

$$\Delta w = w N \Omega k_z v_z, \quad \text{and} \quad a_e = (-1)^N (B_{zo}/B_o) J_{m-N}(\alpha_{mn} R_o).$$

B. TM_{mn} mode

$$\frac{d}{dt} \alpha = a_m (1 - w k_z V_z / k_z^2 c^2) (N/\alpha) J_N(\alpha) \cos \Phi_m \quad (15)$$

$$\frac{d}{dt} \Phi_m = \Delta w - a_m (1 - w k_z v_z / k_z^2 c^2) (N/\alpha) J_N'(\alpha) \sin \Phi_m \quad (16)$$

$$\frac{d}{dt} \gamma = -a_m (\Omega_o / k_z c^2) \left[v_z - (k_z N \Omega / \alpha_{mn}^2) \right] J_N(\alpha) \cos \Phi_m \quad (17)$$

$$\frac{d}{dt} v_z = -a_m (\Omega / k_z) \left[(1 - v_z^2 / c^2) - (w N \Omega / \alpha_{mn}^2 c^2) (1 - k_z V_z / w) \right] J_N(\alpha) \cos \Phi_m \quad (18)$$

where

$$\Phi_m = \Phi_e - \pi/2 \quad \text{and} \quad a_m = (-1)^N (k_z c E_{zo} / m \Omega_o) J_{m-N}(\alpha_{mn} R_o)$$

First, we shall derive two invariants from each set of governing equations. From Eqs. (11), (13) and (14), by taking their relative ratios to cancel out $J_N'(\alpha) \cos \Phi_e$, two invariants are obtained for TE_{mn} mode case:

$$k_z v_z - k_z v_{zo} = (k_z^2 c^2 / w - k_z v_{zo}) (1 - \gamma_o / \gamma) \quad (19)$$

$$(\Omega_o / \alpha_{mn} c)^2 (\alpha^2 - \alpha_o^2) = (\gamma - \gamma_o k_z v_{zo} / w)^2 - \gamma_o^2 (1 - k_z v_{zo} / w)^2 - (k_z c / w)^2 (\gamma - \gamma_o)^2 \quad (20)$$

with the aid of (19), we can express Δw for TE_{mn} mode case to be

$$\Delta w = \Delta w_o + (w_o - k_z^2 c^2 / w) (\gamma - \gamma_o) / \gamma \quad (21)$$

where $\Delta w_o = w - w_o$ and $w_o = N \Omega_o / \gamma_o + k_z v_{zo}$

Similarly, from the relative ratios of Eqs. (15), (17) and (18), two invariants for TM_{mn} mode case are obtained to be

$$(\gamma v_z - \gamma_o v_{zo}) \left[\gamma + \gamma_o v_{zo} - 2 k_z N \Omega_o / \alpha_{mn}^2 \right] = c^2 (\gamma - \gamma_o) \left[\gamma + \gamma_o - 2 N \Omega_o w / \alpha_{mn}^2 c^2 \right] \quad (22)$$

$$\gamma - \gamma_o = \left[k_z (\gamma v_z - \gamma_o v_{zo}) + (\Omega_o / 2 N) (\alpha^2 - \alpha_o^2) \right] / w \quad (23)$$

With the aid of (22), Δw , for TM_{mn} mode case, can be expressed to be

$$\begin{aligned}\Delta w &= \Delta w_o + w_o(\gamma - \gamma_o)/\gamma + (\gamma_o/h) \{w_1 [w_1^2 + (k_z^2 c^2/h_o^2)(\gamma - \gamma_o)(\gamma + \gamma_o - 2N\Omega_o w/\alpha_{mn}^2 c^2)]^{1/2}\} \\ &\approx \Delta w_o + [w_o - 1/2(k_z^2 c^2/h_o^2)(\gamma + \gamma_o - 2N\Omega_o w/\alpha_{mn}^2 c^2)](\gamma - \gamma_o)/\gamma\end{aligned}\quad (24)$$

where

$$w_1 = k_z v_{zo} - (k_z^2/\alpha_{mn}^2)(N\Omega_o/h_o)$$

and

$$w_1^2 \gg (k_z^2 c^2/h_o^2)(\gamma - \gamma_o)(\gamma + \gamma_o - 2N\Omega_o w/\alpha_{mn}^2 c^2)$$

is assumed.

In the above, we have derived two sets of governing rate equations (11)-(14) and (15)-(18) for describing the behavior of the electron beam inside a circular waveguide in the presence of electromagnetic fields of TE_{mn} mode or TM_{mn} mode respectively. In order to close the system of equations, it is necessary to include a field equation that takes into account the effects of the dynamical properties of the medium on the field. Since the purpose of this work is to derive a single nonlinear equation for describing the temporal evolution of the field amplitude of the electron cyclotron maser instability, the field equation used for the present analysis is the energy conservation equation:

$$n_o m_o c^2 \frac{d}{dt} \langle \gamma \rangle + (\epsilon/16\pi) \frac{d}{dt} E_o^2 = 0 \quad (25)$$

where n_o is the electron beam density averaged over the cross-section of the guide, $\langle \rangle$ stands for an average over the initial random phase distortion of the electron beam, and $E_o = (w/\alpha_{mn} c) B_{zo}$ and

$$\begin{aligned}\epsilon &= (1 + k_z^2 c^2/w^2) \{ [1 - (m-1)^2/\alpha_{mn}^2 R_W^2] J_{M-1}^2(\alpha_{mn} R_W) + [1 - (m+1)^2/\alpha_{mn}^2 R_W^2] J_{m+1}^2(\alpha_{mn} R_W) \} \\ &\quad + (\alpha_{mn} c/w)^2 \left[1 - m^2/\alpha_{mn}^2 R_W^2 \right] J_M^2(\alpha_{mn} R_W)\end{aligned}$$

for TE_{mn} mode and $E_o = E_{zo}$ and

$$\epsilon = (k_z/\alpha_{mn})^2 (1 + w^2/k_z^2 c^2) \left[J_{m-1}^2(\alpha_{mn} R_W) + J_{m+1}^2(\alpha_{mn} R_W) \right] + J_m^2(\alpha_{mn} R_W)$$

for TM_{mn} mode. Equation (25) is then integrated, the result is

$$n_o m_o c^2 (\langle \gamma \rangle - \gamma_o) = - (\epsilon/16\pi) [E_o^2(t) - E_o^2(o)] \quad (26)$$

1.2. ANALYSIS

In the present analysis, the effect of depletion of the rotational free energy of the electrons by the unstable waves will be assumed to be insignificant, $E_o(t)$ and $\theta(t)$ are thus expected to vary with time much faster than other variables γ , α and v_z in (11)-(14) and (15)-(18). Therefore, only two rate equations (12) and (13) or (16) and (17) from each set of equations, will be employed in the following analysis. They are further unified into one set of equations expressed approximately as

$$\frac{d}{dt} \Phi = -\Delta w - AE_o \sin \Phi \quad (27)$$

$$\frac{d}{dt} \gamma = DE_o \cos \Phi \quad (28)$$

and

$$\Delta w = \Delta w_o + G(\gamma - \gamma_o) \quad (29)$$

where the notations used for (i) TE_{mn} mode case, are $\Phi = \Phi_0$, $G = (w_0 - k_z^2 c^2 / w) / \gamma_0$,

$$A = (-1)^N (\alpha_{mn} c / B_0) (1 - k_z v_{z0} / w) J_{m-N}(\alpha_{mn} R_0) \left\{ \frac{1}{\alpha_0} \frac{d}{d\alpha_0} [\alpha_0 J_N(\alpha_0)] \right\}$$

and

$$D = (-1)^N (\Omega_0^2 / \gamma_0 B_0 \alpha_{mn} c) J_{m-N}(\alpha_{mn} R_0) [\alpha_0 J_N(\alpha_0)]$$

$|a_0 J_N(\alpha) \sin \Phi| \ll 1$ is assumed to reduce (12) to (27) and for (ii) TM_{mn} mode case, are $\Phi = \Phi_m$, $G = (w_0 - (k_z^2 c^2 / w_1) (1 - N \Omega_0 w / \gamma_0 \alpha_{mn}^2 c^2) / \gamma_0$,

$$A = (-1)^N (k_z c / B_0) (1 - w v_{z0} / k_z c^2) J_{m-N}(\alpha_{mn} R_0) (N / \alpha_0) J_N(\alpha_0)$$

and

$$D = (-1)^{N+1} (\Omega_0 / B_0 c) (v_{z0} - k_z N \Omega_0 / \gamma_0 \alpha_{mn}^2) \times J_{m-N}(\alpha_{mn} R_0) J_N(\alpha_0)$$

γ, α , and v_z replaced by their initial values γ_0, α_0 and v_{z0} in the coefficients A, D and G is followed by the assumptions that they vary with time much slower than $E_0(t)$ and $\Phi(t)$ and the effect of beam energy depletion is insignificant.

We now introduce an average procedure to combine Eqs. (25), (27) and (28) into a single nonlinear equation for describing the temporal evolution of the field amplitude $E_0(t)$. We first take the average over Eq. (28) and compare the result with Eq. (25) to establish the relation:

$$\langle \cos \Phi \rangle = - (\epsilon / 8\pi n_0 m_0 c^2 D) \frac{d}{dt} E_0 \quad (30)$$

We next take the average over Eq. (29) and use the relation (26) to obtain

$$\langle \Delta w \rangle = \Delta w_0 - (G \epsilon / 16\pi N_0 m_0 c^2) [E_0^2(t) - E_0^2(0)] \quad (31)$$

Equation (28) is integrated to obtain $\gamma - \gamma_0$, which is then used to express Δw as

$$\Delta w = \Delta w_0 + GD \int_0^t E_0(t') \cos \Phi' dt' \quad (32)$$

We now multiply (27) by $\sin \Phi$ and $\cos \Phi$ respectively and then take the average over the resultants, two moment equations are obtained

$$\begin{aligned} \frac{d}{dt} \langle \cos \Phi \rangle &= \Delta w_0 \langle \sin \Phi \rangle + \frac{1}{2} A E_0 (1 - \langle \cos 2\Phi \rangle) \\ &+ \frac{1}{2} G D \int_0^t dt' E_0(t') [\langle \sin(\Phi + \Phi') \rangle + \langle \sin(\Phi - \Phi') \rangle] \end{aligned} \quad (33)$$

$$\begin{aligned} \frac{d}{dt} \langle \sin \Phi \rangle &= - \Delta w_0 \langle \cos \Phi \rangle - \frac{1}{2} A E_0 \langle \sin 2\Phi \rangle \\ &- \frac{1}{2} G D \int_0^t dt' E_0(t') [\langle \cos(\Phi + \Phi') \rangle + \langle \cos(\Phi - \Phi') \rangle] \end{aligned} \quad (34)$$

where we have derived two coupled moment equations which are also coupled to the higher order moments $\langle \cos 2\Phi \rangle$, $\langle \sin 2\Phi \rangle$, $\langle \cos(\Phi + \Phi') \rangle$, and $\langle \sin(\Phi + \Phi') \rangle$. In principle, a hierarchy of moment equations can be derived in the similar way, they have, however, to be truncated at certain degree in order to close the system of equations. This is done by neglecting all those of higher order moments in (33) and (34). Further, since $\Phi - \Phi'$ becomes independent of the initial random phase in the lowest order term of its expansion, we may approximate

$$\langle \sin(\Phi - \Phi') \rangle \approx - \sin \Delta \Phi(t - t') \quad \text{and} \quad \langle \cos(\Phi - \Phi') \rangle \approx \cos \Delta \Phi(t - t') \quad (35)$$

where $\Delta\Phi(t-t') = \int_{t'}^t \langle \Delta w(\tau) \rangle d\tau$ and $\langle \Delta w \rangle$ is given by (31).

With those simplifications, (33) and (34) reduce to

$$\frac{d}{dt} \langle \cos \Phi \rangle \approx \Delta w_o \langle \sin \Phi \rangle + \frac{1}{2} A E_o - \frac{1}{2} G D \int_0^t dt' E_o(t') \sin \Delta\Phi(t-t') \quad (36)$$

and

$$\frac{d}{dt} \langle \sin \Phi \rangle \approx -\Delta w_o \langle \cos \Phi \rangle - \frac{1}{2} G D \int_0^t E_o(t') \cos \Delta\Phi(t-t') \quad (37)$$

Finally, a nonlinear differential equation for the field amplitude $E_o(t)$ can be derived by combining (36) and (37) together with the aid of the relation (30), the result is

$$\frac{d^3}{dt^3} E_o(t) + (\Delta w_o^2 + c_o) \frac{d}{dt} E_o(t) = a_o \left\{ 1 - \frac{G \epsilon [E_o^2(t) - E_o^2(o)]}{32 \pi \Delta w_o \Omega_o m_o c^2} \right\} \int_0^t dt' E_o(t') \cos \Delta\Phi(t-t') \quad (38)$$

where $c_o = 4 \pi n_o m_o c^2 D A k$ and $a_o = 8 \pi n_o m_o c^2 \Delta w_o G D^2 k$.

(2) Relativistic Adiabatic Invariants of Electron Motion under Electron Cyclotron Resonance Heating (ECRH)

Three adiabatic invariants of the electron motion under electron cyclotron resonance heating by three differently polarized heater: (1) ordinary mode; (2) extraordinary mode; and (3) electrostatic mode are derived. These relations determine the electron trajectory in the phase space and hence provide necessary information on the process of energy transfer between the electrons and the coherent waves.

2.1. Characteristic Equations

The nonlinear interaction of a single electron with a heating wave of arbitrary polarization near a cyclotron harmonic, $\omega \approx N \Omega$ is analyzed, where ω is the wave frequency, $\Omega = \frac{e B_o}{\gamma m_o c} = \Omega_o / \gamma$ is the relativistic electron cyclotron frequency, $\Omega_o = e B_o / m_o c$, $\gamma = (1 + P^2 / m_o c^2)^{1/2}$ is the relativistic factor, B_o is the background magnetic field, \vec{P} is the momentum of the electron and N is an integer. The relativistic electron orbit equations are

$$\frac{d}{dt} \vec{R} = \vec{P} / \gamma m_o \quad (1)$$

and

$$\frac{d}{dt} \vec{P} = -e [\vec{E} + (\vec{P} / \gamma m_o c) \times (\vec{B} + z B_o)] \quad (2)$$

where one coupled to the energy equation of the electron

$$m_0 c^2 \frac{d}{dt} \gamma = - (e/\gamma m_0) \vec{E} \cdot \vec{P} \quad (3)$$

where (\vec{R}, \vec{P}) are the spatial and the momentum coordinates of the electron in the phase space, m is the rest mass, and \vec{E} and \vec{B} , the heating wave fields of arbitrary polarization, have the following general expressions:

$$\begin{aligned} \vec{E} = & [\hat{x} - (k_z/k_\perp) \hat{z}] \epsilon_o \cos(k_\perp x + k_z z - \omega t) \\ & + \hat{y} \epsilon_z \cos(k_\perp x + k_z z - \omega t + \phi_z) + [\hat{x} + (k_z/k_\perp) \hat{z}] \epsilon_s \sin(k_\perp x + k_z z - \omega t + \phi_s) \\ \vec{B} = & (c/\omega) \vec{k} \times \vec{E} \end{aligned} \quad (4)$$

here $\vec{k} = \hat{x} k_\perp + \hat{z} k_z$, ϵ_o, ϵ_z and ϵ_s represent the field amplitudes associated with the ordinary mode, extraordinary mode and electrostatic modes, respectively, and ϕ_z and ϕ_s are the arbitrary constant phases. The collective effect of the plasma on the wave propagation and polarization is not included in the analysis.

We first decompose Eq. (2) into transverse and axial components. We next combine the two transverse components together by using the complex notation $P^- = P_x - iP_y$, and use (3) to simplify the axial equation for P_z . The results are

$$[\frac{d}{dt} + i(\Omega + \Omega_z)] P^- = -e(1 - k_z v_z/\omega) E^- - e(k_\perp v_z/\omega) E_z \quad (5)$$

$$\frac{d}{dt} P_z = -e(1 - \vec{k} \cdot \vec{v}/\omega) E_z + (k_z/\omega) m c^2 \frac{d}{dt} \gamma \quad (6)$$

where

$$\begin{aligned} E^- = & E_x - iE_y = - (k_z \epsilon_o/k_\perp) \cos(k_\perp x + k_z z - \omega t) - \\ & i \epsilon_z \cos(k_\perp x + k_z z - \omega t + \phi_z) + \epsilon_s \sin(k_\perp x + k_z z - \omega t + \phi_s) \end{aligned}$$

and

$$\Omega_z = eB_z/\gamma m_0 c.$$

Eq. (5) is then integrated formally to be

$$P^- = e^{-i \int_0^t (\Omega' + \Omega_z) dt'} \left\{ P_o^- - e \int_0^t dt' e^{i \int_0^{t'} (\Omega'' + \Omega_z'') dt''} \left[(1 - k_z v_z'/\omega) E^-(t') + (k_\perp v_z'/\omega) E_z(t') \right] \right\} \quad (7)$$

where $P_o^- = P_{ox} - iP_{oy} = P_{o\perp} e^{-i\theta_o}$, $\theta_o = \tan^{-1}(v_{oy}/v_{ox})$ is the initial phase angle of the electron in velocity space, $\Omega' = \Omega(t')$, $\Omega_z' = \Omega_z(t')$, $R'' = R(t'')$, $\Omega_z'' = \Omega_z(t'')$ and $v_z' = v_z(t')$.

Since the wave field \vec{E} itself depends on x and z , i.e., the solution of (1) and (2), it is useful to define a self-consistent trajectory prior to expressing (7) explicitly. Near the cyclotron harmonic resonance, i.e., $\omega \approx N\Omega$, only the slow time varying component of the integral on the RHS of (7) contributes to the resonance trajectory of the electron. One can then define such a set of self-

consistent resonance trajectory as

$$v_x = v_{\perp} \cos \left[\theta_0 + \Psi(t) + \int_0^t \Omega' dt' \right], v_y = v_{\perp} \sin \left[\theta_0 + \Psi(t) + \int_0^t \Omega' dt' \right]$$

$$x = x_0 + (v_y / \Omega)$$

and

$$z = z_0 + \int_0^t v_z' dt',$$

where v_z' is assumed to retain only those of slow time varying components, Ψ is the self-consistent phase shift of electron gyration due to the resonance interaction, and $\Psi(0)=0$. Substituting this set of resonance trajectories into (3), (5), and (8), the governing equations for the slow-time varying components of the variables, γ, v_{\perp}, v_z and Ψ are derived to be

$$\frac{d}{dt} \alpha = a_0 (\omega - k^2 v_z / k_z) (N/\alpha) J_N(\alpha) \cos \phi_N - a_z (\omega - k_z v_z) J_N'(\alpha) \sin(\phi_N + \phi_s) \quad (8)$$

$$- a_s \omega (N/\alpha) J_N(\alpha) \sin(\phi_N + \phi_s)$$

$$\frac{d}{dt} \phi_N = -\Delta \omega \left[1 + a_z J_N(\alpha) \cos(\phi_N + \phi_s) \right] - a_0 (\omega - k^2 v_z / k_z) (N/\alpha) J_N'(\alpha) \sin \phi_N \quad (9)$$

$$- a_z (\omega - k_z v_z) \left\{ \frac{1}{\alpha} \frac{d}{d\alpha} \left[\alpha J_N'(\alpha) \right] \right\} \cos(\phi_N + \phi_s) - a_s \omega (N/\alpha) J_N'(\alpha) \cos(\phi_N + \phi_s)$$

$$\frac{d}{dt} \gamma = a_0 (\omega \Omega_0 / k_z^2 c^2) (k_z^2 N \Omega / k_{\perp}^2 - k_z v_z) J_N(\alpha)$$

$$\cos \phi_N - a_z (\alpha / \gamma) (\Omega_0^2 \omega / k_{\perp}^2 c^2) J_N'(\alpha) \sin(\phi_N + \phi_s)$$

$$- a_s (\omega \Omega_0 / k_{\perp}^2 c^2) (N \Omega + k_z v_z) J_N(\alpha) \sin(\phi_N + \phi_s) \quad (10)$$

$$\frac{d}{dt} \gamma v_z = -a_0 (\Omega_0 / k_z) (\omega - k^2 N \Omega / k_{\perp}^2) J_N$$

$$\cos \phi_N - a_z (\alpha / \gamma) (k_z \Omega_0^2 / k_{\perp}^2) J_N'(\alpha) \sin(\phi_N + \phi_s)$$

$$- a_s (k_z \Omega_0 \omega / k_{\perp}^2) J_N(\alpha) \sin(\phi_N + \phi_s) \quad (11)$$

where

$$\alpha = k_{\perp} v_{\perp} / \Omega, \quad \phi_N = N(\theta_0 + \Psi) + k_{\perp} x_0 + k_z z_0 - \int_0^t \Delta\omega(t') dt', \quad \Delta\omega = \omega - N\Omega - k_z v_z, \quad a_0 = (k_z c \epsilon_0 / \omega B_0),$$

$$a_z = (k_{\perp} c \epsilon_z / \omega B_0), \quad a_s = (k_{\perp} c \epsilon_s / \omega B_0),$$

and $J_N(\alpha)$ and $J'_N(\alpha)$ are the Bessel functions of order N and its derivative, respectively.

2.2. Adiabatic Invariants

We now proceed to derive the adiabatic invariants relations from the characteristic equations (8) - (11). Since different modes will propagate to different locations, we hence derive the invariants separately for each mode. The general procedure to derive the invariants is by taking the ratio of the two relevant equations among the four characteristic equations and then integrating the resultant ratio to obtain each invariant. Three independent combinations can be made and, hence, three invariant relations for each mode can be derived. We consider

A. Ordinarily Polarized Heater, i.e., $a_z = 0 = a_s$:

We first take the ratio of (10) to (11), the result is then integrated to be

$$(\gamma v_z - k_z N \Omega_0 / k_{\perp}^2)^2 - c^2 (\gamma - N \Omega_0 k^2 / k_{\perp}^2 \omega)^2 = \text{const. in time} = A_{01} \quad (12)$$

Similarly, from (8) and (10), yields

$$\gamma - (\omega / k^2 c^2) (k_z \gamma v_z + \Omega_0 \alpha^2 / 2N) = \text{const. in time} = A_{02} \quad (13)$$

where A_{02} is related to A_{01} . The relationship is obtained by substituting (13) into (12) and using the relation

$$\gamma^2 = 1 + (\Omega_0 \alpha / k_{\perp} c)^2 + (\gamma v_z / c)^2 = 1 + P^2 / k^2 c^2$$

the result is

$$A_{01} = (k^2 / k_{\perp}^2) (N \Omega_0 / \omega) \left[2A_{02} + (k_z^2 / k_{\perp}^2) (\omega N \Omega_0 / k^2 c^2) - (k^2 / k_{\perp}^2) (N \Omega_0 / \omega) \right] \quad (14)$$

The last invariant is obtained from (8) and (9) and it is

$$J_N(\alpha) \sin \phi_N - (k_z k_{\perp}^2 / k^2 \Omega_0 a_0) \left[\gamma v_z - (k_z c^2 / 2N \Omega_0) (\Omega_0 / k_{\perp} c)^2 \alpha^2 \right]$$

$$= \text{const. in time} = A_{03}$$

B. Extraordinarily Polarized Heater, i.e., $a_0 = 0 = a_s$:

From (10) and (11), we obtain

$$\gamma (1 - \omega v_z / k_z c^2) = \text{const. in time} = A_{s1}, \quad (16)$$

and then from (8) and (10), and with the aid of (16), yields

$$(\gamma - \gamma_0 k_z v_{z0}/\omega)^2 - (k_z c/\omega)^2 (\gamma - \gamma_0)^2 - (\Omega_0/k_z c)^2 \alpha^2 = \text{const. in time} = A_{z2} \quad (17)$$

Finally, we take the ratio of (8) to (9) and assume that $|(\alpha/N) J_{N+1}(\alpha)| \ll |J_N(\alpha)|$ the resultant ratio can then be integrated with the aids of (16) and (17) to be

$$\begin{aligned} & \left[1 + a_z J_N(\alpha) \cos(\phi_N + \phi_z) \right] \\ & \exp\left\{ (k_z^2 c^2 / 2 N \Omega_0^2) \left[(\Delta\omega_0/\omega) \gamma^2 + (\omega_0/\omega - k_z^2 c^2 / \omega^2) (\gamma - \gamma_0)^2 \right] \right\} \\ & = \text{const. in time.} \\ & = A_{z3} \end{aligned} \quad (18)$$

where $\Delta\omega_0 = \omega - \omega_0$ and $\omega_0 = N \Omega_0 / \gamma_0 + k_z v_{z0}$

C. Electrostatic Heating Wave, i.e., $a_0 = 0 = a_z$

Taking the ratio of (10) to (11) and integrating the resultant ratio, yields

$$\gamma^2 - (\gamma v_z + N \Omega_0 / k_z)^2 / c^2 = \text{const. in time} = A_{s1} \quad (19)$$

next, the result derived from the ratio of (8) to (11) is

$$\alpha^2 - 2(N k_z^2 / k_z \Omega_0) \gamma v_z = \text{const. in time} = A_{s2} \quad (20)$$

where A_{s1} and A_{s2} are related as

$$A_{s1} = 1 - (N \Omega_0 / k_z c)^2 + (\Omega_0 / k_z c)^2 A_{s2} \quad (21)$$

From (8) and (9) and with the aid of (18) and (20), the last invariant is obtained to be

$$J_N(\alpha) \cos(\phi_N + \phi_s) + (\alpha^2 / 2 N - k_z^2 c^2 \gamma / \omega \Omega_0) / a_s = \text{const. in time} = A_{s3} \quad (22)$$

We, therefore, have shown that the electron trajectory under ECRH is governed by three invariants (12), (13) and (15) with 0-mode heating, (16), (17), and (18) with X-mode heating, and (19), (20), and (22) with electrostatic heater. The second term on the LHS of (15) and (22) and the exponential factor on the LHS of (18) manifests the effect of detuning on resonance interaction. There are two sources of detuning, one introduced by the motion of the particle guiding center as is represented by the $k_z v_z$ term and another one comes from the relativistic effect $\Omega = \Omega(t)$. They are included in the phase equation (9) in which the $\Delta\omega$ term accounts for the total detuning effect and hence reflected in the results of invariants.

If we focus on relativistic detuning effect only and thus set $k_z = 0$, i.e., considering normal incident case, the invariants for each mode type of heater

reduces to:

A. Ordinarily Polarized Heater:

$$\gamma^2 v_z^2 - \gamma_o^2 v_{zo}^2 = c^2 (\gamma - \gamma_o) (\gamma + \gamma_o - 2N\Omega_o / \omega)$$

$$\gamma - \gamma_o = (\omega \Omega_o / 2Nk^2 c^2) (\alpha^2 - \alpha_o^2) \quad (23)$$

and

$$J_N(\alpha) \sin \phi_N - (\gamma v_z - \gamma_o v_{zo}) / v_o = A_{os}$$

where $v_o = c\epsilon_o / m\omega$.

B. Extraordinarily Polarized Heater:

$$\gamma v_z = \text{const.} = \gamma_o v_{zo}$$

$$\gamma^2 - \gamma_o^2 = (\Omega_o / kc)^2 (\alpha^2 - \alpha_o^2) \quad (24)$$

$$\left[1 + a_z J_N(\alpha) \cos(\phi_N + \phi_z) \right] \exp\{ (k^2 c^2 / 2N\Omega_o^2) (\gamma - \gamma_o \omega_o / \omega)^2 \} = \text{const. in time}$$

Electrostatic Heater:

$$\gamma v_z = \text{const.} = \gamma_o v_{zo}$$

$$\gamma^2 - \gamma_o^2 = (\Omega_o / kc)^2 (\alpha^2 - \alpha_o^2) \quad (25)$$

$$J_N(\alpha) \cos(\phi_N + \phi_z) + (\alpha^2 / 2N - \omega \gamma / \Omega_o) / a_z = \text{const. in time.}$$

III. Instabilities Excited by Wave-Plasma Interaction

(1) Oscillating Two-Stream Instability of a Ducted Whistler Pump

A magnetically field-aligned zero-frequency mode excited together with two lower hybrid sidebands by a ducted whistler pump is investigated. The thermal focusing force is found to be the dominant nonlinear effect on the excitation of large-scale instabilities, while the nonoscillatory heating current overrides the thermal focusing force in the short wavelength region. Our results show that the thermal instability of whistler waves should be expected to occur in the ionospheric plasmas in the wave injection experiments performed at Siple, Antarctica. The excitation of this instability can also be used to explain the enhancement of air flow and particle precipitation observed during the powerful VLF transmitter cycle from a Russian station and may possibly be the cause of the lower hybrid waves correlated with the occurrence of lightning storms. Further, the proposed instability may become a potential candidate for

γf heating of fusion plasmas. This work has been published in *The Physics of Fluids*.

(2) Excitation of Upper-Hybrid Waves by a Thermal Parametric Instability

A purely growing instability characterized by a four-wave interaction has been analyzed in a uniform magnetized plasma. Up-shifted and down-shifted upper-hybrid waves and a nonoscillatory mode can be excited by a pump wave of ordinary rather than extraordinary polarization in the case of ionospheric heating. The differential ohmic heating force dominates over the ponderomotive force as the wave-wave coupling mechanism. The heating current at zero frequency produces a significant stabilizing effect on the excitation of short-scale modes by counterbalancing the destabilizing effect of the differential ohmic heating. The effect of ionospheric inhomogeneity is estimated, showing a tendency to raise the thresholds of the instability. When applied to ionospheric heating experiments, the present theory can explain the excitation of field-aligned plasma lines and ionospheric irregularities with a continuous spectrum ranging from metre-scale to hundreds of metre-scale. Further, the proposed mechanism may become a competitive process to the parametric decay instability and be responsible for the overshoot phenomena of the plasma line enhancement at Arecibo. This work has been published in *The Journal of Plasma Physics*.

(3) Earth's Magnetic Field Perturbations as the Possible Environmental Impact of the Conceptualized Solar Power Satellite

The results of this study conclude that the earth's magnetic field can be significantly perturbed locally by the microwave beam transmitted from the conceptualized solar power satellite (SPS) at a frequency of 2.45 GHz with incident power density of 230 W/m^2 at the center of the beam. The simultaneous excitation of the earth's magnetic field fluctuations and ionospheric density irregularities is caused by the thermal filamentation instability of microwaves with scale lengths greater than a few hundred meters. Earth's magnetic field perturbations with magnitudes (\approx a few tens of gammas) comparable to those in magnetospheric substorms can be expected. Particle precipitation and air-glow enhancement are the possible, concomitant ionospheric effects associated with the microwave-induced geomagnetic field fluctuations. Our present work adds earth's magnetic field perturbations as an additional effect to those such as ionospheric density irregularities, plasma heating, etc., that should be assessed as the possible environmental impacts of the conceptualized solar power satellite program. This work has been published in *The Journal of Geophysical Research*.

(4) A Theoretical Model of Artificial Spread-F Echoes

Our previous work [Kuo and Schmidt, *Phys. Fluids*, 26, 2529, 1983] on filamentation instability of EM waves in magnetic-plasmas has shown that the irregularities excited by the O-mode pump and by the X-mode pump have different polarization directions. The irregularities excited by the O-mode pump are field-aligned and are polarized in the direction perpendicular to the meridian plane. By contrast, the irregularities excited by the X-mode pump are polarized in the meridian plane and are, in general, not field-aligned. These results are realized to agree with the observations on spread-F phenomena during the ionospheric heating experiments, namely, the excitation of differently polarized irregularities by differently polarized heater is responsible for the different occurrence frequencies of artificial spread-F noticed at Arecibo, Boulder, and Tromsø. To enhance our contribution to the spread-F problem, we further developed a theoretical model for artificial spread-F echoes. In this work, the relationship between the spread-F echoes and the HF wave-induced

irregularities is studied by the proposed model. The effect of the irregularity polarizations, scale length, and the geomagnetic dip angle on the spread-F echoes have been examined. A manuscript has been proposed and submitted to *Radio Science* for publication.

APPENDIX 1.

Analysis of Electron Cyclotron
Maser Instability

REPRINTED FROM:

PHYSICS LETTERS

Volume 103A, No. 9, 30 July 1984

ANALYSIS OF THE ELECTRON CYCLOTRON MASER INSTABILITY

S.P. KUO and B.R. CHEO

Polytechnic Institute of New York, Route 110, Farmingdale, NY 11735, USA

pp. 427-432



NORTH-HOLLAND PHYSICS PUBLISHING - AMSTERDAM

ANALYSIS OF THE ELECTRON CYCLOTRON MASER INSTABILITY

S.P. KUO and B.R. CHEO

Polytechnic Institute of New York, Route 110, Farmingdale, NY 11735, USA

Received 14 February 1984

Revised manuscript received 8 May 1984

A single nonlinear equation which describes the temporal evolution of the field amplitude of the electron cyclotron maser instability is derived self-consistently. The results deduced from this nonlinear equation are found to agree well with those of particle simulation.

Recently there has arisen the need to develop high-power millimeter and submillimeter wave sources for various applications in areas including millimeter wave radar communication and electron cyclotron heating of magnetically confined plasma in thermonuclear fusion devices. Conventional microwave devices such as the traveling wave tube or magnetron rely on a slow wave structure for their operation. Power density as well as voltage breakdown considerations place a lower limit on the dimensions of the structure. The electron cyclotron maser (gyrotron) mechanism [1-4], on the other hand, is through the fast wave coupling (waveguide) to convert the "transverse energy" of the relativistic electron beam into EM radiation. Moreover, gyrotron operation does not rely on the fine structure of a waveguide or cavity, and therefore efficient generation of high power millimeter or submillimeter waves by the new device called gyrotron is possible.

A great deal of the basic understanding of the electron cyclotron maser instability mechanism has been achieved in previous studies [5-8], though continuous efforts in this area are still needed in order to improve the power gain, the conversion efficiency, the coherency of the radiation and the new competing mechanisms, etc. In this work the nonlinear evolution of the electron cyclotron maser instability is studied analytically. Usually there are two mechanisms which are responsible for saturation of the unstable wave in the maser instability. In the following analysis the phase trapping of the gyrating particles in the wave is considered to be the only mechanism for saturation. This is reasonable if the initial beam energy is assumed to be large enough such that the effect of depletion of the rotational free energy of the electrons by the unstable wave becomes insignificant. Our approach to the problem starts with solving the equations of motion of a single electron moving in the wave fields and then follows with averaging the results over the initial random phase distribution to obtain the collective response of electrons to the wave fields. It is then found that the temporal evolution of the wave field amplitude can be governed by a single nonlinear equation which is derived self-consistently.

The motion of electrons in a dc magnetic field and the waveguide mode fields is governed by a set of coupled nonlinear differential equations:

$$d\mathbf{r}/dt = \mathbf{P}/\gamma m_0, \quad d\mathbf{P}/dt = -e[\mathbf{E} + c^{-1}\mathbf{v} \times (\mathbf{B} + zB_0\hat{z})], \quad m_0 c^2 d\gamma/dt = -e\mathbf{E} \cdot \mathbf{v}, \quad (1,2,3)$$

where

$$\gamma = (1 + P^2/m_0^2 c^2)^{1/2}, \quad \mathbf{P} = \gamma m_0 \mathbf{v},$$

and the wave fields \mathbf{E} and \mathbf{B} inside a guide, simplified to be of plane geometry, are given by

$$\mathbf{E} = \hat{y} E_y = \hat{y} E_0(t) \sin k_n(x-a) \cos(k_z z - \omega t),$$

$$\mathbf{B} = \hat{x}(k_z c/\omega) E_0(t) \sin k_n(x-a) \cos(k_z z - \omega t) + \hat{z}(k_n c/\omega) E_0(t) \cos k_n(x-a) \sin(k_z z - \omega t),$$

$k_n = n\pi/2a$ is the perpendicular wave number, $n = 1, 2, 3, \dots$ is the waveguide mode number and $2a$ is the distance between the two parallel plates.

Although the wave field seen by a stationary observer is simple harmonic at frequency ω , the fields and hence the force seen by the gyrating electrons consist of an infinite number of frequency components oscillating at ω

$N'\Omega - k_z v_z$ ($N' = 1, 2, 3, \dots$; $\Omega = eB_0/\gamma m_0 c$, the cyclotron frequency). Thus if the wave frequency ω is near one of the Doppler shifted harmonics, $\omega \approx N'\Omega + k_z v_z$, the $N' = N$ term becomes the slowest term and has the dominant influence on the orbit evolution. At exact resonance, $\omega = N\Omega + k_z v_z$, this term is known as the secular term in resonance heating analyses [9,10]. Following a similar approach, we first define a trajectory:

$$v_x = v_\perp(t) \cos\left(\phi_0 + \psi(t) + \int_0^t \Omega' dt'\right), \quad v_y = v_\perp(t) \sin\left(\phi_0 + \psi(t) + \int_0^t \Omega' dt'\right),$$

$$x = x_0 + v_y/\Omega, \quad z = z_0 + \int_0^t v_z' dt',$$

where $\Omega' \equiv \Omega(t')$, $v_z' \equiv v_z(t')$, $\phi_0 = \tan^{-1}(v_{y0}/v_{x0})$. ψ is the time dependent phase varying slowly along with $v_\perp(t)$ due to interaction with the wave field. We substitute these relations into (2) and (3) and drop all fast oscillating terms in the Lorentz force. With the aid of

$$\exp(i\alpha \sin \phi) = \sum_{l=-\infty}^{\infty} J_l(\alpha) \exp(il\phi),$$

a set of self-consistent governing equations are derived for the slowly varying functions γ , v , v_z and ψ :

$$d\alpha/dt = \frac{1}{2} \delta_{n,N} (k_n/\Omega_0) (eE_0/m_0) (1 - k_z v_z/\omega) J_N'(\alpha) \cos \phi, \quad (4)$$

$$d\phi/dt = -\Delta\omega - \frac{1}{2} \delta_{n,N} (k_n/\Omega_0) (eE_0/m_0) (1 - k_z v_z/\omega) \alpha^{-1} (d/d\alpha) [\alpha J_N'(\alpha)] \sin \phi, \quad (5)$$

$$d\gamma/dt = \frac{1}{2} \delta_{n,N} (\Omega_0/\gamma k_n) (eE_0/m_0 c^2) \alpha J_N'(\alpha) \cos \phi, \quad (6)$$

and

$$dv_z/dt = \frac{1}{2} \delta_{n,N} (\Omega_0/\gamma^2 k_n) (eE_0/m_0 c^2) (k_z c^2/\omega - v_z) \alpha J_N'(\alpha) \cos \phi, \quad (7)$$

where

$$\alpha = k_n v_\perp/\Omega, \quad \delta_{n,N} = 1 + (-1)^{n+N}, \quad \phi = k_n(x_0 - a) + k_z z_0 + N(\phi_0 + \psi) - \int_0^t \Delta\omega(t') dt',$$

$$\Delta\omega = \Delta\omega_0 + N\Omega_0(\gamma - \gamma_0)/\gamma\gamma_0 - k_z(v_z - v_{z0}) = \Delta\omega_0 + (\omega_0 - k_z^2 c^2/\omega)(\gamma - \gamma_0)/\gamma\gamma_0,$$

$$\omega_0 = N\Omega_0/\gamma_0 + k_z v_{z0}, \quad \Delta\omega_0 = \omega - \omega_0 \quad \text{and} \quad \Omega_0 = eB_0/m_0 c = \gamma\Omega.$$

If $\Delta\omega_0 = 0$, it can be shown that the wave is suffering the cyclotron damping only and no instability can be excited. However, if $\Delta\omega_0 > 0$, i.e. initially there is a mismatch frequency between wave and gyrating electrons, those electrons that lose energy to the wave ($\gamma - \gamma_0 < 0$) tend to reduce the mismatch frequency so as to increase

the interaction period of losing energy to the wave. On the other hand, those electrons that gain energy from the wave ($\gamma - \gamma_0 > 0$) will then increase the mismatch frequency and reduce the period of gaining energy from the wave. On the average electrons will lose energy to the wave. Therefore, $\Delta\omega$ plays a role similar to the population inversion function in the two level system. This can be seen by defining a population inversion function $W = n_0 \gamma m_0 c^2 (\langle \Delta\omega \rangle + \Delta\omega_0) / 2\hbar\omega^2$ and the averaged polarization current density $J_p = -en_0(\Omega\alpha/k_n)\langle \cos \phi \rangle$, where n_0 is the average electron density and $\langle \rangle$ stands for an average over the initial random distribution.

From eq. (6) and the definition of $\Delta\omega = \Delta\omega_0 + (\omega_0 - k_z^2 c^2 / \omega)(\gamma - \gamma_0) / \gamma\gamma_0$, the population inversion equation is obtained as

$$dW/dt = (\delta_{n,N} / 4\hbar\omega) \gamma_0 (1 - k_z^2 c^2 / \omega_0^2) J'_N(\alpha) J_p E_0. \quad (8)$$

Since the effect of depletion of the rotational free energy of the electrons by the unstable wave is assumed to be insignificant in the present analysis, $E_0(t)$ and $\phi(t)$ are thus expected to vary with time much faster than other variables γ , α and v_z in (4)–(7). Neglecting the slow time variation of α and γ , eq. (6) is integrated to obtain γ_0 , which is then used to express $\Delta\omega$ as

$$\Delta\omega = \Delta\omega_0 + A_0 \int_0^t dt' E_0(t') \cos \phi', \quad (9)$$

where $A_0 = \beta_1 (e m_0 c) (\omega_0^2 - k_z^2 c^2) J'_N(\alpha) / \omega_0 \gamma_0^2$, $\beta_1 = v_1 / c$, $\phi' = \phi(t')$ and $\delta_{n,N} = 2$, $\gamma \approx \gamma_0$ and $\omega \approx \omega_0$ have been used.

From the definition of J_p , we obtain

$$J_p \approx en_0(\Omega_0 \alpha k_n \gamma_0) (\sin \phi \ddot{\phi} + \cos \phi \dot{\phi}^2).$$

In the following, we derive the explicit expression of $(\sin \phi \ddot{\phi} + \cos \phi \dot{\phi}^2)$, only the linear terms and the lowest order nonlinear terms will be included in the derivation. With the aid of (9), the time derivative of (5) becomes

$$\ddot{\phi} = -A_0 E_0 \cos \phi - D_0 (\sin \phi dE_0/dt - E_0 \Delta\omega \cos \phi) + \frac{1}{2} D_0^2 E_0^2 \sin 2\phi, \quad (10)$$

where

$$D_0 = (e \gamma_0 m_0 c \beta_1) (1 - k_z v_{z0} / \omega_0) (d/dt) [\alpha J'_N(\alpha)],$$

and $v_z \approx v_{z0}$ is assumed.

Taking the square of (5), yields

$$\dot{\phi}^2 = \Delta\omega_0^2 + A_0 (\Delta\omega + \Delta\omega_0) \int_0^t dt' E_0(t') \cos \phi' + 2D_0 \Delta\omega E_0 \sin \phi + D_0^2 E_0^2 \sin^2 \phi. \quad (11)$$

Thus,

$$\langle \sin \phi \ddot{\phi} \rangle \approx -\frac{1}{2} D_0 dE_0/dt + \frac{1}{2} D_0 E_0 \langle \Delta\omega \sin 2\phi \rangle + \frac{1}{4} D_0^2 E_0^2 \langle \cos \phi \rangle \quad (12)$$

and

$$\begin{aligned} \langle \cos \phi \dot{\phi}^2 \rangle \approx & \Delta\omega_0^2 \langle \cos \phi \rangle + A_0 \left\langle (\Delta\omega + \Delta\omega_0) \cos \phi \int_0^t dt' E_0(t') \cos \phi' \right\rangle + D_0 E_0 \langle \Delta\omega \sin 2\phi \rangle \\ & + \frac{1}{4} D_0^2 E_0^2 \langle \cos \phi \rangle, \end{aligned} \quad (13)$$

where the higher-order terms $\langle \cos 2\phi \rangle$, $\langle \sin 2\phi \rangle$ and $\langle \cos 3\phi \rangle$ have been neglected.

We further approximate

$$\begin{aligned}
\left\langle \sin \phi \int_0^t dt' E_0(t') \cos \phi' \right\rangle &= \frac{1}{2} \int_0^t dt' E_0(t') (\sin(\phi - \phi') + \sin(\phi + \phi')) \\
&\approx \frac{1}{2} \int_0^t dt' E_0(t') \sin \langle \Delta \omega \rangle (t - t') + \dots,
\end{aligned} \quad (14)$$

$$\begin{aligned}
\left\langle \sin 2\phi \int_0^t dt' E_0(t') \cos \phi' \right\rangle \\
\approx \frac{1}{2} \langle \sin \phi \rangle \int_0^t dt' E_0(t') \cos \langle \Delta \omega \rangle (t - t') + \frac{1}{2} \langle \cos \phi \rangle \int_0^t dt' E_0(t') \sin \langle \Delta \omega \rangle (t - t'),
\end{aligned} \quad (15)$$

and

$$\left\langle (\Delta \omega + \Delta \omega_0) \cos \phi \int_0^t dt' E_0(t') \cos \phi' \right\rangle \approx \frac{1}{2} (\langle \Delta \omega \rangle + \Delta \omega_0) \int_0^t dt' E_0(t') \cos \langle \Delta \omega \rangle (t - t'), \quad (16)$$

where $\langle \Delta \omega \rangle$ will be defined later.

With the aid of (14), we also have

$$\langle \sin \phi \dot{\phi} \rangle \approx -\Delta \omega_0 \langle \sin \phi \rangle - \frac{1}{2} A_0 \int_0^t dt' E_0(t') \sin \langle \Delta \omega \rangle (t - t') - \frac{1}{2} D_0 E_0, \quad (17)$$

from which we obtain

$$\langle \sin \phi \rangle \approx -\langle \sin \phi \dot{\phi} \rangle / \Delta \omega_0 = (A_0 / 2\Delta \omega_0) \int_0^t dt' E_0(t') \sin \langle \Delta \omega \rangle (t - t') - D_0 E_0 / 2\Delta \omega_0. \quad (18)$$

Substituting (18) into (15) and subsequently substituting (15) and (16) into (12) and (13), together with the aid of the relations $\langle \cos \phi \rangle = -(k_n / en_0 \Omega \alpha) J_p$ and $\langle \sin \phi \dot{\phi} \rangle = (k_n / en_0 \Omega \alpha) \dot{J}_p$, the explicit expression of $\langle \sin \phi \ddot{\phi} + \cos \phi \times \dot{\phi}^2 \rangle$ is then obtained, and the equation for the polarization current is derived as

$$\begin{aligned}
\ddot{J}_p + 2s\dot{J}_p + \Delta \omega_1^2 J_p &= \frac{a_0 \omega_0^2 \hbar W}{8\pi J'_N(\alpha) \gamma_0 n_0 m_0 c^2 \Delta \omega_0} \int_0^t dt' E_0(t') \cos \langle \Delta \omega \rangle (t - t') \\
&- \frac{S}{8\pi J'_N(\alpha)} \left(2c_0 E_0 + \frac{a_0}{\Delta \omega_0} \int_0^t dt' E_0(t') \sin \langle \Delta \omega \rangle (t - t') \right) - \frac{c_0}{8\pi J'_N(\alpha)} \frac{dE_0}{dt},
\end{aligned} \quad (19)$$

where

$$S = \frac{3\omega_0 c_0}{\gamma_0 \Delta \omega_0} \frac{(1 - k_z^2 c^2 / \omega_0^2) E_0}{32\pi \gamma_0 n_0 m_0 c^2} \int_0^t E_0(t') \cos \langle \Delta \omega \rangle (t - t') dt',$$

$$a_0 = 2(\omega_p^2 / \gamma_0^2 \omega_0) \beta_{\perp}^2 (\omega_0^2 - k_z^2 c^2) W_N(\alpha) \Delta \omega_0, \quad c_0 = (\omega_p^2 / \gamma_0 \omega_0) (\omega_0 - k_z v_{z0}) Q_N(\alpha),$$

$$\Delta\omega_1^2 = \Delta\omega_0^2 + \frac{4c_0}{\beta_1^2} \frac{Q_N}{W_N} \frac{(1 - k_z v_{z0}/\omega_0)E_0^2}{32\pi\gamma_0 n_0 m_0 c^2} + \frac{6\omega_0 c_0}{\gamma_0} \frac{(1 - k_z v_{z0}/\omega_0)E_0}{32\pi\gamma_0 n_0 m_0 c^2} \int_0^t dt' E_0(t') \sin \langle \Delta\omega \rangle (t - t'),$$

$\omega_p^2 = 4\pi n_0 e^2/m_0$, n_0 is the electron beam density averaged over the cross section of the guide, $W_N(\alpha) = J_N'^2(\alpha)$ and $Q_N(\alpha) = J_N'(\alpha)(d/d\alpha)[\alpha J_N'(\alpha)]$. This equation is analogous to the polarization equation of the laser medium.

Eqs. (8) and (19) describe the behavior of the electron beam in the presence of an electromagnetic field. In order to close the system of equations, it is necessary to include a field equation that takes into account the effects of the dynamical properties of the medium back on the field. Since eqs. (8) and (19) only include the field amplitude, energy conservation equation should be sufficient for the present analysis. Thus

$$n_0 m_0 c^2 d\langle \gamma \rangle/dt + (1/16\pi) dE_0^2/dt = 0. \quad (20)$$

From (8) and (20), the following relations are obtained:

$$\langle \Delta\omega \rangle = \Delta\omega_0 - \frac{(\omega_0 - k_z^2 c^2/\omega_0)E_0^2}{16\pi n_0 \gamma_0 m_0 c^2}. \quad (21)$$

$$W = \frac{n_0 \gamma_0 m_0 c^2}{\hbar \omega^2} \left(\Delta\omega_0 - \frac{(\omega_0 - k_z^2 c^2/\omega_0)E_0^2}{32\pi n_0 \gamma_0 m_0 c^2} \right), \quad (22)$$

and

$$4\pi \delta_{n,N} J_N'(\alpha) J_p = dE_0/dt. \quad (23)$$

Substituting (22) and (23) into (19), a nonlinear equation for the field amplitude $E_0(t)$ is obtained:

$$\frac{d^3 E_0}{dt^3} + 2s \frac{d^2 E_0}{dt^2} + (\Delta\omega_1^2 + c_0) \frac{dE_0}{dt} = a_0 \left(1 - \frac{\omega_0^2 - k_z^2 c^2}{\omega_0 \Delta\omega_0} \frac{E_0^2}{32\pi n_0 \gamma_0 m_0 c^2} \right) \int_0^t dt' E_0(t') \cos \langle \Delta\omega \rangle (t - t') \\ + s \left(2c_0 E_0 + \frac{a_0}{\Delta\omega_0} \int_0^t dt' E_0(t') \sin \langle \Delta\omega \rangle (t - t') \right). \quad (24)$$

If we drop the nonlinear terms and assume that $E_0(t) = E_0(0)e^{i\Gamma t}$ in (24), the linear dispersion relation is recovered

$$1 = \delta_{n,N} \frac{\omega_p^2}{\gamma_0 \omega_0} \left(\frac{\beta^2 \Delta\omega_0 (\omega_0^2 - k_z^2 c^2) W_N(\alpha)}{(\Gamma^2 + \Delta\omega_0^2)^2} - \frac{1}{2} \frac{(\omega_0 - k_z v_{z0}) Q_N(\alpha)}{(\Gamma^2 + \Delta\omega_0^2)} \right). \quad (25)$$

Thus we have derived a single equation which describes the nonlinear evolution of the field amplitude in electron cyclotron maser instabilities. This constitutes the main contribution of this paper. It can be shown that in (14), the field amplitude E_0 , including that which appeared in the coefficients, can be normalized to $\epsilon(\tau) = E_0(t)/(32\pi n_0 \gamma_0 m_0 c^2)^{1/2}$, a small quantity; and the time scale to $\tau = \Delta\omega_0 t$, a slow scale. Although the physics contained in eq. (14) is not immediately apparent and the complexity of the equation defies analytical solution, it nevertheless offers significant advantage in numerical work as compared with brute force particle simulation approach. Even after one first removes the fast field oscillations while dealing with a set of equations of a slow variable [e.g. eqs. (4)–(7) plus some relationship which closes the system], the savings in computational effort can still be significant.

As a comparison we integrated (14) numerically using the normalizations in E_0 and t mentioned earlier and the parameters of ref. [6]. The results are plotted in figs. 1a and 1b. Compared with those given by figs. 14 and 15

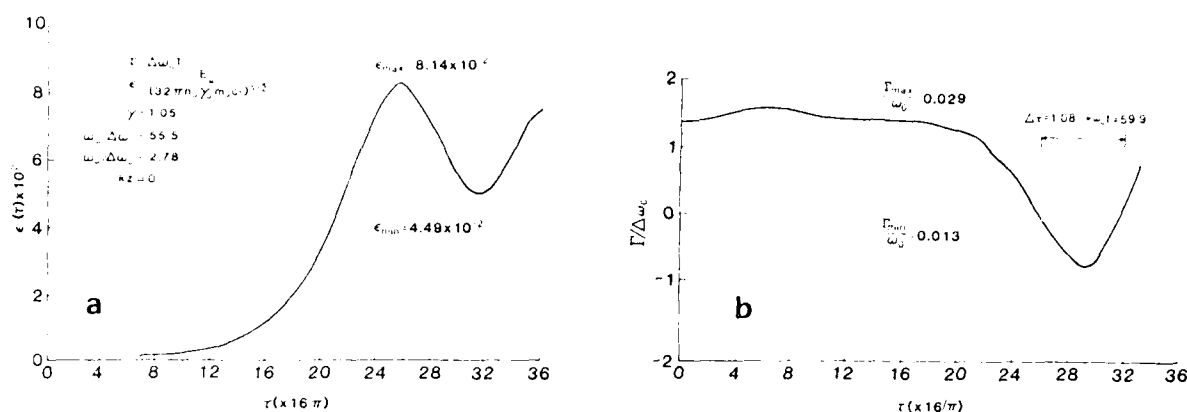


Fig. 1. (a) Radiation field amplitude evolving in time, $\epsilon_{\max} = 8.14 \times 10^{-2}$ and $\epsilon_{\min} = 4.49 \times 10^{-2}$ are in good agreement with the results of particle simulation. (b) Growth rate versus time.

of ref. [6], the agreement is remarkable. It is seen that the maximum values of the field and the growth rate, and the time between the two points when the growth rate is equal to zero given here agree with those shown by figs. 14 and 15 of ref. [6] to an accuracy as much as one may extract from the graphs. The main discrepancy between the two results appears at the value of ϵ_{\min} . This may be because only the lowest-order nonlinear terms in the phase expansion are included in the present approach. Thus the phase does not evolve reciprocally so that the effect of electrons regaining energy from the radiation field is less pronounced. Although this is a point of important physical interests, in operations of gyrotrons, such a regime should not be reached in practice. Thus one can expect to directly derive the power gain, the conversion efficiency and also the dynamic properties of the collective response of the electron beam to the excited wave fields from this single equation without relying on particle simulation.

Finally, we would like to comment on what difficulty one may encounter in dealing with this nonlinear differential-integral equation numerically. This we can do only based on our experiences. In the effort discussed above, we have employed a simple trapezoidal integration routine. Equal time steps Δt varying from $\pi/100$ to $\pi/1000$ have been used. The method is insensitive to the initial conditions. In fact during one computer run, an initial growth rate three times larger than the correct value was used. The field evolves and converges quickly to the correct values except during the initial period while still in the linear regime. The results t are also insensitive to the step size before numerical instabilities sets which occur some time after the growth rate Γ goes from negative to positive again. No serious effort beyond varying the step size was made to remedy this problem. We are not aware of any published results of particle simulation which are carried out to this extent.

We would like to acknowledge the contributions of Dr. Li-hsiang S. Cheo of William Paterson College in her numerical work and the discussions with her on the numerical instability problem. This work is supported by the Air Force Office of Scientific Research, Air Force Systems Command, U.S. Air Force, under Grant No. AFOSR-83-0001.

- [1] R.Q. Twiss, *Austr. J. Phys.* 11 (1958) 564.
- [2] J.L. Hirshfield and J.M. Wachtel, *Phys. Rev. Lett.* 12 (1964) 533.
- [3] V.L. Granatstein, M. Herndon, P. Sprangle, Y. Carmel and J.A. Nation, *Plasma Phys.* 17 (1975) 23.
- [4] V.L. Granatstein, P. Sprangle, R.K. Parker and M. Herndon, *J. Appl. Phys.* 46 (1975) 2021.
- [5] P. Sprangle and W.M. Manheimer, *Phys. Fluids* 18 (1975) 224.
- [6] P. Sprangle and A.T. Drobot, *IEEE Trans. MTT-25* (1977) 528.
- [7] K.R. Chu and J.L. Hirshfield, *Phys. Fluids* 21 (1978) 461.
- [8] Y.Y. Lau, *IEEE Trans. ED-29* (1982) 320.
- [9] S.P. Kuo and B.R. Cheo, *Phys. Fluids* 24 (1981) 784.
- [10] S.P. Kuo and B.R. Cheo, *Phys. Fluids* 26 (1983) 3018.

. APPENDIX 2.

Oscillating Two Stream Instability
of Ducted Whistler Pump

Oscillating two-stream instability of a ducted whistler pump

S. P. Kuo

Polytechnic Institute of New York, Long Island Center, Farmingdale, New York 11735

M. C. Lee

Regis College Research Center, Weston, Massachusetts 02193

(Received 25 October 1983; accepted 24 February 1984)

A magnetically field-aligned zero-frequency mode excited together with two lower hybrid sidebands by a ducted whistler pump is investigated. The thermal focusing force is found to be the dominant nonlinear effect on the excitation of large-scale instabilities; while the nonoscillatory beating current overrides the thermal focusing force in the short wavelength instabilities.

Applications of these studies to space and laboratory plasmas are discussed.

I. INTRODUCTION

Interest in the radio frequency (rf) heating of plasmas has stimulated extensive studies on the parametric instabilities driven by whistler pumps in either the ducted or non-ducted mode. The excited sideband modes may be electromagnetic waves¹⁻⁵ (i.e., the daughter whistler waves) or electrostatic waves⁶⁻⁸ (i.e., the lower hybrid waves) when the pump wave frequency is near the lower hybrid frequencies. In the former process the concomitant low-frequency mode can be an ion (or electron) acoustic wave or a shear Alfvén wave. The possible low-frequency modes discussed widely in the latter process include a backward ion cyclotron (or ion Bernstein) mode and a quasi-ion mode.

In this paper, we investigate the parametric excitation of a magnetically field-aligned zero-frequency mode together with two lower hybrid sidebands by a ducted whistler pump. This is the oscillating two-stream instability of a whistler pump analyzed by a four-wave interaction process. The influence of various nonlinear effects on this instability is evaluated. The thermal focusing force that results from the differential Ohmic heating of the whistler pump and the lower hybrid sidebands dominates in exciting this instability in the large-scale regime. However, the nonoscillatory beating current that is driven by the whistler pump field on the density fluctuations of lower hybrid sidebands overrides the thermal focusing force effect in the short-scale regime of the instability. In any case, the ponderomotive force (i.e., the radiation pressure force) does not have a significant effect on this instability as long as the phase velocity of the whistler pump far exceeds the electron thermal velocity.

The coupled mode equations for the lower hybrid sidebands and the field-aligned purely growing modes are derived in Sec. II. These modes are coupled through the whistler pump wave. A dispersion relation is obtained in Sec. III, where the relative importance of the nonlinearities contributed from the thermal focusing force, the ponderomotive force, and the nonoscillatory beating current is evaluated. The applications of our work to space plasma and laboratory plasma studies are discussed in Sec. IV with specific examples. Conclusions are finally drawn in Sec. V.

II. COUPLED MODE EQUATIONS

We consider the propagation of a ducted whistler wave in infinite, spatially uniform plasmas embedded in a uniform

magnetic field $\mathbf{B}_0 = \hat{z}B_0$,

$$\mathbf{E}_0 = \epsilon_0(\hat{x} + i\hat{y}) \exp[i(k_0 z - \omega_0 t)],$$

where ω_0 and k_0 are the angular wave frequency and wave-number, satisfying the dispersion relation

$$1 - [\omega_{pe}^2 / \omega_0(\omega_0 - \Omega_e)] = k_0^2 c^2 / \omega_0^2, \quad (1)$$

wherein ω_{pe} and Ω_e are the electron plasma frequency and the electron cyclotron frequency, respectively.

The zeroth-order velocity responses of electrons and ions to the whistler wave may be written as

$$\mathbf{v}_{0e,i} = \mp i(e\epsilon_0/m_{e,i})[(\hat{x} + i\hat{y})/(\omega_0 \mp \Omega_{e,i})], \quad (2)$$

where the subscripts e and i refer to electrons and ions and correspond to the $-$ and $+$ signs, respectively.

We now analyze a parametric process whereby the whistler pump wave excites two lower hybrid sidebands (ω_{\pm}, k_{\pm}) and a field-aligned purely growing mode ($\tilde{\omega}, k$). The wave frequency and wave vector matching relations for this four-wave interaction require that $\omega_+ - \omega_- = \omega_0 = \omega_- + \omega_+^*$ and $k_+ - k_- = k_0 = k_- + k$. We take $k = \hat{x}k$ and $\omega_i = i\gamma$ for the purely growing mode, where a positive γ is the linear growth rate. Then, the matching conditions become $\omega_{\pm} = \omega_0 + i\gamma = \omega$ and $k_{\pm} = \hat{z}k_0 \pm \hat{x}k$.

The lower hybrid sidebands are excited through the beating current density driven by the whistler pump field on the density perturbation of the purely growing mode. The coupled mode equation for these high-frequency sidebands can be derived from the following fluid equations for electrons and ions:

$$\mathbf{k}_{\pm} \cdot \mathbf{v}_{e\pm} = \omega(\delta n_{e\pm}/n_0) - (n_{s\pm}/n_0)\mathbf{k}_{\pm} \cdot \mathbf{v}_{0e}, \quad (3)$$

$$\tilde{\omega}\mathbf{v}_{e\pm} + i\Omega_e\mathbf{v}_{e\pm} \times \hat{z} = -\mathbf{k}_{\pm}(e/m_e)\phi_{\pm} + i\mathbf{v}_{e\pm} \cdot \mathbf{v}_{0e}, \quad (4)$$

$$\mathbf{k}_{\pm} \cdot \mathbf{v}_{i\pm} = \omega(\delta n_{i\pm}/n_0) - (n_{s\pm}/n_0)\mathbf{k}_{\pm} \cdot \mathbf{v}_{0i}, \quad (5)$$

and

$$\tilde{\omega}\mathbf{v}_{i\pm} - i\Omega_i\mathbf{v}_{i\pm} \times \hat{z} = (e/m_i)\mathbf{k}_{\pm}\phi_{\pm} + i\mathbf{v}_{i\pm} \cdot \mathbf{v}_{0e}. \quad (6)$$

Equations (3) and (4) [(5) and (6)] come from the linearized electron (ion) continuity equation and the electron (ion) momentum transfer equation, respectively. The variables, $\mathbf{v}_{e,i\pm}$, $\delta n_{e,i\pm}$ and ϕ_{\pm} , represent the velocity, density, and electric potential perturbations associated with the excited sidebands. Under the quasineutrality assumption (i.e., $n_e = n_i = n_s$), the density perturbation associated with the purely growing mode is denoted by n_s ($= n_{s+} = n_{s-}^*$). Here

$\bar{\omega} = \omega + iv_e$ in (4) and $\bar{\omega}_i = \omega + iv_i$ in (6), where v_e and $v_i = v_e (m_e/m_i)$ are the electron-ion and ion-electron collision frequencies, respectively. The thermal pressure terms have been neglected in (4) and (6), because we assume that $k^2 T_e/m_e \Omega_e^2$, $k_0^2 T_e/m_e \omega_0^2$, and $k^2 T_i/m_i \omega_0^2$ are much less than 1, where T_e and T_i are the electron and ion temperatures, respectively. Hence, the Landau damping effects may be ignored in our fluid description of plasma dynamics.

Solving (3)–(6) for $\delta n_{e,\pm}$ and $\delta n_{i,\pm}$ and substituting them into the Poisson's equation $k^2 \phi_{\pm} = 4\pi e(\delta n_{e,\pm} - \delta n_{i,\pm})$, we obtain the following coupled mode equations for the lower hybrid sidebands:

$$(\omega^2 - \omega_R^2 + iv_e \omega_R \omega_{lh} / \Omega_e \Omega_i) \phi_{\pm} = 4\pi e(\omega_R + iv_e) \omega_{lh}^2 \mathbf{k}_{\pm} \cdot (\mathbf{v}_{0i} - \mathbf{v}_{0e}) \mathbf{n}_{\pm} / k^2 \omega_{pi}^2, \quad (7)$$

where ω_{lh} is the lower hybrid resonance frequency defined by $\omega_{pi} / (1 + \omega_{pe}^2 / \Omega_e^2)^{1/2}$; $\omega_R = \omega_{lh} (1 + m_i k_0^2 / m_e k^2)^{1/2}$ is the dispersion relation for lower hybrid waves. The coupling term, arranged on the right-hand side of (7), shows that the driving sources for the lower hybrid sidebands are the beating currents produced by the interaction of the density perturbation n_{\pm} (i.e., the purely growing mode) with the pump driven velocities $\mathbf{v}_{0e,i}$.

The nonlinear effects responsible for the excitation of the purely growing mode include the thermal focusing force, the ponderomotive force, and the beating current driven by the whistler pump field on the density perturbations of the lower hybrid sidebands. Their relative importance, as discussed in Secs. IV and V, depends upon the scale lengths of the instability. All the nonlinear effects on electron and ion dynamics are included in the derivation of the coupled mode equation for the purely growing mode. This coupling equation can be derived from the following equations:

$$\gamma(n_s/n_0) + ik(\delta v_{ex} + \delta v_{ex}^*) = 0, \quad (8)$$

$$i\mathbf{F}_e = -ik(\delta T_e + T_e n_s/n_0) - e\mathbf{E}_s - m_e \Omega_e \delta \mathbf{v}_e \times \hat{\mathbf{z}} - m_e v_e (\delta \mathbf{v}_e - \delta \mathbf{v}_i), \quad (9)$$

$$\delta T_e = 2(H_e + 3v_i \delta T_i - iT_e k \delta v_{ex}) / 3\gamma_e, \quad (10)$$

$$\gamma(n_s/n_0) + ik(\delta v_{ix} + \delta v_{ix}^*) = 0, \quad (11)$$

$$\gamma m_i \delta \mathbf{v}_i + i\mathbf{F}_i = -ik(\delta T_i + T_i n_s/n_0) + e\mathbf{E}_s + m_i \Omega_i \delta \mathbf{v}_i \times \hat{\mathbf{z}} + m_e v_e (\delta \mathbf{v}_e - \delta \mathbf{v}_i), \quad (12)$$

$$\delta T_i = 2(H_i + 3v_i \delta T_e - iT_i k \delta v_{ix}) / 3\gamma_i. \quad (13)$$

Equations (8)–(10) [(11)–(13)] come from the linearized electron (ion) continuity equation, the electron (ion) momentum transfer equation, and the electron (ion) energy transfer equation, respectively. The electron inertia term is neglected in (9), but the ion inertia term is retained in (12). Here $\delta v_{e,i}$, $\delta T_{e,i}$ and $\mathbf{E}_s (= \hat{\mathbf{z}} E_s)$ are the velocity, temperature, and the electrostatic field perturbations caused by the purely growing mode. $\delta v_{e,i}^{\text{NL}} = (\delta n_{e,i}^* - v_{0e,i} \delta n_{e,i} + \delta n_{e,i} + v_{0e,i}^* \delta n_{e,i}) / n_0$ are the induced velocity perturbations due to the beating of the density perturbation of the lower hybrid sidebands and the velocity responses of electrons and ions in the whistler pump field. Here $\mathbf{F}_{e,i} = -im_{e,i} [\mathbf{v}_{0e,i} \cdot \nabla \mathbf{v}_{e,i}^* + \mathbf{v}_{e,i}^* \cdot \nabla \mathbf{v}_{0e,i} + \mathbf{v}_{0e,i}^* \cdot \nabla \mathbf{v}_{e,i} + \mathbf{v}_{e,i} \cdot \nabla \mathbf{v}_{0e,i} \pm (\Omega_{e,i} / B_0) (\mathbf{v}_{e,i}^* \times \mathbf{b}_0 + \mathbf{v}_{e,i} \times \mathbf{b}_0^*)]$ are the ponderomotive forces, where $\mathbf{b}_0 = -i(k_0 c / \omega_0) \mathbf{E}_0$ is

the whistler wave magnetic field. $H_{e,i} = 2m_{e,i} \mathbf{v}_{e,i} (\mathbf{v}_{0e,i} \cdot \mathbf{v}_{e,i}^* + \mathbf{v}_{0e,i}^* \cdot \mathbf{v}_{e,i})$ result from the differential ohmic heating of the whistler pump wave and the excited sidebands and give rise to the thermal focusing forces, $-\nabla(n_0 \delta T_{e,i})$. In (10) and (13), $\gamma_{e,i} = \gamma + 2v_i + v_{e,i} k^2 v_{te,i}^2 / \Omega_{e,i}^2$, where $v_{te,i} = (T_{e,i} / m_{e,i})^{1/2}$ are the electron and ion thermal velocities; v_{ii} is the ion-ion collision frequency.

We now proceed to derive the coupled mode equation for the purely growing mode from Eqs. (8)–(13). Subtracting (11) from (8) yields

$$\delta v_{ix} - \delta v_{ex} = \delta v_{ex}^{\text{NL}} - \delta v_{ix}^{\text{NL}}. \quad (14)$$

The x component of the resultant vector equation from the sum of (9) and (12) is

$$\gamma m_i \delta v_{ix} + i(F_{ex} + F_{ix}) = -ik(\delta T_e + \delta T_i + m_i c_s^2 n_s / n_0) + m_i \Omega_i (\delta v_{iy} - \delta v_{ey}), \quad (15)$$

where $c_s = [(T_e + T_i) / m_i]^{1/2}$ is the ion acoustic velocity. From (14) and the y component of (9), the expression for $(\delta v_{iy} - \delta v_{ey})$ in terms of δv_{ix} is obtained. Then, substituting it into (15) leads to

$$\delta v_{ix} = -i(v_e / m_i) \{ F_{ex} + F_{ix} + k(\delta T_e + \delta T_i + m_i c_s^2 n_s / n_0) - (\Omega_e / v_e) [F_{ey} + im_e \Omega_e (\delta v_{ix}^{\text{NL}} - \delta v_{ex}^{\text{NL}})] \} / (\Omega_e \Omega_i + v_e \gamma). \quad (16)$$

Eliminating $\delta T_{e,i}$ from (16) with the aid of (10) and (13) yields

$$P \delta v_{ix} = -iv_e \{ kc_s^2 n_s / n_0 + (F_{ex} + F_{ix} - \Omega_e F_{ey} / v_e) / m_i + (2k / 3m_i) [H_e / \gamma_e + H_i / \gamma_i + 2v_i (H_e + H_i) / \gamma_e \gamma_i] (1 - 4v_i^2 / \gamma_e \gamma_i) - i[(\Omega_e \Omega_i / v_e) + (2k^2 T_e / 3m_i \gamma_e) \times (1 + 2i / \gamma_i) / (1 - 4v_i^2 / \gamma_e \gamma_i)] (\delta v_{ix}^{\text{NL}} - \delta v_{ex}^{\text{NL}}) \}, \quad (17)$$

where $P = \Omega_e \Omega_i + v_e \gamma + (2k^2 v_e / 3m_i) [T_e / \gamma_e + T_i / \gamma_i + 2m_e v_e c_s^2 / \gamma_e \gamma_i] / (1 - 4v_i^2 / \gamma_e \gamma_i)$.

Combining (11) and (17) by eliminating δv_{ix} , we obtain the coupled mode equation for the purely growing mode

$$(\gamma P + v_e k^2 c_s^2) (n_s / n_0) = -(kv_e / m_i) (F_{ex} + F_{ix} - \Omega_e F_{ey} / v_e) - (2k^2 v_e / 3m_i) [H_e / \gamma_e + H_i / \gamma_i + 2v_i (H_e + H_i) / \gamma_e \gamma_i] / (1 - 4v_i^2 / \gamma_e \gamma_i) + i[(kv_e / m_i) \times [m_e \Omega_e^2 / v_e + (2k^2 T_e / 3\gamma_e) \times (1 + 2v_i / \gamma_i) / (1 - 4v_i^2 / \gamma_e \gamma_i)] \times (\delta v_{ix}^{\text{NL}} - \delta v_{ex}^{\text{NL}}) - kP \delta v_{ix}^{\text{NL}}]. \quad (18)$$

The right-hand side of (18) contains the coupling terms that have been grouped specifically into three terms corresponding, respectively, to the contribution of the three nonlinear effects, namely, the ponderomotive force, the thermal focusing force, and the beating current.

Equations (7) and (18) form the set of coupled mode equations that describe the coupling of lower hybrid sidebands and the purely growing mode through the whistler

pump wave. We are going to show that these coupled modes can become unstable when the pump field exceeds a threshold.

III. DISPERSION RELATION

With the aid of (2)–(6), the phasor amplitudes of $\delta v_{e,ix}^{nl}$, $F_{e,ix}$, F_{ey} , and $H_{e,i}$ are expressed in terms of ϕ_{\pm} as follows:

$$\delta v_{e,ix}^{nl} = i \left\{ (e/m_{e,i})^2 / \Omega_{1,2} \right\} \left\{ [k^2 / \Omega_{1,2}^2 \pm k_0^2 / (\omega_0^2 + \nu_e^2)] A - i(\nu_e / \omega_0) [k^2 / \Omega_e^2 \pm k_0^2 / (\omega_0^2 + \nu_e^2)] B \right\}, \quad (19)$$

where $A = \epsilon_0 \tilde{\phi}_{-}^{*} - \epsilon_0^{*} \tilde{\phi}_{+}$, $B = \epsilon_0 \tilde{\phi}_{-}^{*} + \epsilon_0^{*} \tilde{\phi}_{+}$, $\Omega_1 = \Omega_e$, $\Omega_2 = \omega_0$, and the quantities with a tilde represent the phasors of the associated perturbations.

$$\tilde{F}_{e,ix} = -im_{e,i} (e/m_{e,i})^2 (\omega_0 / \Omega_{1,2}) \left\{ [k^2 / \Omega_{1,2}^2 + \Omega_{e,i} k_0^2 / \omega_0 \times (\omega_0^2 + \nu_e^2)] B - i(\nu_e / \omega_0) \times [k^2 / \Omega_e^2 - \Omega_{e,i} k_0^2 / \omega_0 (\omega_0^2 + \nu_e^2)] A \right\}, \quad (20)$$

$$\tilde{F}_{ey} = im_e (e/m_e)^2 \{ (\nu_e / \omega_0) [2k^2 \omega_0^2 / \Omega_e^4 + k_0^2 / (\omega_0^2 + \nu_e^2)] B + i[k^2 / \Omega_e^2 - k_0^2 / (\omega_0^2 + \nu_e^2)] A \}, \quad (21)$$

$$\tilde{H}_{e,i} = -i(e/m_{e,i})^2 (2k\nu_e m_e / \Omega_{1,2}) [B \pm i(\nu_e / \Omega_e) A]. \quad (22)$$

From (7), we obtain the following two expressions for A and B , respectively:

$$A = 2(\nu_e / \omega_R) \left\{ (\omega_R^2 \omega_{th}^2 / \Omega_e \Omega_i) + (\omega_R^2 - \omega_0^2) \right\} [\omega_R \omega_{th}^2 \times (k_0^2 c^2 - \omega_0^2) / \omega_0 \omega_{pi}^2 k] |\epsilon_0|^2 (\bar{n}_i / n_0) / [(\omega_0^2 - \omega_R^2)^2 + \nu_e^2 \omega_R^2 \omega_{th}^4 / \Omega_e^2 \Omega_i^2], \quad (23)$$

$$B = -2i(\omega_0^2 - \omega_R^2 + \nu_e^2 \omega_{th}^2 / \Omega_e \Omega_i) \times [\omega_R \omega_{th}^2 (k_0^2 c^2 - \omega_0^2) / \omega_0 \omega_{pi}^2 k] |\epsilon_0|^2 \times (\bar{n}_i / n_0) / [(\omega_0^2 - \omega_R^2)^2 + \nu_e^2 \omega_R^2 \omega_{th}^4 / \Omega_e^2 \Omega_i^2]. \quad (24)$$

$$\gamma^2 + \gamma \nu_e \left\{ \frac{13}{3} \left(\frac{k^2 \nu_e^2}{\Omega_e^2} \right) + \left(\frac{\nu^*}{\nu_e \Omega_i \omega_0} \right) \left[(\omega_0^2 - \omega_R^2) \left(1 - \frac{k_0^2 \Omega_e}{k^2 \omega_0} \right) + \left(\frac{\nu_e^2 \omega_{th}^2}{\Omega_e \Omega_i} \right) \right] + \nu_e^2 \left(2 \left(\frac{k^2 \nu_e^2}{\Omega_e^2} \right)^2 - \left(\frac{4\nu^*}{3\nu_e \Omega_e \Omega_i} \right) \left[(\omega_0^2 - \omega_R^2) \left(1 - \frac{7}{4} \frac{k^2 \nu_e^2}{\Omega_e \omega_0} \right) + \left(\frac{\nu_e^2 \omega_{th}^2}{\Omega_e \Omega_i} \right) \right] \right\} \times \left[1 - \frac{k_0^2 \nu_e^2}{2\nu_e^2} \frac{\Omega_e}{\omega_0} \left(1 - \frac{k^2 \omega_0^2}{k_0^2 \Omega_e^2} + \frac{3}{2} \frac{k^2 \nu_e^2}{k_0^2 \Omega_e^2} \right) \right] \right\} = 0. \quad (26)$$

Setting $\gamma = 0$ in the dispersion relation leads to the threshold field intensities as

$$\epsilon_{th}^2 = \frac{1}{4} (m_e / e)^2 (k^2 \nu_e^4 \Omega_i / \omega_R \omega_{th}^2) \times \frac{[(\omega_0^2 - \omega_R^2)^2 + \nu_e^2 \omega_R^2 \omega_{th}^4 / \Omega_e^2 \Omega_i^2]}{[(\omega_0^2 - \omega_R^2)(h - j_1) + (\nu_e^2 \omega_{th}^2 / \Omega_e \Omega_i)(h + j_2)]}, \quad (27)$$

wherein the relation $(k_0^2 c^2 - \omega_0^2) \simeq \omega_0 \omega_{pe}^2 / \Omega_e$ from (1) has been used; h and j (j_1 and j_2) represent the contributions of nonlinear effects produced by the thermal focusing force, and the beating current, respectively. They are $h = 1$, $j_1 = 7 k^2 \nu_e^2 / 4 \Omega_e \omega_R$, and $j_2 = k^2 \nu_e^2 \omega_R / 2 \Omega_e \nu_e^2 \eta$, where

$$\eta = \left(1 + \frac{m_i}{m_e} \frac{k_0^2}{k^2} \right) \left(1 - \frac{m_i}{m_e} \frac{k_0^2}{k^2} \frac{\Omega_e^2}{\omega_{pe}^2} \right)^{-1}.$$

To simplify the problem, we assume that $\Omega_i \ll \omega_0 \ll \Omega_e$, $\nu_e \ll \Omega_e$, $\gamma \ll \omega_0$, $\nu_i \ll \omega_0$, and $\gamma \nu_e \ll \Omega_e \Omega_i$ in the following derivation of the dispersion relation. Then, it is seen that $|\delta v_{ix}^{nl}| \sim (m_e / m_i)^2 (\Omega_e / \omega_0)^3 |\delta v_{ex}^{nl}| \ll |\delta v_{ix}^{nl}|$, and $|H_i| \sim (\Omega_i^2 / \omega_0^2) |H_e| \ll |H_e|$. If $T_e \sim T_i$ is further assumed, the parameters, $\gamma_{e,i}$ and P in (18) may be approximated as $\gamma_i \simeq \gamma_e = \gamma + 2\nu_i + \frac{\nu_e k^2}{\nu_e^2 \Omega_e^2} \times \nu_e^2 / \Omega_e^2$ and $P \simeq \Omega_e \Omega_i + 2\nu_e k^2 c^2 / 3\gamma$, where $\gamma = \gamma + \nu_e k^2 \nu_e^2 / \Omega_e^2$. The dispersion relation is finally obtained by substituting Eqs. (19)–(24) into (18). It is

$$[\gamma \bar{\gamma} + \nu_e (k^2 c^2 / \Omega_e \Omega_i) (\bar{\gamma} + 2\gamma / 3)] (\Omega_e \Omega_i / \bar{\gamma} \nu^*) = (\omega_0^2 - \omega_R^2) \{ (4\nu_e / 3\bar{\gamma})_H + (k_0^2 \Omega_e^2 / k^2 \omega_0^2)_F - [(4\nu_e / 3\bar{\gamma}) (k^2 \nu_e^2 / \Omega_e \omega_0) + (\Omega_e / \omega_0)]_J \} + (\nu_e^2 \omega_{th}^2 / \Omega_e \Omega_i) \{ (4\nu_e / 3\bar{\gamma})_H - [(\Omega_e / \omega_0) + (4\nu_e / 3\bar{\gamma}) (k^2 \nu_e^2 / 2 \Omega_e \omega_0) \times (k_0^2 \Omega_e^2 / k^2 \nu_e^2 - \omega_0^2 / \nu_e^2)]_J \}, \quad (25)$$

where $\nu^* = 2\nu_e (m_e / m_i) k^2 (\omega_R \omega_{th}^2 / \omega_{pi}^2 \omega_0) [(k_0^2 c^2 - \omega_0^2) / \Omega_e^2] (e\epsilon_0 / m_e)^2 / [(\omega_0^2 - \omega_R^2)^2 + \nu_e^2 \omega_R^2 \omega_{th}^4 / \Omega_e^2 \Omega_i^2]$. We use the subscripts, H , F , and J , to indicate that the corresponding terms are contributed from the thermal focusing force, the ponderomotive force, and the nonlinear beating current, respectively.

In process of obtaining (25), it is found that while the ponderomotive force is additive to the thermal focusing force, the ponderomotive force and the nonlinear beating current effect are partially counterbalanced by each other. The relative importance of these nonlinear effects to be seen later depends upon the scale length of the excited field-aligned modes. The dispersion relation [Eq. (25)] is a quadratic equation of γ and can be written as

The beating current terms are the net results after having been partially balanced by the contribution of the ponderomotive force effect. The residual ponderomotive force effect is found to be negligibly small.

Since the right-hand side of (27) has to be positive, a criterion for the instability is drawn from its denominator as

$$\omega_0^2 \geq \omega_R^2 - (\nu_e^2 \omega_{th}^2 / \Omega_e \Omega_i) (b/a) \quad (28)$$

for $k^2 \nu_e^2 / \Omega_e \omega_R \leq 4/7$, where $a = 1 - 7k^2 \nu_e^2 / 4 \Omega_e \omega_R (= h - j_1)$, $b = 1 + k^2 \nu_e^2 \omega_R / 2 \Omega_e \nu_e^2 \eta (= h + j_2 \simeq j_2)$, and $\omega_0^2 \gg \nu_e^2$ has been assumed. The instability zone defined by (28) shows a scale-length dependence. Here ϵ_{th}^2 has a minimum, which occurs at

$$\omega_0^2 = \omega_m^2 \simeq \omega_R^2 + (\nu_e^2 \omega_{th}^2 / \Omega_e \Omega_i) \times \{ -b + [b^2 + (\omega_R^2 / \nu_e^2) a^2]^{1/2} \} / a. \quad (29)$$

The minimum threshold field is thus obtained by substituting (29) into (27), the result is

$$\epsilon_{th}^{(m)} = (3v_e/2\Omega_e)^{1/2} (m_e/e) k v_{te}^2 \times \{ [a^2 + (v_e b/\omega_R)^2]^{1/2} - \{v_e b/\omega_R\} \}^{1/2} / |a|. \quad (30)$$

The growth rate obtained by solving (26) is given by

$$\gamma \sim (6/13) v_e (k^2 v_{te}^2 / \Omega_e^2) [(E_0/E_{th}^{(m)})^2 - 1], \quad \text{for } (E_0/E_{th}^{(m)})^2 \ll 10, \quad (31)$$

$$\sim \sqrt{2} v_e (k^2 v_{te}^2 / \Omega_e^2) (E_0/E_{th}^{(m)}), \quad \text{for } (E_0/E_{th}^{(m)})^2 \gg 10. \quad (32)$$

It is of interest to determine the wavelength regime wherein the thermal focusing or beating current is the dominant nonlinear effect. This can be done by examining the denominator of (27) with the aid of (29). It is found that the thermal focusing effect becomes dominant when $k^2 v_{te}^2 / \Omega_e \omega_R \ll 1$ and $k^2 < (\Omega_e^2 / \omega_{pe}^2) (m_i/m_e) k_0^2$ (i.e., $\eta < 0$ and $b < 0$). In this regime (30) reduces to $\epsilon_{th}^{(m)} \sim (\sqrt{3}/2) (k^2 v_{te}^2 / \Omega_e) (m_e/e) \times [1 + (1 + 4\Omega_e^2 v_e^2 \eta^2 / k^4 v_{te}^4)^{1/2}]^{1/2} / |\eta|^{1/2}$ which decreases as the wavelength increases. However, the effect of nonlinear beating current overrides the thermal focusing effect as $k^2 > (\Omega_e^2 / \omega_{pe}^2) (m_i/m_e) k_0^2$ and $k^2 v_{te}^2 / \Omega_e v_e \gg 1$. In this regime the minimum threshold field becomes $\epsilon_{th}^{(m)} \sim (3/2)^{1/2} \times (m_e/e) v_e v_{te} |\eta|^{1/2}$, that is independent of both the wavelength and the magnetic field.

IV. APPLICATIONS

A. Space plasmas

The plasma in the upper atmosphere is weakly magnetized, namely, $\omega_{pe}^2 > \Omega_e^2$ and, therefore, $\omega_{th} \sim (\Omega_e \Omega_i)^{1/2}$. In this case study, we use the following topside ionospheric parameters: $\omega_{pe}/2\pi = 2.83$ MHz, $\Omega_e/2\pi = 1.1$ MHz, $v_{te} = 1.3 \times 10^5$ m/sec, m_e/m_i (O^+) = 3.4×10^{-5} and $v_e = 126$ Hz, where the value of v_e is computed from the formula $\omega_{pe} \times (2/\pi)^{1/2} \ln(16\pi^2 n_0^2 \lambda_D^6) / 24\pi_0 \lambda_D^3$, where n_0 and λ_D are the plasma density and the electron Debye length, respectively. According to (28) and (29), the pump wave frequency ($\omega_0/2\pi$) has to exceed 5.6 kHz for exciting the present decay process. When ($\omega_0/2\pi$) is greater than 17 kHz, the thermal focusing force is the dominant nonlinear effect since $\eta < 0$ in this case. For instance, let $\omega_0/2\pi = 18$ kHz, modes with scale lengths around 14 m can be generated. The threshold field intensity is about 0.23 (mV/m), that can be easily achieved at the altitude of 600 km with the available VLF transmitters at, for example, Siple. The growth rate, calculated from (32), is $\gamma \sim 0.056 \epsilon_0$ (sec^{-1}), where ϵ_0 is measured in (mV/m). On the other hand, the nonlinear beating current nonlinearity dominates if the pump wave frequency is set at, for example, 6 kHz. Then, modes with scale lengths around 3.2 m can be excited at the threshold field ~ 0.122 (mV/m) and with the growth rate $\sim 2\epsilon_0$ (sec^{-1}).

B. Laboratory plasmas

The following Alcator C parameters are adopted in our study of the oscillating two-stream instability of whistler

pumps in laboratory plasmas: $\Omega_e/2\pi = 280$ GHz (i.e., $B_0 = 1.0 \times 10^5$ G), $\omega_{pe}/2\pi = 200$ GHz (i.e., $n_0 = 5 \times 10^{20}$ m^{-3}), m_e/m_i (D^+) = 2.72×10^{-4} , $T_e = 1$ keV (i.e., $v_{te} = 1.3 \times 10^7$ m/sec), $\omega_{th} \sim 0.8\omega_{pe} \sim 2.64$ GHz, and $v_e = 7.7 \times 10^5$ Hz. It is found from (28) and (29) that if the nonlinear beating current or the thermal focusing force is the dominant nonlinearity for the instability depends upon if $\omega_0 < \omega_{pe} \sim 3.3$ GHz or $\omega_0 > \omega_{th}$ [$1 + (7m_i v_{te}^2 \omega_{pe}^2 / 4m_e \times c^2 \Omega_e^2) \eta^2$] $^{1/2} \sim 5.6$ GHz. The latter case is, however, not considered here since the required threshold field is found to be extremely high. Therefore, we choose $\omega_0/2\pi = 3$ GHz. The factor, $f = (k_0/k)^2 (m_i/m_e)$, that is computed from the frequency matching relation $\omega_0 = \omega_R = \omega_{th} (1 + f)^{1/2}$ has the value of 0.29. The scale length determined from $\lambda = (2\pi/k_0) \times (0.29 m_e/m_i)^{1/2}$ is 1.29×10^{-4} m.

In this case, since $(k^2 v_{te}^2 / \Omega_e v_e) \sim 2.8 \times 10^5$ and $(k_0^2 m_i \times \Omega_e^2 / k^2 m_e \omega_{pe}^2) \sim 1.6 \times 10^{-2}$, the beating current rather than the thermal focusing force certainly provides the dominant nonlinearity for the instability. The minimum threshold field is then

$$\epsilon_{th}^{(m)} \sim \sqrt{3/2} (m_e/e) v_e v_{te} |\eta|^{1/2} \sim 121 \text{ (V/m)}. \quad (33)$$

The corresponding growth rates are found to be

$$\gamma = \sqrt{2} v_e (k^2 v_{te}^2 / \Omega_e^2) (E_0/E_{th}^{(m)}) \sim 5.77 \times 10^6 \text{ (sec}^{-1}\text{)}. \quad (34)$$

The ϵ_0 in (34) is taken to be 3 (kV/m) (i.e., 0.1 esu/cm). The growth time of the instabilities defined by γ^{-1} is 0.173 μsec . Since these short-scale instabilities have large growth rates, they have the potential application to the rf heating of laboratory plasmas.

In this wavelength regime, the magnetic field has no effect on the threshold fields. This is because the scale lengths of these instabilities are much less than the ion gyro-radius ($\sim 2.7 \times 10^{-2}$ m). Therefore, the cross-field diffusion damping on the instabilities is not important as compared to the collisional damping. However, on the other hand, the excitation of the field-aligned modes relies on the cross-field mobility. The magnetic field reduces the cross-field mobility, whereas the collisions facilitate it. This may explain the dependence of the growth rates on collisions and the magnetic field as shown in (34).

The threshold for these instabilities is less by a large factor of $3(\omega_0/v_e)^{1/2}$ than that for the excitation of lower hybrid waves and quasi-ion modes.⁸ This fact indicates that purely growing modes can be produced much more easily than quasi-ion modes in laboratory plasmas by whistler pump waves.

V. CONCLUSION

A whistler pump wave may excite two lower hybrid sidebands and a magnetically field-aligned purely growing mode via the oscillating two-stream instability. This process is controlled by different nonlinear effects in the different scale-length regimes of the instability. The thermal focusing force provides the dominant nonlinearity for the instability with scale lengths greater than $2\pi v_{te} / (\Omega_e \omega_R)^{1/2}$ and $2\pi (m_e/m_i)^{1/2} c / (\Omega_e \omega_R)^{1/2}$. This thermal instability of whistler waves is expected to occur in ionospheric plasmas in the wave injection experiments performed at, for instance, Siple.

In contrast, the nonoscillatory beating current overrides the thermal focusing force in producing the short-wavelength-scale instability, namely, $\lambda < 2\pi v_{te}/(\Omega_e v_e)^{1/2}$ and $2\pi(m_e/m_i)^{1/2} c/(\Omega_e \omega_R)^{1/2}$. This short-wavelength-scale instability can be excited in the fusion plasma devices (for example, the Alcator C), and may become a potential candidate for rf heating of fusion plasmas. In either case, the ponderomotive force does not contribute a significant effect to the nonlinearity for this instability.

ACKNOWLEDGMENTS

This work was supported jointly in part by the National Science Foundation Grant No. ATM-8315322 and in part by the Air Force Office of Scientific Research Grant No.

AFOSR-83-0001 at Polytechnic Institute of New York and by the Air Force Geophysics Laboratory Contract No. 19628-83-K-0024 at the Regis College Research Center.

¹D. W. Forslund, J. M. Kindel, and E. L. Lindman, Phys. Rev. Lett. **29**, 249 (1972).

²K. F. Lee, Phys. Fluids **17**, 1343 (1974).

³A. I. Akhiezer, I. A. Akhiezer, R. V. Polovin, A. G. Sitenko, and K. N. Stepanov, *Plasma Electrodynamics* (Pergamon, New York, 1975), Vol. 1, p. 295.

⁴L. Chen, Plasma Phys. **19**, 47 (1977).

⁵S. N. Antani, D. J. Kaup, and P. K. Shukla, Phys. Fluids **26**, 483 (1983).

⁶J. M. Kindel, H. Okuda, and J. M. Dawson, Phys. Rev. Lett. **29**, 995 (1972).

⁷M. Porklab, Phys. Fluids **20**, 2058 (1977); and references therein.

⁸R. L. Berger and F. W. Perkins, Phys. Fluids **19**, 406 (1976).

APPENDIX 3.

Excitation of Upper Hybrid Waves by a
Thermal Parametric Instability

Excitation of upper-hybrid waves by a thermal parametric instability

By M. C. LEE

Regis College Research Center, Weston, Massachusetts 02193

AND S. P. KUO

Polytechnic Institute of New York, Long Island Center,
Farmingdale, New York 11735

(Received 15 March 1983 and in revised form 15 August 1983)

A purely growing instability characterized by a four-wave interaction has been analysed in a uniform, magnetized plasma. Up-shifted and down-shifted upper-hybrid waves and a non-oscillatory mode can be excited by a pump wave of ordinary rather than extraordinary polarization in the case of ionospheric heating. The differential Ohmic heating force dominates over the ponderomotive force as the wave-wave coupling mechanism. The beating current at zero frequency produces a significant stabilizing effect on the excitation of short-scale modes by counterbalancing the destabilizing effect of the differential Ohmic heating. The effect of ionospheric inhomogeneity is estimated, showing a tendency to raise the thresholds of the instability. When applied to ionospheric heating experiments, the present theory can explain the excitation of field-aligned plasma lines and ionospheric irregularities with a continuous spectrum ranging from metre-scale to hundreds of metre-scale. Further, the proposed mechanism may become a competitive process to the parametric decay instability and be responsible for the overshoot phenomena of the plasma line enhancement at Arecibo.

1. Introduction

In many cases of parametric instabilities excited by high-frequency electromagnetic waves in ionospheric heating experiments, the dominant nonlinear effect in the wave-wave interaction is produced by the differential Ohmic heating force rather than by the ponderomotive force (e.g. Fejer 1979; Gurevich 1978; Perkins, Oberman & Valeo 1974). The thermal effect generated by the electric field of the wave in collisional plasmas may drastically reduce the thresholds of the instabilities under favourable conditions.

The parametric wave process discussed in this paper is a thermal plasma instability triggered by electromagnetic waves. Since it involves a purely growing mode, a four-wave interaction process is analysed, including a pump wave, wave-vector up-shifted and down-shifted upper-hybrid waves, and a non-oscillatory mode. The differential Ohmic heating force is seen to dominate over the ponderomotive force as the primary mechanism for wave coupling. In addition,

the beating current at zero frequency is included as a nonlinear effect. This non-oscillatory beating current tends to weaken the effect of the differential Ohmic heating, i.e. to impede the excitation of the instability. The stabilizing effect of the non-oscillatory beating current is especially prominent in the generation of short-scale modes.

To begin with the analysis of a four-wave interaction in §2, a uniform medium theory is developed. The relevance of all the possible nonlinear effects in the wave-plasma interaction of interest is evaluated in §3. The criteria of the instability are investigated in §4 primarily for pump waves of ordinary and extraordinary polarization in the ionosphere. With the intention of applying the present theory to ionospheric heating experiments, we estimate in §5 the influence of ionospheric inhomogeneity on the instability and compare the theory with some experimental results.

2. A four-wave interaction

The four-wave interaction under consideration is a parametric instability excited by a high-frequency electromagnetic wave in a collisional, magnetized plasma (e.g. the ionosphere). Wave-vector up-shifted and down-shifted upper-hybrid modes and a purely growing mode are generated. The four-wave interaction may be represented by two sets of three-wave coupling as follows:

$$\begin{aligned}\omega_u &= \omega_i + \omega_0, & \mathbf{k}_u &= \mathbf{k}_i + \mathbf{k}_0, \\ \omega_0 &= \omega_i + \omega_d, & \mathbf{k}_0 &= \mathbf{k}_i + \mathbf{k}_d,\end{aligned}$$

where the subscripts 0, u , d , and i represent the pump wave, the up-shifted high-frequency mode, the down-shifted high-frequency mode, and the purely growing mode.

To simplify the problem, we assume that $k_0 = 0$ (thus, $\mathbf{k}_u = \mathbf{k}_i = -\mathbf{k}_d$) for a dipole pump field and $\omega_i = 0$ (thus, $\omega_u = \omega_0 = \omega_d$) for the non-oscillatory growing mode. This condition is achievable in the ionosphere, when an HF radio wave transmitted vertically from the ground reaches its reflexion height. A Cartesian system of co-ordinates is chosen with its z axis along the d.c. magnetic field. Its x axis coincides with the wave vectors of the excited field-aligned modes (i.e. $\mathbf{k}_i = \mathbf{k}_u = -\mathbf{k}_d = -k\hat{x}$). The purely growing mode is field aligned, because the concomitantly excited upper-hybrid modes are field-aligned in nature.

The coupled mode equation, which describes the process of exciting field-aligned high-frequency modes by scattering the pump wave off the low-frequency electrostatic density perturbations, can be derived from the electron continuity equation, the electron momentum equation, and the Poisson's equation:

$$\frac{\partial}{\partial t} n_e + \nabla \cdot n_e \mathbf{V}_e = 0, \quad (1)$$

$$m \left(\frac{\partial}{\partial t} + \mathbf{V}_e \cdot \nabla \right) \mathbf{V}_e = - \frac{\nabla p_e}{n_e} - e \mathbf{E} - \frac{e B_0}{c} \mathbf{V}_e \times \hat{z} = -v_{Te} m (\nabla_{\perp}^2 \mathbf{V}_e), \quad (2)$$

$$\nabla \cdot \mathbf{E} = -4\pi e n_e. \quad (3)$$

where $\nabla p_e = 3T_0 \nabla n_e$ and $\mathbf{V}_i = 0$ is set for high-frequency modes; e , m , n_e , T_0 , ν_e , \mathbf{V}_e , \mathbf{V}_i , \mathbf{E} and B_0 are electric charge, electron mass, electron density, unperturbed electron temperature, electron-ion collision frequency, electron velocity, ion velocity, electric field, and the d.c. magnetic field strength, respectively. As shown in Appendix A, if the excited field-aligned high-frequency waves are electrostatic modes (i.e. the upper-hybrid waves), the coupled-mode equation in a uniform medium is given by

$$\left(\frac{\partial}{\partial t} + \nu_e\right) \left(\frac{\partial^2}{\partial t^2} + \nu_e \frac{\partial}{\partial t} + \omega_p^2 - v_t^2 \nabla_\perp^2\right) \nabla_\perp^2 \Phi_1 + \Omega_e^2 \frac{\partial}{\partial t} \nabla_\perp^2 \Phi_1 \\ = \omega_p^2 \left[\left(\frac{\partial}{\partial t} + \nu_e\right) \nabla_\perp \cdot \left(\frac{\delta n_e}{n_0} \mathbf{E}_p\right) - \Omega_e \nabla_\perp \cdot \left(\frac{\delta n_e}{n_0} \mathbf{E}_p \times \hat{z}\right) \right], \quad (4)$$

where n_0 is the unperturbed plasma density, which is assumed to be constant; δn_e is the electron density perturbation due to the excited zero-frequency mode; $\Omega_e = eB_0/mc$ is the electron gyrofrequency; $\omega_p = (4\pi e^2 n_0/m)^{1/2}$ is the electron plasma frequency; $v_t = (3T_e/m)^{1/2}$ is the electron thermal velocity; $\mathbf{E}_p = \mathbf{E}_p \exp(-i\omega_0 t)$ is the dipole pump field; $\nabla_\perp^2 = \partial^2/\partial x^2 + \partial^2/\partial y^2$; and Φ_1 is the electrostatic potential of the upper-hybrid waves. The coupling terms on the right-hand side of (4), appearing as the driving source of the field-aligned high-frequency side-bands, originate in the nonlinear beating current. This current at the pump frequency is produced by the beating of the oscillating electron velocity in the pump field (\mathbf{E}_p) with the non-oscillating density perturbations (δn_e). If wave-like perturbations of the $\delta p = \delta \tilde{p} \exp[i(\mathbf{k} \cdot \mathbf{r} - \omega t)]$ type are assumed, the up-shifted and down-shifted modes and the zero frequency mode can be designated respectively by $\delta \tilde{p}_u \exp[-i(kx + \omega t)]$, $\delta \tilde{p}_d \exp[i(kx - \omega t)]$, and $\delta \tilde{p}_i \exp(\gamma t - ikx)$, where $\omega = \omega_0 + i\gamma$ and a positive γ represents the growth rate of the instability.

Substituting

$$\mathbf{E}_p = \tilde{\mathbf{E}}_p \exp(-i\omega_0 t), \quad \delta n_e = \delta \tilde{n}_e \exp(\gamma t - ikx), \\ \Phi_1 = \tilde{\Phi}_1 \exp[i(kx - \omega t)], \quad \text{and} \quad \Phi_2 = \tilde{\Phi}_2 \exp[-i(kx + \omega t)]$$

into (4) leads to

$$\Phi_1 = \frac{\omega_p^2}{k} [(\omega_0 + i\nu_e) E_{px} - i\Omega_e E_{py}] \frac{\delta n_e^*}{n_0} [(\omega_0^2 + \Omega_e^2) \nu_e + i\omega_0 \Gamma]^{-1}, \quad (5a)$$

$$\Phi_2 = -\frac{\omega_p^2}{k} [(\omega_0 + i\nu_e) E_{px} - i\Omega_e E_{py}] \frac{\delta n_e}{n} [(\omega_0^2 + \Omega_e^2) \nu_e + i\omega_0 \Gamma]^{-1}, \quad (5b)$$

where δn^* is the complex conjugate of δn ; E_{px} and E_{py} are the x and y components of \mathbf{E}_p ; $\Gamma = \omega_k^2 + \Omega_e^2 + \nu_e^2 - \omega_0^2$, where $\omega_k^2 = \omega_p^2 + k^2 v_t^2$. The subscripts 1 and 2 are used to represent the down shifted and up-shifted side bands respectively. All the tildes over the amplitudes of the perturbed quantities and the pump field have been omitted without causing any confusion. In obtaining (5a) and (5b), $\gamma \ll \omega_0$, ν_e have been assumed and can be justified.

To derive the dispersion relation, one more equation relating δn_e to Φ_1 and Φ_2 is needed. Both electron and ion kinetics have to be considered for the purely

growing mode (δn_e). In addition to (1) and (2), the following four equations are also employed to derive the coupled mode equation for the non-oscillatory mode:

$$\partial n_i / \partial t + \nabla \cdot n_i \mathbf{V}_i = 0, \quad (6)$$

$$M \left(\frac{\partial}{\partial t} + \mathbf{V}_i \cdot \nabla \right) \mathbf{V}_i = - \frac{\nabla p_i}{n_i} + e \mathbf{E} + \frac{e B_0}{c} \mathbf{V}_i \times \hat{z} + \nu_{in} \frac{m^* e}{n_i} (\mathbf{V}_e - \mathbf{V}_i) - \nu_{in} M \mathbf{V}_i, \quad (7)$$

$$\frac{\partial}{\partial t} T_e + \frac{2}{3} T_0 \nabla \cdot \mathbf{V}_e = \frac{2 \nabla}{3 n_e} \cdot (R_{\parallel}^e \nabla_{\parallel} + R_{\perp}^e \nabla_{\perp}) T_e - 2 \nu_e \frac{m}{M} (T_e - T_0) + \frac{2}{3} \nu_e m \langle v_e^2 \rangle, \quad (8)$$

$$\delta n_e \simeq \delta n_i = \delta n, \quad (9)$$

where $\nabla p_i = T_0 \nabla n_i$; M and ν_{in} are ion mass and ion-neutral collision frequency; $R_{\parallel}^e = 3 n_0 T_0 / 2 m \nu_e$ and $R_{\perp}^e = (\nu_e / \Omega_e)^2 3 n_0 T_0 / 2 m \nu_e$, where T_0 is the electron or ion temperature in thermal equilibrium; the angle brackets used in (8) indicate the time average over a time-scale of order of a few high-frequency periods. The electron energy equation is included, because differential Ohmic heating in electron gas contributes to the nonlinearity in generating the field-aligned purely growing modes. The derivation of this coupled mode equation is briefly described in the next section with a discussion of the various nonlinear effects which may be involved in the wave coupling of the proposed instability.

3. Nonlinear effects

3.1. Beating current at zero frequency

The linearized electron continuity equation can be written as

$$\gamma \delta n_e - i k n_0 \delta V_{ex} - i k \mathcal{J} = 0, \quad (10)$$

where $\mathcal{J} = \delta n_{e1}^* V_{px} + \delta n_{e2} V_{px}^*$ represents the beating current at zero frequency. This non-oscillatory beating current is driven by the pump field in the oscillating electron density perturbations of the excited high-frequency waves. In the appendix of Fejer (1979), a warning is addressed concerning the use of the low-frequency beating current term. This problem is examined in Appendix B, where we show that the paradox discussed in Fejer (1979) can be removed in our case.

3.2. Nonlinear Lorentz force and differential Ohmic heating force

Using the quasi-neutrality condition to combine the linearized electron and ion continuity equations, one obtains

$$\delta v_{ix} - \delta v_{ex} = (\delta n_{e1}^* v_{px} + \delta n_{e2} v_{px}^*) n_0^{-1}. \quad (11)$$

The x component of the combined linearized electron and ion momentum equations leads to

$$\delta v_{ix} = i k \left[(v_{px} v_{ix}^* + v_{px}^* v_{ix}) \frac{m}{M} + c_s^2 \frac{\delta n_e}{n_0} + \frac{\delta T_e}{M} \right] / v_{ex} + (\delta v_{ix} - \delta v_{ex}) \Omega_e / v_{ex}, \quad (12)$$

where $\tilde{v}_{in} = v_{in} + \gamma$, $c_s^2 = (T_e + T_i)/M = 2T_0/M$, and $\delta V_{ix} \gg \delta V_{ex} m/M$ has been assumed. The y component of the electron momentum equation gives

$$\delta v_{iy} - \delta v_{ey} = -\delta v_{ex} \frac{\Omega_e}{\tilde{v}_e} - (v_{px} v_{1y}^* + v_{px}^* v_{2y}) \frac{ik}{\tilde{v}_e}, \quad (13)$$

where $\tilde{v}_e = v_e + \gamma$.

Eliminating δv_{ix} and $(\delta v_{iy} - \delta v_{ey})$ from (11) and (12) yields

$$\delta V_{ex} = ik \left[\mathcal{F} + c_s^2 \frac{\delta n}{n_0} + \frac{\delta T_e}{M} \right] / \tilde{v}_{in} \left(1 + \frac{\Omega_e \Omega_i}{\tilde{v}_{in} \tilde{v}_e} \right) - n_0^{-1} \mathcal{J} / \left(1 + \frac{\Omega_e \Omega_i}{\tilde{v}_{in} \tilde{v}_e} \right), \quad (14)$$

where

$$\mathcal{F} = (v_{px} v_{1x}^* + v_{px}^* v_{2x}) m/M - (v_{px} v_{1y}^* + v_{px}^* v_{2y}) \Omega_i / \tilde{v}_e,$$

representing the nonlinear Lorentz force term, which is derived from the convective term of the electron momentum equation and is reduced to the ponderomotive force in the case of an unmagnetized plasma.

The perturbation of electron temperature (δT_e) in (14) can be obtained from the electron energy equation. It is

$$\delta T_e = \frac{2}{3} [ikT_0 \delta V_{ex} + \mathcal{H}] / [\gamma + 2\nu_e m/M + \frac{2}{3} R_{\perp}^2 k^2 / n_0], \quad (15)$$

where $\mathcal{H} = 2\nu_e m(\mathbf{v}_p \cdot \mathbf{v}_1^* + \mathbf{v}_p^* \cdot \mathbf{v}_2)$ is the differential Ohmic heating term arising from the electron energy dissipation in the high-frequency wave field.

Substituting (15) into (14) and, then, eliminating δv_{ex} from (10) and (14) yields the following result:

$$\delta n = A \{B\mathcal{F} + C\mathcal{H} + D\mathcal{J}\}, \quad (16)$$

where

$$A = \{[\gamma \Omega_e \Omega_i / \tilde{v}_e + k^2 c_s^2] [\gamma + 2\nu_e m/M + \frac{1}{3} k^2 r_e^2 \nu_e + \frac{1}{3} \gamma k^2 c_s^2]\}^{-1},$$

$$B = -k^2 n_0 [\gamma + 2\nu_e m/M + \frac{1}{3} k^2 r_e^2 \nu_e],$$

$$C = \frac{2}{3} (-k^2 n_0 / M),$$

$$D = ik \{(\Omega_e \Omega_i / \tilde{v}_e) [\gamma + 2\nu_e m/M + \frac{1}{3} k^2 r_e^2 \nu_e] + \frac{1}{3} k^2 c_s^2\},$$

where r_e and c_s are the electron gyroradius and the ion-acoustic velocity, respectively. \tilde{v}_e 's have been replaced by v_e 's in (16) since $v_e \gg \gamma$ is assumed.

3.3. The significance of nonlinearities

Equation (16) has been written in a form which expresses the contribution from different nonlinear effects to the excitation of zero-frequency plasma density perturbations. We now evaluate the significance of these nonlinear effects.

The perturbations of electron velocity and density ($\mathbf{v}_1, \mathbf{v}_2, \delta n_{e1}, \delta n_{e2}$) caused by the excited high-frequency modes and the electron velocity (\mathbf{v}_p) responding to the pump field can be obtained from (2) and (3). They are

$$\delta n_{e1}^* = -(k^2/4\pi e) \Phi_1^*, \quad \delta n_{e2} = -(k^2/4\pi e) \Phi_2,$$

$$\mathbf{v}_1^* = -(e/m) [\omega_0/(\omega_0^2 - \Omega_e^2)] k(1 + k^2/k_D^2) [1 + 2i\omega_0 \nu_e/(\omega_0^2 - \Omega_e^2)] \\ \times [(1 - i\nu_e/\omega_0) \hat{x} - i(\Omega_e/\omega_0) \hat{y}] \Phi_1^*.$$

$$\mathbf{v}_2^* = (e/m) [\omega_0/(\omega_0^2 - \Omega_e^2)] k(1 + k^2/k_D^2) [1 - 2i\omega_0 \nu_e/(\omega_0^2 - \Omega_e^2)] \\ \times [(1 + i\nu_e/\omega_0) \hat{x} + i(\Omega_e/\omega_0) \hat{y}] \Phi_2.$$

$$\begin{aligned} \mathbf{v}_p = & -i(e/m)[\omega_0/(\omega_0^2 - \Omega_e^2)][1 - 2i\omega_0\nu_e/(\omega_0^2 - \Omega_e^2)] \\ & \times \{[\hat{x}(1 + i\nu_e/\omega_0)E_{px} - i(\Omega_e/\omega_0)E_{py}] \\ & + \hat{y}[(1 + i\nu_e/\omega_0)E_{py} + i(\Omega_e/\omega_0)E_{px}]\} - i(e/m)\omega_0^{-1}(1 - i\nu_e/\omega_0)E_{pz}\hat{z}, \end{aligned}$$

where $k_D = \lambda_D^{-1} = (4\pi e^2 n_0/T_0)^{1/2}$ is the electron Debye wavenumber.

Substituting the above expressions into (16) gives the other coupled mode equation for the field-aligned mode,

$$\delta n = A\{F + H + J\}, \quad (17)$$

where

$$\begin{aligned} F = & -i(e^2 k^3/mM\omega_0^2)[\gamma + 2\nu_e m/M + \frac{1}{3}k^2 r_e^2 \nu_e](E_{px}\Phi_1^* + E_{px}^*\Phi_2), \\ H = & \frac{4}{3}i\nu_e(e^2 k^3/mM\omega_0^2)\{2i\Omega_e/\omega_0(E_{py}\Phi_1^* - E_{py}^*\Phi_2) - (E_{px}\Phi_1^* + E_{px}^*\Phi_2)\}, \\ J = & \frac{2}{3}(k^3 e^2/mM\omega_0^2)(k^2/k_D^2)\{[(2\Omega_e\nu_e/\omega_0^2)(E_{py}\Phi_1^* - E_{py}^*\Phi_2) - (E_{px}\Phi_1^* - E_{px}^*\Phi_2)] \\ & + i[(\nu_e/\omega_0)(E_{px}\Phi_1^* + E_{px}^*\Phi_2) + (\Phi_e/\omega_0)(E_{py}\Phi_1^* + E_{py}^*\Phi_2)]\}, \end{aligned}$$

corresponding to the nonlinear Lorentz force, the differential Ohmic heating force, and the non-oscillatory beating current, respectively. The ponderomotive force is seen to be less than the differential Ohmic heating force by a factor of $k^2 r_e^2$ for modes with scale lengths less than $\pi r_e(2M/m)^{1/2}$ and by a factor of m/M otherwise. Therefore, the contribution of the ponderomotive force is negligible in the generation of modes with scale lengths much larger than the electron gyroradius (r_e). In obtaining (17), $(k/k_D)^2 \ll 1$ has been assumed, i.e., the scale lengths of the excited modes are much larger than the electron Debye length, and $\omega_0^2 \gg \Omega_e^2 \gg \nu_e^2$ (this is true in ionospheric heating experiments in the F region).

The dispersion relation of the instability is finally obtained from (5a), (5b), and (17) as

$$\begin{aligned} & \{[\gamma + 2\nu_e m/M + \nu_e k^2 T_e/m\Omega_e^2][\gamma\Omega_e/\nu_e + k^2 c_s^2] + \frac{1}{3}\gamma k^2 r_e^2\} \\ & \times (\omega_0^2 \nu_e^2 + \Gamma^2)(3mM/4\nu_e^2 e^2 k^2) = \{2(\Gamma - \nu_e^2)|E_{px}|^2 + 4(\Omega_e^2/\omega_0^2)\Gamma|E_{py}|^2 \\ & + i(E_{px}E_{py}^* - E_{px}^*E_{py})(\Omega_e/\omega_0)(3\Gamma - 2\nu_e^2) - (E_{px}E_{py}^* + E_{px}^*E_{py}) \\ & \times (\Omega_e\nu_e/\omega_0)(\omega_0 + 2\Gamma/\omega_0)\}_H - \frac{1}{2}(2\pi\lambda_D/\lambda)^2\{2(\omega_0^2 + \Gamma)|E_{px}|^2 \\ & + 2\Omega_e^2|E_{py}|^2 + i(E_{px}E_{py}^* - E_{px}^*E_{py})(\Omega_e/\omega_0)(\Gamma + 2\omega_0^2) \\ & - (E_{px}E_{py}^* + E_{px}^*E_{py})\Omega_e\nu_e\}_J, \end{aligned} \quad (18)$$

where λ_D and λ are the electron Debye length and the scale length of the excited modes. The right-hand side of (18) is intentionally written to retain two terms labelled by H and J corresponding, respectively, to the original differential Ohmic heating term and the non-oscillatory beating current term. It is clear from (18) that the beating current tends to counterbalance the Ohmic heating effect.

Physically, this arises from the fact that the zero-frequency electrostatic mode is a nonlinearly driven mode, but not a normal mode. The induced non-oscillatory beating current imposes a stabilizing effect on the destabilization caused by the nonlinearity due to the differential Ohmic heating. This beating current is dependent on the scale lengths of excited modes. It is qualitatively clear from

(18) that shorter-scale modes are more significantly affected than larger-scale modes. A quantitative evaluation of this effect will be made after we specify the nature of the pump wave.

4. Conditions of the instability

4.1. Pump waves of ordinary polarization

Since HF radio waves of both ordinary and extraordinary polarization have been used as pump waves in ionospheric heating experiments, let us first consider the oblique incidence of an O-mode pump wave. By oblique incidence, we mean that, near its reflexion height, the O-mode pump wave does not propagate exactly perpendicular to the d.c. magnetic field. Consequently, there are perpendicular components of pump field, which can be approximately related as $E_{py} = -iE_{px}$. The dispersion relation for the case of obliquely incident O-mode heater waves can, therefore, be written as

$$\frac{1}{2}(mM/\nu_e e^2 k^2)(\omega_0^2 \nu_e^2 + \Gamma^2) \{ [\gamma + 2\nu_e m/M + \frac{1}{3}\nu_e k^2 r_e^2] [\gamma \Omega_e \Omega_i / \nu_e + k^2 c_s^2] + \frac{1}{3}\gamma k^2 c_s^2 \} \\ \simeq (1 - 2\Omega_e/\omega_0) [2\Gamma - 2\nu_e^2 - \omega_0^2 (2\pi\lambda_D/\lambda)^2] |E_{px}|^2. \quad (19)$$

The threshold power for exciting the instability can be determined from (19) by setting $\gamma = 0$. It is given by

$$|eE_{px}/m|_{th}^2 = \frac{1}{2}v_e^2(\omega_0^2 \nu_e^2 + \Gamma^2) [2m/M + \frac{1}{3}k^2 r_e^2] (1 - 2\Omega_e/\omega_0)^{-1} \\ \times [2\Gamma - 2\nu_e^2 - \omega_0^2 (2\pi\lambda_D/\lambda)^2]^{-1}. \quad (20)$$

Since the right-hand side of (19) or (20) has to be positive, it requires that

$$\Gamma > \nu_e^2 + \frac{1}{2}\omega_0^2 (2\pi\lambda_D/\lambda)^2. \quad (21)$$

The threshold power has a minimum value at

$$\Gamma = \Gamma_0 = a + (a^2 + \nu_e^2 \omega_0^2)^{\frac{1}{2}}, \quad (22)$$

where

$$a = \nu_e^2 + \frac{1}{2}\omega_0^2 (2\pi\lambda_D/\lambda)^2. \quad (23)$$

The minimum threshold power is given by

$$|eE_{px}/m|_{min}^2 = \frac{1}{2}v_e^2(\omega_0^2 \nu_e^2 + \Gamma_0^2) [2m/M + \frac{1}{3}k^2 r_e^2] (1 - 2\Omega_e/\omega_0)^{-1} (a^2 + \omega_0^2 \nu_e^2)^{-\frac{1}{2}}. \quad (24)$$

Note that the second term, $\frac{1}{2}\omega_0^2 (2\pi\lambda_D/\lambda)^2$, of the parameter a defined by (23) originates in the non-oscillatory beating current. If the following parameters are adopted: $\omega_0/2\pi = 6$ MHz, $\Omega_e/2\pi = 1.2$ MHz, $\nu_e = 1$ kHz, $\lambda_D = 0.5 \times 10^{-2}$ m (typical for the F region heating experiments), it is seen that

$$\Gamma_0 \simeq \nu_e \omega_0 \quad \text{for } \lambda \gg 2\pi\lambda_D(\omega_0/2\nu_e)^{\frac{1}{2}} \simeq 4m$$

and

$$|eE_{px}/m|_{min}^2 = \frac{1}{2}v_e^2 \omega_0 \nu_e [2m/M + \frac{1}{3}k^2 r_e^2] / [1 - 2\Omega_e/\omega_0] \quad (25a)$$

$$\Gamma_0 \simeq (2\pi\lambda_D/\lambda)^2 (\omega_0^2/2) \quad \text{for } \lambda < 2\pi\lambda_D(\omega_0/2\nu_e)^{\frac{1}{2}}$$

and

$$|eE_{px}/m|_{min}^2 = (\pi^2 \lambda_D^2 \nu_e^2 \omega_0^2 / \lambda^2) [2m/M + \frac{1}{3}k^2 r_e^2] / [1 - 2\Omega_e/\omega_0]. \quad (25b)$$

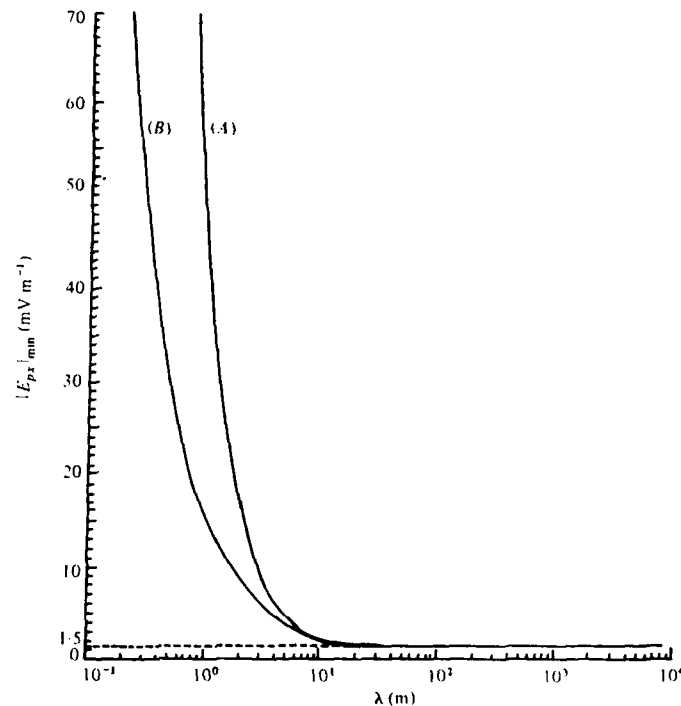


FIGURE 1. Threshold fields of the instability to excite field-aligned modes with a broad scale length ranging from tens of centimetres to a few kilometres in the ionosphere. Curves (A) and (B) correspond respectively to the results 25(b) and 25(a) obtained with and without the non-oscillatory beating current.

Note that $\Gamma_0 = \omega_p^2 + k^2 v_i^2 + \Omega_e^2 + \nu_e^2 - \omega_0^2$. Therefore, the stabilizing effect imposed by the non-oscillatory beating current can only affect the excitation of modes with scale lengths less than a few metres.

The excited field-aligned high-frequency modes can be identified from (25a) and (25b). In either case, $\omega_p^2 + k^2 v_i^2 + \Omega_e^2 + \nu_e^2 \simeq \omega_0^2$. This result shows that (i) the field-aligned high-frequency waves are upper-hybrid modes, (ii) a purely growing instability can be excited in an underdense plasma, i.e. $\omega_0 > \omega_p$.

Solving (19) for γ gives the growth rate of the instability

$$\gamma = \frac{1}{2} \nu_e \left\{ -b + \left[b^2 + \frac{8}{3} k^2 r_e^2 (b - \frac{8}{3} k^2 r_e^2) \left(\frac{|E_{px}|^2}{|E_{px}|_{\min}^2} - 1 \right) \right]^{\frac{1}{2}} \right\}, \quad (26)$$

where $b = 2m/M + \frac{1}{3} k^2 r_e^2$. The growth time of the instability can be defined as the period for the amplitude of excited modes to exceed their thermal level by five e -folds of magnitude, namely, $T_5 = 5\gamma^{-1}$. $|E_{px}|_{\min}$ (V m⁻¹) and T_5 (s) as a function of scale lengths (λ) are plotted, respectively, in figures 1 and 2 with the following parameters used: $m/M = 3.4 \times 10^{-5}$ (i.e. O^+ is the only ion species considered), $\nu_e = 1$ kHz, $\omega_0/2\pi = 6$ MHz, $v_i = 1.8 \times 10^5$ (m s⁻¹), $\Omega_e/2\pi = 1.2$ MHz, $r_e = 2.4 \times 10^{-2}$ m, and $|E_{px}| = 0.1$ V m⁻¹. The striking effect of the non-oscillatory beating current is to raise the thresholds and increase (decrease) the growth times (growth rates) of the instability for the short scale modes (i.e. $\lambda < 4$ m). This

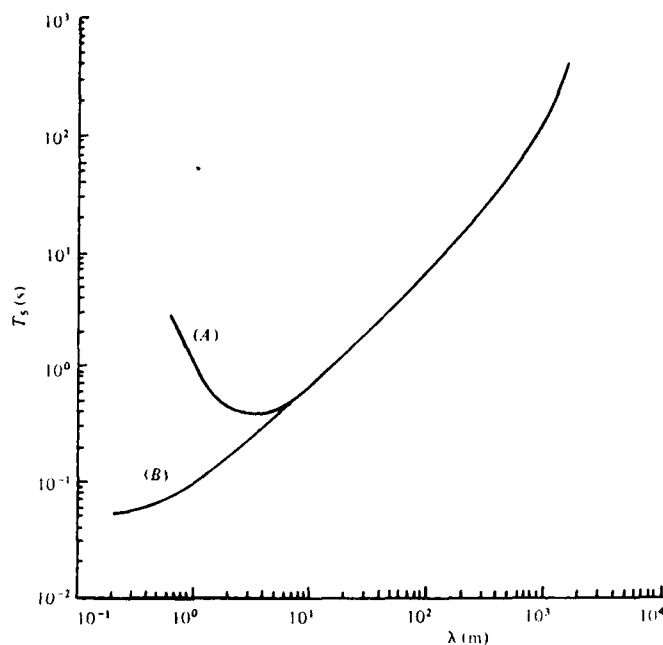


FIGURE 2. Growth times of the instability. Curves (A) and (B) correspond, respectively, to the cases with and without the non-oscillatory beating current in the analysis of the instability.

effect is so significant that a minimum (maximum) growth time (growth rate) of the instability is formed in the metre-scale range as shown in figure 2.

For λ larger than approximately 10 metres, $|E_{px}|_{\min}$ has a constant value of $1.5 \text{ (mV m}^{-1}\text{)}$. In other words, the minimum threshold power for exciting large-scale field-aligned modes by the present instability is independent of the scale lengths of the excited modes. However, the growth times (rates) of larger-scale modes are generally greater (less) than those of shorter-scale lengths. The results indicate that modes with large scale lengths (say, over 1 km) cannot be favourably excited by the present instability.

4.2. Pump waves of extraordinary polarization

In the case of X-mode pump waves, the corresponding dispersion relation can be similarly obtained from (18) with the substitution of $E_{py} = iE_{px}$. It is

$$\begin{aligned} & \{[\gamma + 2\nu_e m/M + \nu_e k^2 T_0/m\Omega_e^2][\gamma\Omega_e\Omega_i/\nu_e + k^2 c_s^2] + \frac{1}{3}\gamma k^2 c_s^2\} \\ & \times (\omega_0^2 \nu_e^2 + \Gamma^2) \frac{1}{2} m M / \nu_e e^2 k^2 \\ & = (1 + 2\Omega_e/\omega_0) [\Gamma - \nu_e^2 - \frac{1}{2}\omega_0^2 (k/k_D)^2] |E_{px}|^2. \end{aligned} \quad (27)$$

The positive right-hand side of (27) requires that

$$\Gamma = \omega_p^2 + k^2 \nu_i^2 + \Omega_e^2 + \nu_e^2 - \omega_0^2 > \nu_e^2 + \frac{1}{2}\omega_0^2 (2\pi\lambda_n/\lambda)^2.$$

If an HF X-mode radio wave is transmitted vertically into the ionosphere from the ground, $\omega_0 = \frac{1}{2}\Omega_e + \frac{1}{2}(\Omega_e^2 + 4\omega_p^2)^{\frac{1}{2}}$ at its reflexion height. Then,

$$\Gamma = \frac{1}{2}\Omega_e^2 + k^2 \nu_i^2 + \nu_e^2 - \frac{1}{2}\Omega_e(\Omega_e^2 + 4\omega_p^2)^{\frac{1}{2}}$$

cannot be positive in the ionosphere. Therefore, HF pump waves of extraordinary polarization transmitted vertically from the ground are not able to reach the upper-hybrid resonance zone to excite the present instability in the ionosphere.

However, extraordinary modes are accessible as pump waves to excite upper-hybrid waves, if they are incident upon the plasmas from either the higher-density side or the higher magnetic field side. The example for the former case is the incidence of pump waves from the topside of the ionosphere. The latter case is achievable in laboratory plasmas (Porkolab & Goldman 1976). The distinction between Porkolab & Goldman's results and ours centres on the different nonlinearities of the instabilities. The ponderomotive force plays a major role in exciting the instability in their case but only an insignificant role in ours as compared with the differential Ohmic heating force. The marked difference can be seen from the threshold fields of the instabilities. Ours (equation (20)) is considerably lower than Porkolab & Goldman's (their equation (A 10) by setting $\gamma = 0$) by a factor of $\frac{1}{2}[2m/M + \frac{1}{2}k^2r_e^2]/(1 - 2\Omega_e/\omega_0)$, which is much less than unity with the substitution of relevant parameters for ionospheric heating experiments.

5. Discussion

It is interesting to note that the ion-neutral collision term does not appear in the final expressions, although it has been included in the ion momentum equation. Ion-neutral collisions seem to have no direct effect on the excitation of field-aligned modes. A simple physical picture can be given as follows. The force experienced by ions is the non-oscillating self-consistent electric field

$$\mathbf{E}_s \propto \exp(\gamma t)$$

across the d.c. magnetic field (\mathbf{B}_0). Two drifts are caused by these crossed electric and magnetic fields, namely, a polarization drift (\mathbf{V}_p) along the direction of \mathbf{E}_s and an $\mathbf{E} \times \mathbf{B}$ drift (\mathbf{V}_D), where $\mathbf{V}_p = \gamma \mathbf{E}_s / \Omega_i B_0$ and $\mathbf{V}_D = \mathbf{E}_s \times \mathbf{B}_0 / B_0^2$. Ion-neutral collisions give rise to additional drifts anti-parallel to \mathbf{V}_p and \mathbf{V}_D . The resultant ion drift (\mathbf{V}_R) along the direction of \mathbf{E}_s has, therefore, three components: $\mathbf{V}_R = \mathbf{V}_p - \nu_{in} \mathbf{V}_p / \gamma + \mathbf{E}_s \times \mathbf{B}_0 / B_0^2$. The last term originates in ν_{in} , causing drift anti-parallel to \mathbf{V}_D . The apparent electric field associated with this drift is given by $\mathbf{E}_a = -\nu_{in} \mathbf{V}_D M / e$. The last two terms can be shown to cancel each other. This explains why ion-neutral collisions impose no net effect on the excitation of field-aligned modes.

The purely growing instability discussed in this paper is similar to the oscillating two-stream instability in unmagnetized plasmas (e.g. Nishikawa 1968) except that (i) the present process takes place in the underdense region (i.e. $\omega_0 > \omega_p$), rather than in the overdense region (i.e. $\omega_0 < \omega_p$); (ii) the differential Ohmic heating, rather than the ponderomotive force, is the dominant nonlinear effect. This parametric instability has been analysed in a uniform, magnetized plasma with application to ionospheric heating experiments. We now evaluate the influence of ionospheric inhomogeneity on the present instability, since ionospheric inhomogeneity tends to impede the excitation of HF wave-induced perturbations as indicated in Tromso experiments (Stubbe *et al.* 1982). The

importance of ionospheric inhomogeneity has been pointed out in the study of other parametric instabilities (e.g. Vaskov & Gurevich 1977; Grach *et al.* 1977; Das & Fejer 1979; Dysthe *et al.* 1983).

The effect of density inhomogeneity can be seen from (21), which determines the locations of the instability. Physically, (21) indicates that the upper-hybrid waves must be excited slightly off resonance. The location for the instability to have the minimum threshold field is given by (22). This height is only about 10 m above the upper-hybrid resonance layer (determined by $\Gamma = 0$) in the *F* region, where Γ is defined as $\omega_p^2 + \Omega_e^2 + k^2 v_t^2 + \nu_e^2 - \omega_0^2$. Let us assume a horizontally stratified ionosphere and the magnetic dip angle to be α . The excited field-aligned modes generally have a finite wave vector component k_m in the meridian plane, and thus a component $k_m \cos \alpha$ in the vertical direction. The modes excited near the upper-hybrid resonance layer can, therefore, extend to the stable region (i.e. below the $\Gamma = 0$ layer). Consequently, the nonlinear effect produced in the unstable region (i.e. above the $\Gamma = 0$ layer) is counterbalanced partially by that produced in the stable region. Higher thresholds for the instability are thus expected.

The effect of ionospheric inhomogeneity on the instability concerned can be estimated as follows. The instability zone extends from the upper-hybrid resonance layer up to the cut-off layer of the ordinary pump wave. This zone is about 5–6 km wide in the ionospheric *F* region. At heights distant from the upper-hybrid resonance layer, Γ is approximately equal to Ω_e^2 rather than $\nu_e \omega_0$ or $\frac{1}{2} \omega_0^2 (2\pi \lambda_D / \lambda)^2$ as given by (25a) or (25b). The threshold fields of the instability, therefore, increase by a factor of $\Omega_e / (\omega_0 \nu_e)^{1/2} \simeq 30$ for large-scale modes or by a factor of $\Omega_e (2\pi \lambda_D / \lambda)^{-1} (\omega_0 / 2)^{-1} \simeq 10 \lambda$ for $\lambda < 4m$. Since the minimum threshold fields shown in figure 1 are generally quite small, such field intensities may still be reasonably attainable in ionospheric heating experiments (cf. the pump field intensity $\simeq 1 \text{ V m}^{-1}$).

We have shown that the upper-hybrid waves can be excited in the ionospheric *F* region by ordinary but not by extraordinary heater waves transmitted vertically from the ground. These upper-hybrid waves, if excited in the ionosphere above Boulder, Colorado, may be detected by the VHF/UHF radars at White Sands Missile Range, New Mexico, and at Menlo Park, California. These plasma modes, termed 'field-aligned plasma lines', are found to have narrower spectral widths and stronger intensities than the plasma lines detected by the 430 MHz incoherent radar in the Arecibo experiments (Minkoff, Kugelmann & Weissman 1974; Carpenter 1974; Minkoff & Kreppel 1976). These striking distinctions result from the different origins of these plasma lines. The 'field-aligned' plasma lines (i.e. the upper-hybrid waves), excited together with zero frequency modes, are generated directly by the ordinary heater wave. The enhanced plasma lines detected by the Arecibo incoherent radar, on the other hand, stem from the scattering of unstable Langmuir waves and the ordinary heater wave off the thermal ion-acoustic waves (Fejer & Kuo 1973; Perkins *et al.* 1974), where the unstable Langmuir waves are produced by the ordinary heater waves via parametric decay instability.

Our proposed mechanism is effective in exciting not only short scale but also

large-scale ionospheric irregularities. A continuous spectrum with scale lengths ranging from a few metres to several hundreds of metres can be produced by this instability with threshold fields well below the incident pump field. With the background ionospheric inhomogeneity taken into account, the calculated growth times of short-scale irregularities (a few seconds) and those of large-scale irregularities (tens of seconds) are in general agreement with the experiments. Further, the prediction that metre-scale modes have maximum growth rates agrees with the observation that the largest backscatter radar cross-sections are associated with the excited metre-scale ionospheric irregularities (Rao & Thome 1974; Minkoff 1974).

Parametric decay instability can be excited in the ionosphere near the reflexion height of O-mode heater waves. Plasma line enhancement detected by the Arecibo incoherent radar has been attributed to the excitation of such an instability (Fejer & Kuo 1973; Perkins *et al.* 1974). Our analyses show that upper-hybrid waves can be generated at heights lower than that of parametric decay instability. The competition of the proposed instability with parametric decay instability may result in the 'overshoot' phenomena of plasma lines observed by Showen & Kim (1978) at Arecibo. The possible process is that the short-scale irregularities developed within seconds by the proposed instability at lower heights can scatter the heater waves and drastically reduce the pump intensity in the parametric decay instability zone. Finally, the applicability of the proposed instability should be pointed out. If the polarization vector of ordinary heater waves coincides exactly with the geomagnetic field, the instability proposed in this paper cannot be excited. This is because a perpendicular component of the wave field is the driving force of this instability. Therefore, ionospheric irregularities are not expected to be excited by the proposed instability at the equator. By contrast, this instability should operate efficiently at high latitudes.

This work was supported by AFGL contract F19628-83-K-0024 at Regis College Research Center and in part by NSF grant ATM-8114427, in part by Air Force Office of Scientific Research Grant AFOSR 83-0001 at Polytechnic Institute of New York.

Appendix A. Derivation of the coupled mode equation given by (4)

The coupled mode equation derived here describes the process of exciting high-frequency modes by scattering the pump waves off the low-frequency electrostatic density perturbations. Mathematically, the coupled mode equation relates the excited high-frequency perturbations to the pump wave field (E_p) and the low-frequency electron density perturbations (δn_e).

Since only electrons can respond quickly in high-frequency fields, the ion velocity term in the electron momentum equation (2) can be set to be zero. Taking the time derivative of (1) and substituting (2) into (1) to replace $\partial V_e/\partial t$ leads to

$$\frac{\partial^2 n}{\partial t^2} + \nu \frac{\partial n}{\partial t} - \frac{e\nabla}{m} \cdot (n\mathbf{E}) - \frac{\nabla^2 p}{m} - \Omega \nabla \cdot (n\mathbf{V} \times \hat{\mathbf{z}}) - \nabla \cdot [\nabla \cdot (n\mathbf{V}\mathbf{V})] = 0 \quad (\text{A } 1)$$

The subscript e has been dropped in (A 1) since no other species except electrons are considered.

To eliminate the $\nabla \cdot (n\mathbf{V} \times \hat{z})$ term in (A 1), the following equation is obtained from the summation of (2) $\times \hat{z}$ and (1) $\cdot (\mathbf{V} \times \hat{z})$:

$$\left(\frac{\partial}{\partial t} + \nu\right) n(\mathbf{V} \times \hat{z}) = \nabla \cdot [n\mathbf{V}(\mathbf{V} \times \hat{z})] - \frac{\nabla p \times \hat{z}}{m} - \frac{en}{m} \mathbf{E} \times \hat{z} + n\mathbf{V}_\perp \Omega. \quad (\text{A } 2)$$

Taking the $(\partial/\partial t + \nu)$ derivative of (A 2), with some manipulation one can obtain

$$\begin{aligned} \left[\left(\frac{\partial}{\partial t} + \nu\right)^2 + \Omega^2\right] n(\mathbf{V} \times \hat{z}) &= \left(\frac{\partial}{\partial t} + \nu\right) \nabla \cdot [n\mathbf{V}(\mathbf{V} \times \hat{z}) - \Omega \nabla \cdot (n\mathbf{V}\mathbf{V}_\perp)] \\ &\quad - \left(\frac{\partial}{\partial t} + \nu\right) \times \left(\frac{\nabla p \times \hat{z}}{m} + \frac{en}{m} \mathbf{E} \times \hat{z}\right) - \Omega \left(\frac{\nabla_\perp p}{m} + \frac{en}{m} \mathbf{E}_\perp\right). \end{aligned} \quad (\text{A } 3)$$

Taking the $[(\partial/\partial t + \nu)^2 + \Omega^2]$ derivative of (A 1) and then substituting (A 3) for $[(\partial/\partial t + \nu)^2 + \Omega^2] n(\mathbf{V} \times \hat{z})$ in (A 1) finally yields

$$\begin{aligned} \left[\left(\frac{\partial}{\partial t} + \nu\right)^2 + \Omega^2\right] \left[\frac{\partial^2 n}{\partial t^2} + \nu \frac{\partial n}{\partial t} - \frac{e\nabla}{m} \cdot (n\mathbf{E}) - \frac{\nabla^2 p}{m}\right] &+ \Omega^2 \left[\frac{\nabla_\perp^2 p}{m} + \frac{e\nabla}{m} \cdot (n\mathbf{E}_\perp)\right] \\ &+ \Omega \left(\frac{\partial}{\partial t} + \nu\right) \frac{e}{m} \nabla \cdot (n\mathbf{E} \times \hat{z}) = \left(\frac{\partial}{\partial t} + \nu\right)^2 \nabla \cdot [\nabla \cdot (n\mathbf{V}\mathbf{V})] + \Omega^2 \frac{\partial}{\partial z} [\nabla \cdot (n\mathbf{V}_z)] \\ &\quad - \Omega \left(\frac{\partial}{\partial t} + \nu\right) \nabla \cdot \nabla \cdot [n\mathbf{V}(\mathbf{V} \times \hat{z})]. \end{aligned} \quad (\text{A } 4)$$

All the terms on the right-hand side of (A 4) are negligible, because they represent the higher-order effects. After linearization, (A 4) can be written in the form

$$\begin{aligned} \left[\left(\frac{\partial}{\partial t} + \nu\right)^2 + \Omega^2\right] \left[\frac{\partial^2}{\partial t^2} n_i + \nu \frac{\partial n_i}{\partial t} - \frac{e\nabla}{m} \cdot (n_0 \mathbf{E}_i) - \frac{3T_e}{m} \nabla^2 n_i\right] \\ + \Omega^2 \left[\frac{3T_e}{m} \nabla_\perp^2 n_i + \frac{e\nabla}{m} \cdot (n_0 \mathbf{E}_i)\right] - \frac{\Omega e}{m} \left(\frac{\partial}{\partial t} + \nu\right) \nabla \cdot (n_0 \mathbf{E} \times \hat{z}) \\ = \frac{e}{m} \left[\left(\frac{\partial}{\partial t} + \nu\right)^2 + \Omega^2\right] \nabla \cdot (\delta n_s \mathbf{E}_p) \\ - \frac{e\Omega^2}{m} \nabla \cdot (\delta n_s \mathbf{E}_p) - \frac{e\Omega}{m} \left(\frac{\partial}{\partial t} + \nu\right) \nabla \cdot (\delta n_s \mathbf{E}_p \times \hat{z}), \end{aligned} \quad (\text{A } 5)$$

where \mathbf{E}_i , n_i , \mathbf{E}_p , and δn_s are the field of the excited high-frequency modes, the high-frequency electron density perturbations, the pump wave field, and the low-frequency electron density perturbations, respectively; ∇p has been replaced by $3T_e \nabla n_i$ in (A 5).

In the case of interest, the excited high-frequency modes are electrostatic waves propagating across the geomagnetic field (taken along the z axis), namely, $\mathbf{E}_i = -\nabla_\perp \Phi_i$. Then (A 5) reduces to

$$\begin{aligned} \left(\frac{\partial}{\partial t} + \nu\right) \left(\frac{\partial^2}{\partial t^2} + \nu \frac{\partial}{\partial t} + \omega_p^2 - v_i^2 \nabla_\perp^2\right) \nabla_\perp^2 \Phi_i + \Omega^2 \frac{\partial}{\partial t} \nabla_\perp^2 \Phi_i \\ = \omega_p^2 \left[\left(\frac{\partial}{\partial t} + \nu\right) \nabla \cdot \left(\frac{\delta n_s}{n_0} \mathbf{E}_p\right) - \Omega \nabla \cdot \left(\frac{\delta n_s}{n_0} \mathbf{E}_p \times \hat{z}\right)\right] \end{aligned} \quad (\text{A } 6)$$

This is the coupled mode equation given by (4) in the text. In obtaining (A 6), a uniform medium has been assumed and the Poisson's equation in the form of $n_i = (4\pi e)^{-1} \nabla_{\perp}^2 \Phi_i$ has been used.

Appendix B. Discussion on the beating current at zero frequency

A paradox is discussed in Fejer (1979) as a caution against the use of a low-frequency beating current term in the wave-plasma interaction. In the following discussion, we examine the correctness of the zero-frequency (i.e. non-oscillatory) beating current used in our work and show that the paradox discussed by Fejer does not exist in our case.

Let us first examine the non-oscillatory beating current in collisionless, unmagnetized plasmas. To employ the results in the text directly, we let $E_{py} = 0$ and then $\mathbf{E}_p \parallel \mathbf{k} = k\hat{x}$; where \mathbf{E}_p is the pump electric field, and \mathbf{k} is the wave vector of the excited modes. The non-oscillatory beating current, which appears in the electron continuity equation, is defined by

$$\mathbf{J}_b = n_{e1}^* \mathbf{V}_p + n_{e2} \mathbf{V}_p^* + \text{c.c.},$$

where $\mathbf{V}_p = -i(e/m) \mathbf{E}_p / \omega_0$ is the electron velocity responding to the pump field \mathbf{E}_p . This current is driven by the pump field \mathbf{E}_p in the oscillating electron density perturbations δn_{e1} , δn_{e2} of the excited Langmuir waves.

From Poisson's equation,

$$\delta n_{e1} = -(k^2/4\pi e) \Phi_1 \quad \text{and} \quad \delta n_{e2} = -(k^2/4\pi e) \Phi_2,$$

where Φ_1 and Φ_2 are obtained from the coupled mode equations (5a) and (5b), respectively, as

$$\Phi_1 = \frac{-i\omega_p^2}{k} \frac{1 - i\gamma/\omega_0}{\Gamma} E_p \frac{\delta n_e^*}{n_0}, \quad (\text{B } 1)$$

$$\Phi_2 = \frac{i\omega_p^2}{k} \frac{1 - i\gamma/\omega_0}{\Gamma} E_p \frac{\delta n_e}{n_0}, \quad (\text{B } 2)$$

where $\delta n_e = \delta \tilde{n}_e \exp(\gamma t - ikx)$ is the electron density perturbation due to the purely growing mode; n_0 , ω_p , ω_0 , γ are the unperturbed plasma density, the electron plasma frequency, the pump wave frequency, the growth rate of purely growing instabilities, and

$$\Gamma \equiv \omega_p^2 + k^2 v_i^2 + \Omega_e^2 + \nu_e^2 - \omega_0^2 = \omega_p^2 + k^2 v_i^2 - \omega_0^2$$

in collisionless, unmagnetized plasmas. An additional term, $i\gamma/\omega_0$, has been retained in (B 1) and (B 2) for exact consistency between Fejer's result and ours. In reality, this term is negligible in the case of collisional, magnetized plasmas considered in our work. To be consistent with Fejer's notation, we let

$$E_p = \frac{1}{2} i \tilde{E}_p \exp(-i\omega_0 t)$$

where \tilde{E}_p is real.

Then,

$$\delta n_{e1} = -\frac{k^2}{4\pi e} \frac{\omega_p^2}{k} \frac{1 - i\gamma/\omega_0}{\Gamma} \frac{\tilde{E}_p}{2} \exp(-i\omega_0 t) \frac{\delta \tilde{n}_e^*}{n_0} \exp(-ikx + \gamma t). \quad (\text{B } 3)$$

and

$$\delta n_{e2} = \frac{k^2}{4\pi e} \frac{\omega_p^2}{k} \frac{1 - i\gamma/\omega_0}{\Gamma} \frac{\tilde{E}_p}{2} \exp(-i\omega_0 t) \frac{\delta \tilde{n}_e}{n_0} \exp(-ikx + \gamma t). \quad (\text{B } 4)$$

The non-oscillatory heating current is, therefore, given by

$$J_b = \delta n_{e1}^* v_p + \delta n_{e2} v_p^* + \text{c.c.} = -\frac{1}{2} \frac{\gamma}{\omega_0} \sigma \frac{e \tilde{E}_p}{m \omega_0} \sin kx, \quad (\text{B } 5)$$

where $\sigma = (k/2\pi e)(\omega_p^2/\Gamma)(\delta \tilde{n}_e/n_0)e^{\gamma t}$. This result agrees with that obtained in Fejer (1979). The charge density (δn_h) of the excited Langmuir waves is

$$\delta n_h = \delta n_{e1} + \delta n_{e2} + \delta n_{e1}^* + \delta n_{e2}^* = -\sigma \sin kx (\sin \omega_0 t + (\gamma/\omega_0) \cos \omega_0 t), \quad (\text{B } 6)$$

which has the form of a standing wave.

We now show that the paradox discussed in Fejer (1979) can be removed if we consider a four-wave interaction process for purely growing modes wherein the charge density of the excited Langmuir waves has been shown to have a standing-wave format given by (B 6). Accordingly, we replace $\sigma_2 \sin(\omega_2 t - \mathbf{k}_2 \cdot \mathbf{p})$, which is the travelling-wave format used in Fejer (1979), by (B 6) for the charge density of the Langmuir waves in the oscillating frame. The charge density in the stationary frame is then

$$\begin{aligned} & -\sigma_2 \sin k_2 \rho \left(\sin \omega_2 t + \frac{\gamma}{\omega_2} \cos \omega_2 t \right) \\ & = -\sigma_2 \sin k_2 x \left(\sin \omega_2 t + \frac{\gamma}{\omega_2} \cos \omega_2 t \right) + \frac{\sigma_2 \cos k_2 x}{2} \frac{k_2 e \tilde{E}_p}{m \omega_1^2} \left\{ \cos(\omega_1 - \omega_2) t \right. \\ & \quad \left. - \cos(\omega_1 + \omega_2) t + \frac{\gamma}{\omega_2} [\sin(\omega_1 + \omega_2) t - \sin(\omega_1 - \omega_2) t] \right\}, \end{aligned}$$

which has the component,

$$\frac{\sigma_2 \cos k_2 x}{2} \frac{k_2 e \tilde{E}_p}{m \omega_1^2} \left[\cos(\omega_1 - \omega_2) t - \frac{\gamma}{\omega_2} \sin(\omega_1 - \omega_2) t \right]$$

at the frequency $\omega_1 - \omega_2$. This component, for $\omega_1 = \omega_2 = \omega_0$, leads to a non-oscillatory current density as

$$J_b = -\frac{1}{2} \frac{\gamma}{\omega_0} \sigma_2 \frac{e \tilde{E}_p}{m \omega_0} \sin k_2 x \quad (\text{B } 7)$$

which is derived from the continuity equation $\nabla \cdot \mathbf{J}_b + (\partial/\partial t) \delta n_h = 0$ and agrees with (B 5). If, on the other hand, the charge density of Langmuir waves,

$$-\sigma_2 \sin k_2 x (\sin \omega_2 t + (\gamma/\omega_2) \cos \omega_2 t),$$

is simply multiplied by the electron velocity induced by the pump wave,

$$\mathbf{v}_p = (e/m)(\tilde{E}_p/\omega_0) \cos \omega_0 t,$$

then the current density is obtained as

$$\begin{aligned} J_b = & -\frac{\sigma_2 \sin k_2 x}{2} \frac{e \tilde{E}_p}{m \omega_0} \left\{ \sin(\omega_2 + \omega_0) t + \sin(\omega_2 - \omega_0) t \right. \\ & \left. + \frac{\gamma}{\omega_2} [\cos(\omega_2 - \omega_0) t - \sin(\omega_2 + \omega_0) t] \right\}. \end{aligned}$$

For $\omega_2 = \omega_0$, the non-oscillatory current density is

$$J_b = -\frac{1}{2} \frac{\gamma}{\omega_0} \sigma_2 \frac{eE_p}{m\omega_0} \sin k_2 x,$$

which has the same form as that derived from the continuity equation shown in (B 7), and no paradox results.

In conclusion, the non-oscillatory beating current can be consistently derived in different ways, if we take into account the fact that the phase relation between the Langmuir waves and the pump wave is not random but uniquely determined by the coupled mode equations in our case. This is the key factor which determines the characteristic of the charge density of Langmuir waves, namely, the format of a standing wave rather than a travelling wave. The non-oscillatory beating current is, indeed, negligibly small in collisionless, unmagnetized plasmas as discussed above. However, collisions and the imposed magnetic field effect can change the phase relation between the excited Langmuir waves and the pump wave. Consequently, δn_h and V_p are no longer out of phase in collisional, magnetized plasmas. As shown in the text, the non-oscillatory beating current is found to be an important nonlinear phenomenon affecting the excitation of upper-hybrid modes and purely growing modes with short scale lengths.

REFERENCES

- CARPENTER, G. B. 1974 *Radio Sci.* **9**, 965.
 DAS, A. C. & FEJER, J. A. 1979 *J. Geophys. Res.* **84**, 6701.
 DYSTHE, K. B., MJØLHUS, E., PECSELI, H. L. & RYPDAL, K. 1983 *Phys. Fluids*, **26**, 146.
 FEJER, J. A. 1979 *Rev. Geophys. Space Phys.* **17**, 135.
 FEJER, J. A. & KUO, Y. Y. 1973 *AGARD Conf. Proc.* **138**, 11.
 GRACH, S. M., KARASHTIN, A. N., MITYAKOV, N. A., RAPOPORT, V. O. & TRAKHTENGERTS, V. YU. 1977 *Radiophys. Quantum Electron.* **20**, 1254.
 GUREVICH, A. V. 1978 *Nonlinear Phenomena in the Ionosphere (Physics and Chemistry in Space 10)*. Springer.
 MINKOFF, J. 1974 *Radio Sci.* **9**, 997.
 MINKOFF, J. & KREPPPEL, R. 1976 *J. Geophys. Res.* **81**, 2844.
 MINKOFF, J., KUGELMAN, P. & WEISSMAN, I. 1974 *Radio Sci.* **9**, 941.
 NISHIKAWA, K. 1968 *J. Phys. Soc. (Japan)*, **24**, 916.
 PERKINS, F. W., OBERMAN, C. & VALEO, E. J. 1974 *J. Geophys. Res.* **79**, 1478.
 PORKOLAB, M. & GOLDMAN, M. V. 1976 *Phys. Fluids*, **19**, 872.
 RAO, P. B. & THOME, G. D. 1974 *Radio Sci.* **9**, 987.
 SHOWEN, R. L. & KIM, D. M. 1978 *J. Geophys. Res.* **83**, 623.
 STUBBE, P., KOPKA, H., JONES, T. B. & ROBINSON, T. 1982 *J. Geophys. Res.* **87**, 1551.
 VASKOV, V. V. & GUREVICH, A. V. 1977 *Soviet Phys. JETP*, **46**, 487.

APPENDIX 4.

Relativistic Adiabatic Invariants of
Electron Motion under ECRH

Relativistic Adiabatic Invariants of Electron Motion Under ECRH

S. P. Kuo and B. R. Cheo

Polytechnic Institute of New York
Long Island Center
Farmingdale, New York 11735ABSTRACT

Three adiabatic invariants of the electron motion under electron cyclotron resonance heating have been derived. The relativistic effect has been included in the analysis. It is shown that the relativistic effect always tends to reduce the parallel energy of the electrons during the early stage of heating.

Heating of plasmas in the electron cyclotron frequency range appears to be a very promising method. This is due in part to the availability of a new type of powerful millimeter-wave source, the gyrotron [1], and in part to a successful demonstration of ECRH in fusion research devices [2,3]. Since the heating efficiency depends on the rate of net energy gain by electrons throughout the entire period of wave-electron interaction, the effectiveness of the ECRH process strongly relies on the resonance condition. However, the assumption of an exact resonance condition is impractical in reality, and since a small mismatch to the resonance condition may mean a strong deterioration in the heating efficiency, a better understanding of the ECRH process is needed in order to improve this resonance heating process to become more effective.

Several theories [4-11] have thus been developed to achieve this goal. In our previous study [5] it was found that the bouncing motion of electrons could serve to alleviate the detuning effect of frequency mismatch and efficient heating could be achieved. It was further shown that the heated electrons tended to focus themselves to the midplane of the bouncing motion configuration due to the interaction between electrons and the parallel component of the wave electric field. It worked to enhance the confinement of those electrons in an "equivalent" mirror trap. Our purpose in this letter is to present the relativistic effect on ECRH process. Three adiabatic invariants of electron motion under ECRH condition are derived, from which we have shown that on the average over the mismatch periods the relativistic effect always tends to reduce the parallel energy of the electrons during the early stage of heating, a similar feature to that caused by the bouncing motion of the electrons [5].

We study the problem from single particle approach. The nonlinear interaction of a single electron with a heating wave of ordinary mode near a cyclotron harmonic, $\omega \sim N\Omega$ is analyzed, where ω is the wave frequency, $\Omega = eB_0/\gamma mc$ is the relativistic electron cyclotron frequency, $\gamma = (1 + P^2/m^2 c^2)^{1/2}$ is the relativistic factor, B_0 is the background magnetic field, P is the momentum of the electron and N is an integer. The relativistic electron orbit equations are

$$\frac{d}{dt} \vec{r} = \vec{P}/\gamma m \quad (1)$$

$$\frac{d}{dt} \vec{P} = -e[\vec{E} + (\vec{P}/\gamma mc) \times (\vec{B} + \hat{z}B_0)] \quad (2)$$

where (\vec{r}, \vec{P}) are the spatial and the momentum coordinates of the electron, m is the rest mass, and \vec{E} and \vec{B} are the electromagnetic heating wave fields of ordinary mode, i.e., $\vec{E} = [\hat{z} - (k_z/k_\perp)\hat{x}]E$ and $\vec{B} = (c/\omega)\vec{k} \times \vec{E}$, where $E = \vec{E} \cos(k_\perp x + k_z z - \omega t)$ and $\vec{k} = \hat{x}k_\perp + \hat{z}k_z$. The energy equation of the electron is

$$mc^2 \frac{d}{dt} \gamma = -(e/\gamma m) \vec{E} \cdot \vec{P} \quad (3)$$

We first decompose Eq. (2) into axial and transverse components

$$\frac{d}{dt} P_z = -e(1 - \vec{k} \cdot \vec{v}/\omega)E + (k_z/\omega)mc^2 \frac{d}{dt} \gamma \quad (4)$$

$$\frac{d}{dt} P^- = (k_z/k_\perp)e(1 - \vec{k} \cdot \vec{v}/\omega)E - i\Omega P^- + (k_\perp/\omega)mc^2 \frac{d}{dt} \gamma \quad (5)$$

where Eq. (3) has been incorporated to obtain (4) and (5), and $P^- = P_x - iP_y$.

Equation (5) is then integrated formally to be

$$P^- = e^{-i \int_0^t \Omega' dt'} \left\{ P_0^- - e \int_0^t dt' e^{i \int_0^{t'} \Omega'' dt''} [(k_1 \vec{v}'/\omega) \cdot \vec{E}(t') - (k_z/k_1)(1 - \vec{k} \cdot \vec{v}'/\omega) E(t')] \right\} \quad (6)$$

where $P_0^- = P_{0x} - iP_{0y} = P_{01} e^{-i\theta_0}$, $\theta_0 = \tan^{-1}(v_{0y}/v_{0x})$ is the initial phase angle of electron in velocity space, $\Omega' = \Omega(t')$, $\Omega'' = \Omega(t'')$ and $\vec{v}' = \vec{v}(t')$.

Since the wave field \vec{E} itself depends on x and z , i.e., the solution of (1) and (2), therefore, it is useful to define a self-consistent trajectory prior to express (6) explicitly. Near the cyclotron harmonic resonance, i.e., $\omega - N\Omega$, only the slow time varying component of the integral on the RHS of (6) contributes to the resonance trajectory of the electron. One can then define such a set of self-consistent resonance trajectory as $v_x = v_1 \cos(\theta_0 + \psi + \int_0^t \Omega' dt')$, $v_y = v_1 \sin(\theta_0 + \psi + \int_0^t \Omega' dt')$, $x = x_0 + (v_y/\Omega)$ and $z = z_0 + \int_0^t v_z' dt'$, where $v_z' = v_z(t')$ is assumed to retain only those of slow time varying components, ψ is the nonlinear phase due to the resonance interaction, and $\psi(0) = 0$. Substituting this set of resonance trajectory into (3) - (5), the governing equations for the slow time-varying components of the variables γ , v_1 , v_z and ψ are derived to be

$$\frac{d}{dt} \alpha = (c\tilde{E}/B_0)(k_z - k_z^2 v_z/\omega)(N/\alpha) J_N(\alpha) \cos \varphi_N \quad (7)$$

$$\frac{d}{dt} \varphi_N = -\Delta\omega - (c\tilde{E}/B_0)(k_z - k_z^2 v_z/\omega)(N/\alpha) J_N'(\alpha) \sin \varphi_N \quad (8)$$

$$mc^2 \frac{d}{dt} \gamma = e\tilde{E}(k_z N\Omega/k_1^2 - v_z) J_N(\alpha) \cos \varphi_N \quad (9)$$

$$\frac{d}{dt} \gamma v_z = -(e\tilde{E}/m)(1 - k_z^2 N\Omega/k_1^2 \omega) J_N(\alpha) \cos \varphi_N \quad (10)$$

where $\alpha = k_{\perp} v_{\perp} / \Omega$, $\varphi_N = N(\theta_0 + \psi) + k_{\perp} x_0 + k_z z_0 - \int_0^t \Delta\omega(t') dt'$, $\Delta\omega = \omega - N\Omega - k_z v_z$, and $J_N(\alpha)$ and $J'_N(\alpha)$ are the Bessel function of order N and its derivatives, respectively.

Equations (7) - (10) are the characteristic equations for describing the resonance interaction between electrons and the ordinarily polarized heating wave. Two sources of detuning, one introduced by the motion of the particle guiding center as is manifested by the $k_z v_z$ term and another one comes from the relativistic effect $\Omega = \Omega(t)$, are included in the phase equation (8) in which the $\Delta\omega$ term accounts for the total detuning effect. These equations are all coupled to each other; however, three invariants of the motion can be determined and used for separating the coupling between each of the rate equations.

We now proceed to derive the adiabatic invariant relations from the characteristic equations (7) - (10). This will be done by taking the ratio of the two relevant equations among the four characteristic equations and then integrating the resultant ratio to obtain each invariant. Three independent combinations can be made and, hence, three invariant relations can be derived. We first take the ratio of (9) to (10), the result is then integrated to be

$$(\gamma v_z - k_z N \Omega_0 / k_{\perp}^2)^2 - c^2 (\gamma - N \Omega_0 k^2 / k_{\perp}^2 \omega)^2 = \text{constant in time} = A_1. \quad (11)$$

Similarly, from (7) and (9), yields

$$\gamma - (\omega / k^2 c^2) (k_z \gamma v_z + \Omega_0 \alpha^2 / 2N) = \text{constant in time} = A_2 \quad (12)$$

where A_2 is related to A_1 . The relationship is obtained by substituting (12) into (11) and using the relation $\gamma^2 = 1 + (\Omega_0 \alpha / k_{\perp} c)^2 + (\gamma v_z / c)^2 = 1 + P^2 / m^2 c^2$, the result is

$$A_1 = (k^2/k_{\perp}^2)(N\Omega_o/\omega) [2A_2 + (k_z^2/k_{\perp}^2)(\omega N\Omega_o/k^2 c^2) - (k^2/k_{\perp}^2)(N\Omega_o/\omega)] \quad (13)$$

The last invariant is obtained from (7) and (8) and it is

$$J_N(\alpha) \sin \phi_N - (k_z^2/k_{\perp}^2) [(\gamma v_z - \gamma_o v_{zo}) - (k_z^2 c^2 / 2N\Omega_o)(\Omega_o/k_{\perp} c)^2 (\alpha^2 - \alpha_o^2)] / v_q = \\ = \text{constant in time} = A_3 \quad (14)$$

where $v_q = e\tilde{E}/m\omega$.

We, therefore, have shown that the electron trajectory in the phase space of polar coordinates (α, ϕ_N) is governed by the invariant relation (14), which is coupled to the other two invariants (11) and (12). The second term on the LHS of (14) manifests the effect of detuning on resonance interaction, where the first term $(\gamma v_z - \gamma_o v_{zo})$ in the parenthesis is attributed to the relativistic effect and the second term in that arises from the oblique propagation of the heating wave (i.e. $k_z \neq 0$).

If we focus on relativistic detuning effect only and thus set $k_z = 0$, i.e., considering normal incidence case, the three invariants (11), (12), and (14) then reduce to

$$\gamma^2 v_z^2 - \gamma_o^2 v_{zo}^2 = c^2 (\gamma - \gamma_o)(\gamma + \gamma_o - 2N\Omega_o/\omega) \quad (15)$$

$$\gamma - \gamma_o = (\omega\Omega_o/2Nk^2 c^2)(\alpha^2 - \alpha_o^2) \quad (16)$$

and

$$J_N(\alpha) \sin \phi_N - (\gamma v_z - \gamma_o v_{zo}) / v_q = A_3 \quad (17)$$

respectively.

Without the second term on the LHS of (17), it reduces to the non-relativistic result $J_N(\alpha) \sin \phi_N = \text{constant in time}$ which shows that the result of resonance interaction is to change α and ϕ_N continuously and

simultaneously, following a closed contour in the polar $\alpha - \varphi_N$ coordinate space. However, the relativistic effect provides a coupling between v_{\perp} and v_z , as shown by (15) and (16), and also causes the detuning of resonance interaction. From the change of the electron cyclotron frequency with the energy, this effect can be expressed in a form as the second term on the LSH of (17). The continuous heating process then cannot be sustained. This effect, however, can be reduced by increasing the intensity of the heating wave (i.e., v_q). From the ratio of (15) to (16), the result of the ratio of parallel energy gain to the perpendicular energy gain for each electron is obtained as

$$(\gamma^2 v_z^2 - \gamma_o^2 v_{zo}^2) / (\gamma^2 v_{\perp}^2 - \gamma_o^2 v_{\perp o}^2) = \frac{1}{2N} \left(\frac{\Delta\omega_o}{\Omega(o)} + \frac{\Delta\omega}{\Omega} \right) \approx (\Delta\omega_o + \Delta\omega) / 2\omega \quad (18)$$

where $\Delta\omega = \omega - N\Omega_o / \gamma$ and $\Delta\omega_o = \Delta\omega(o)$. It shows that if $\Delta\omega_o + \Delta\omega < 0$, γv_{\perp} and γv_z change in a different way. Furthermore, if $\Delta\omega_o < 0$ and $\Delta\omega < 0$, i.e. $\Delta\omega_o \Delta\omega > 0$, then, during the period that the electron gains energy from the wave the mismatch frequency is also reduced so that the interaction period of gaining energy from the wave is increased. On the other hand, during that period when electron loses energy to the wave the mismatch frequency is increased and the period of losing energy to the wave is reduced. On the average over the mismatch period, the electron will then gain energy from the wave in this case. Since the change of $\gamma^2 v_z^2$ is a small fraction of the change of $\gamma^2 v_{\perp}^2$, we thus conclude that the relativistic effect will give rise to the perpendicular heating and simultaneously cause the parallel cooling. While in the case both $\Delta\omega_o > 0$ and $\Delta\omega > 0$, i.e. $\Delta\omega_o \Delta\omega > 0$, similar argument gives the conclusion that electron is losing energy to the wave on the average. Since γv_z and γv_{\perp} have to change in the same

manner, i.e., increase or decrease together, the result of the interaction between wave and electrons in this case is therefore also to reduce the parallel energy of the electrons on the average.

In both cases, $|\gamma v_z|$ is decreasing on the average, when $\Delta\omega_0 \Delta\omega > 0$. Since the condition $\Delta\omega_0 \Delta\omega > 0$ always holds in the beginning phase of heating, on the average the relativistic effect always tends to reduce the parallel energy of the electrons during this phase.

ACKNOWLEDGMENT

This work was sponsored by the Air Force Office of Scientific Research, Air Force Systems Command, U. S. Air Force, under Grant No. AFOSR-83-0001.

REFERENCES

- [1] Y. Carmel, K. R. Chu, M. Read, A. K. Ganguly, D. Dialens, R. Seeley, J. S. Levine, and V. L. Granatstein, Phys. Rev. Lett. 50 (1983) 112.
- [2] R. M. Gilgenbach, M. E. Read, K. E. Hackett, R. Lucey, B. Hui, V. L. Granatstein, K. R. Chu, A. C. England, C. M. Loring, D. C. Eldrige, H. C. Howe, A. G. Kulchar, E. Lazarus, M. Murakami and J. B. Wilgen, Phys. Rev. Lett. 44 (1980) 647.
- [3] R. A. Dandl, H. O. Eason and H. Ikegami, Oak Ridge National Laboratory Report, TM-6703 (1979).
- [4] S. P. Kuo and B. R. Cheo, Phys. Fluids 24 (1981) 784.
- [5] S. P. Kuo and B. R. Cheo, Phys. Fluids 26 (1983) 3018.
- [6] D. B. Batchelor, R. C. Goldfinger and H. Weitzer, IEEE Trans. Plasma Sci. PS-8 (1980) 78.
- [7] T. M. Antonson, Jr., and W. M. Manheimer, Phys. Fluids 21 (1978) 2295.
- [8] H. Weitzner and D. B. Batchelor, Phys. Fluids 23 (1980) 1359.
- [9] J. C. Sprott, Phys. Fluids 14 (1971), 15 (1972) 2247.
- [10] F. Jaeger, A. J. Lichtenberg, and M. A. Lieberman, Plasma Phys. 14 (1972) 1073.
- [11] M. A. Lieberman and A. J. Lichtenberg, Plasma Phys. 15 (1973) 125.

APPENDIX 5.

Earth's Magnetic Field Perturbations as
the Possible Environmental Impact
of the Conceptualized Solar
Power Satellite (SPS)

Earth's Magnetic Field Perturbations as the Possible Environmental Impact of the Conceptualized Solar Power Satellite

M. C. LEE

Regis College Research Center, Weston, Massachusetts

S. P. KUO

Polytechnic Institute of New York, Long Island Center, Farmingdale

It is predicted that the earth's magnetic field can be significantly perturbed locally by the microwave beam transmitted from the conceptualized solar power satellite (SPS) at a frequency of 2.45 GHz with incident power density of 230 W/m^2 at the center of the beam. The simultaneous excitation of earth's magnetic field fluctuations and ionospheric density irregularities is caused by the thermal filamentation instability of microwaves with scale lengths greater than a few hundred meters. Earth's magnetic field perturbations with magnitudes (\sim a few tens of gammas) comparable to those in magnetospheric substorms can be expected. Particle precipitation and airglow enhancement are the possible, concomitant ionospheric effects associated with the microwave-induced geomagnetic field fluctuations. Our present work adds earth's magnetic field perturbations as an additional effect to those such as ionospheric density irregularities, plasma heating, etc., that should be assessed as the possible environmental impacts of the conceptualized solar power satellite program.

1. INTRODUCTION

The solar power satellite (SPS) is a conceptualized energy proposal for the conversion of solar into microwave energy on a geostationary satellite (see Glaser [1977] for the details). The subsequent transmission of microwaves from the satellite toward the earth naturally gives rise to a concern of the possible environmental impacts of this bold large-scale energy program. The wave-ionosphere interaction assessed by the scientific community includes the substantial heating of the ionosphere and the generation of ionospheric density irregularities [Perkins and Rohle, 1978; Gordon and Duncan, 1978; Perkins and Goldman, 1981; Rush, 1981; Gordon and Duncan, 1983].

It is shown in this paper that earth's magnetic field can be significantly perturbed by the microwave beam of the SPS at the envisioned frequency of 2.45 GHz with the incident power density of 230 W/m^2 at the center of the beam. Large microwave-produced earth's magnetic field perturbations (δB) are associated with the simultaneous excitation of large-scale field-aligned ionospheric density irregularities (δn) via the thermal filamentation instability. This instability excited by the incident microwave generates an electromagnetic sideband mode and purely growing modes (δB and δn). This instability has been investigated for the cases of the HF ionospheric heating experiment [Kuo and Lee, 1983], the envisioned MF ionospheric heating experiment and the VLF wave injection experiment [Lee and Kuo, 1984]. In these three cases, the incident radio wave is described as either a right-hand (i.e., an R wave) or a left-hand (i.e., an L wave) circularly polarized wave. However, the ionosphere does not impose a significant effect of birefringence on microwave propagation and the microwave beam of SPS does not propagate generally along the earth's magnetic field.

The thermal filamentation instability of microwaves in the ionosphere is illustrated in section 2 with a physical picture that shows how the earth's magnetic field perturbations (δB) and the ionospheric density irregularities (δn) can be excited

simultaneously. Described in section 3 are the characteristics of the instability and the evaluation of the conditions for the simultaneous excitation of δB and δn in ionospheric E and F regions. The consequence of microwave-induced earth's magnetic field perturbations as the possible environmental impact of SPS is finally discussed in section 4 with a conclusion.

2. SIMULTANEOUS EXCITATION OF δB AND δn

In the transionospheric propagation of microwaves, plasmas generally experience two types of nonlinear force known as the ponderomotive force (or generally called the nonlinear Lorentz force) and the thermal pressure force due to the wave field interaction with charged particles. If the microwave field intensity is sufficiently large, a microwave sideband and purely growing modes associated with earth's magnetic field perturbations (δB) and ionospheric density irregularities (δn) can be excited by the thermal filamentation instability. The nonlinearity is dominantly contributed from the thermal pressure force rather than the ponderomotive force.

The thermal filamentation instability has been analyzed for radio waves in the HF band [Kuo and Lee, 1983] and in the MF as well as the VLF bands [Lee and Kuo, 1984]. The main characteristics of this instability are summarized as follows for a radio wave propagating along the earth's magnetic field as either an R or an L wave represented by

$$E_0(\mathbf{r}, t) = e_0(\hat{x} \pm i\hat{y}) \exp[i(k_0 z - \omega_0 t)] + \text{c.c.}$$

Here e_0 , k_0 , and ω_0 are the constant wave field amplitude, wave vector, and wave frequency, respectively; the \pm signs correspond to the R and the L wave modes. The earth's magnetic field or the wave propagation direction has been chosen to be the z axis of the rectangular coordinate system.

The excited sideband mode has the wave field given by

$$e_1 = (e_{1\perp} \cos ky + \hat{z} e_{1z} \sin ky) \exp(\gamma t)$$

where $\mathbf{k} = k\hat{y}$ is the filamentation wave vector and γ is the growth rate of the thermal filamentation instability. The excited purely growing modes have the general form of $\delta P = \delta \hat{P}(\cos ky) \exp(\gamma t)$ associated with the simultaneous generation of earth's magnetic field perturbations (i.e., $\delta \hat{P} = \hat{z} \delta \hat{B}$)

Copyright 1984 by the American Geophysical Union.

Paper number 4A1115.
0148-0227/84/004A-1115\$02.00

mass, the electric charge, the electron gyrofrequency, the ion plasma frequency, the ion-neutral collision frequency, the electron (ion) thermal velocity, and the ion acoustic velocity, respectively.

This dispersion relation can be much simplified when it is applied to the case of microwave-ionosphere interaction. The effect of ionospheric refringence on microwaves is relatively immaterial because the microwave frequency is larger than the electron gyrofrequency by three orders of magnitude. Therefore, (4) and (5) can be approximated by $P_{\perp} \approx 1$ and $q_{\pm} \rightarrow \pm \infty$, respectively. The polarization of the microwave is assumed to be within a meridian plane for the efficient excitation of field-aligned modes.

The threshold field and the growth rate derived from (3) for this case are given, respectively, by

$$\left| \frac{eE_{th}}{mc} \right| = 0.6 \frac{\omega_0}{\omega_{pe}} k V \left(2 \frac{m}{M} + \frac{k^2 V_t^2}{\Omega_e^2} \right)^{1/2} \quad (6)$$

and

$$\gamma = \left(\frac{1}{2} \right) [-a + (a^2 + 4b)^{1/2}] \quad (7)$$

where

$$a = 2v_e [(m/M) - (C_s \omega_{pe} \epsilon_0 / c \Omega_e \epsilon_{th})^2] \\ b = 8(\pi v_e C_s / \lambda \Omega_e^2) [(\epsilon_0 / \epsilon_{th})^2 - 1]$$

The threshold condition shown in (6) is determined by the energy balance between the driving (heat) source of the instability (i.e., the collisional dissipation of microwave pump and the excited sideband mode) and the damping processes denoted by the two terms: $2(m/M)$ and $k^2 V_t^2 / \Omega_e^2$. These two damping terms, appearing in the electron energy equation, represent the collisional damping of the heat source and the cross-field heat conduction loss, respectively. The former term dominates over the latter term if the scale length ($\lambda = 2\pi/k$) of the instability is larger than $(2M/m)^{1/2} \pi V_t / \Omega_e$; it is reversed otherwise. Since both the driving source and the damping processes are

caused by collisions, the threshold field of the instability given by (6) is independent of the collision frequency consequently. In contrast, the growth rate is proportional to the collisional frequency. This is because the collective oscillation (i.e., the field-aligned purely growing modes) relies on the cross-field mobility that is facilitated by collisions.

Our theoretical model, which is now applied to the study of microwave-ionosphere interaction, was originally formulated for wave beams with large cross sections propagating along the geomagnetic field in the ionosphere and in the magnetosphere. The inhomogeneity of the background plasma density can be reasonably ignored in our previous studies of VLF, MF, and HF cases because the proposed process becomes effective for modes with scale lengths less than the scale sizes of the background plasma density gradients by at least two orders of magnitude. However, the applicability of our model to the case of microwave-ionosphere interaction needs to be examined carefully because the microwave beam is about 10 km with a propagation angle (i.e., the angle between the axis of the microwave beam and the magnetic field) of, say, 45°. The inhomogeneity effect imposed by the microwave beam, i.e., the heat conduction along the magnetic field, cannot be neglected in this case. Therefore, the parallel scale length (λ_{\parallel}) has a given value of the order of the beam size (~ 10 km) rather than the scale size (~ 50 km) of the ionospheric density gradients, namely,

$$\lambda_{\parallel} = L / \cos \theta = 10 \text{ km} / \cos 45^\circ \sim 14 \text{ km}$$

where L and θ are the beam size and the beam wave propagation angle, respectively.

With the inclusion of a nonzero parallel wave number ($k_{\parallel} = 2\pi/\lambda_{\parallel}$), equation (2) is modified as follows:

$$\frac{\delta n_e}{n_0} \approx \left\{ 1 + \frac{v_e}{\gamma} \left(\frac{2\pi c}{\lambda_{\perp} \omega_{pe}} \right)^2 \left[1 + \frac{\Omega_e \Omega_i}{v_e v_{in}} \left(\frac{\lambda_{\perp}}{\lambda_{\parallel}} \right)^2 \right] \right\} \left(\frac{\delta B}{B_0} \right) \quad (2')$$

where λ_{\perp} and λ_{\parallel} are the perpendicular and the parallel scale lengths of the thermal filamentation instability. If the newly added factor, $[1 + (\Omega_e \Omega_i / v_e v_{in}) (\lambda_{\perp} / \lambda_{\parallel})^2]$, is much greater than unity, viz., $(\Omega_e \Omega_i / v_e v_{in}) (\lambda_{\perp} / \lambda_{\parallel})^2 \gg 1$, then the product of $(v_e / \gamma) (2\pi c / \lambda_{\perp} \omega_{pe})^2$ and $(\Omega_e \Omega_i / v_e v_{in}) (\lambda_{\perp} / \lambda_{\parallel})^2$ can greatly exceed unity and consequently, the geomagnetic field fluctuations may become insignificant. This situation occurs in the ionospheric region where $v_e v_{in}$ is rather small compared with $\Omega_e \Omega_i$.

The finite parallel wave number (k_{\parallel}) gives rise to a heat conduction loss along the earth's magnetic field that introduces a new term in equation (6) for the threshold condition of the instability, that is,

$$\left| \frac{eE_{th}}{mc} \right| \approx 0.6 \frac{\omega_0}{\omega_{pe}} k_1 v_i \left(2 \frac{m}{M} + \frac{k_{\perp}^2 v_i^2}{\Omega_e^2} + \frac{k_{\parallel}^2 v_i^2}{v_e^2} \right)^{1/2} \quad (6')$$

The third term in the parentheses corresponds to the parallel heat conduction loss. As mentioned before, $2m/M \gg k_{\perp}^2 v_i^2 / \Omega_e^2$ for the excitation of modes with $\lambda_{\perp} \gg (2M/m)^{1/2} \pi v_i / \Omega_e \sim 11$ m, for instance, for the F region parameters: $M(O^+)/m = 16 \times 1840$, $v_i = 1.3 \times 10^5$ m/s (i.e., $T_e \sim 1000$ K), and $\Omega_e / 2\pi = 1.4$ MHz. However, $k_{\parallel}^2 v_i^2 / v_e^2$ may be significantly larger than $2m/M$ for a small v_e . The threshold condition (6') in such a case is thus determined primarily by the parallel heat conduction loss and it can lead to a highly stringent condition for the instability.

We examine the effects of a finite parallel wave number on the proposed mechanism in the ionospheric F and E regions separately. For $\lambda_{\parallel} = 14$ km and the typical F region parameters: $M(O^+)/m = 16 \times 1840$, $v_i = 1.3 \times 10^5$ m/s (i.e., $T_e \sim$

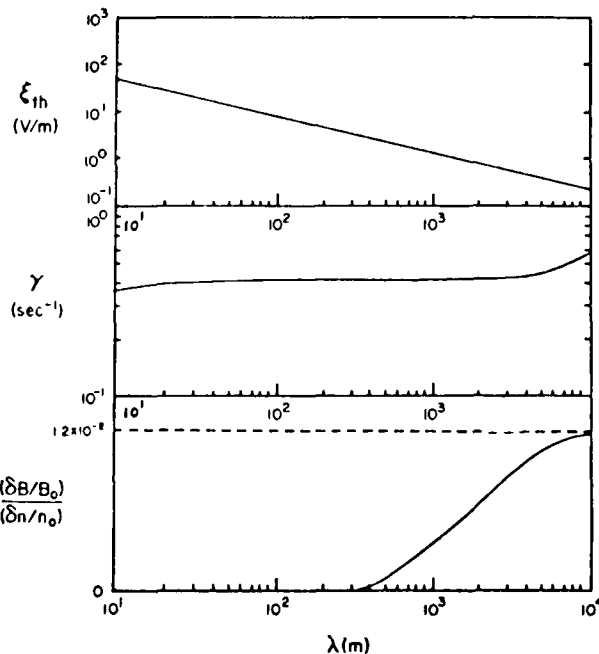


Fig. 3. The threshold field (ϵ_{th}), the growth rate (γ), and the ratio of $(\delta B/B_0)$ to $(\delta n/n_0)$ as a function of the scale length (λ).

1000 K), $\Omega_e/2\pi = 1.4$ MHz, $\omega_{pe}/2\pi = 6$ MHz, $v_{in} = 0.5$ Hz, and $v_e = 500$ Hz, $k_{\perp}^2 v_i^2 / v_e^2$ ($\sim 1.36 \times 10^{-2}$) is much greater than $2m/M$ ($\sim 6.8 \times 10^{-5}$). The parallel heat conduction loss, therefore, enhances the threshold field by a factor of $(k_{\parallel} v_i / v_e)(M/2m)^{1/2} \sim 14.2$. The new factor in (2') is

$$[1 + (\Omega_e \Omega_i / v_e v_{in})(\lambda_{\perp} / \lambda_{\parallel})^2] \sim 1.34 \times 10^4$$

for $\lambda_{\perp} = 500$ m. With this large factor, (2') can be approximately expressed as

$$\delta n/n_0 \approx [1 + (\Omega_e \Omega_i / \gamma v_{in})(2\pi c / \lambda_{\parallel} \omega_{pe})^2](\delta B/B_0) \\ \sim 1.7 \times 10^6 (\delta B/B_0)$$

for the estimated $\gamma = 10^{-3} \text{ s}^{-1}$. The excited geomagnetic field fluctuations, $\delta B \sim 3.0 \times 10^{-3}$ gammas for $\delta n/n_0 = 10\%$ (cf. the background geomagnetic field, $B_0 = 5 \times 10^4$ gammas or 0.5 G), are negligibly small. We thus conclude that the large heat conduction loss along the geomagnetic field inhibits the proposed mechanism from producing significant geomagnetic field perturbations in the F region.

As shown below, the condition for the instability is quite different in the E region whose relevant parameters are taken to be $M(\text{NO}^+)/m = 30 \times 1840$, $v_i = 4.0 \times 10^4$ m/s (i.e., $T_e \sim 200^\circ \text{K}$), $\Omega_e/2\pi = 1.4$ MHz, $\omega_{pe}/2\pi = 3.0$ MHz, $v_{in} = 1.0 \times 10^3$ Hz, and $v_{en} = 1.0 \times 10^4$ Hz. The parallel heat conduction loss, $k_{\parallel}^2 v_i^2 / v_e^2 \sim 3.8 \times 10^{-8}$, is drastically reduced by the large effective electron collisions contributed dominantly from the electron-neutral collisions. The parallel heat conduction loss is greater than the cross-field heat conduction loss, $k_{\perp}^2 v_i^2 / \Omega_e^2 \sim 3.3 \times 10^{-9}$ (for $\lambda_{\perp} = 500$ m) but very much less than the collisional damping of the heat source represented by $2m/M \sim 3.6 \times 10^{-5}$ in (6) and (6'). The factor associated with k_{\parallel} in (2'), $(\Omega_e \Omega_i / v_e v_{in})(\lambda_{\perp} / \lambda_{\parallel})^2$, is, for instance, 0.11 for $\lambda_{\perp} = 500$ m and 11.00 for $\lambda_{\perp} = 5$ km. These calculations show that if $\lambda_{\perp} / \lambda_{\parallel} \ll 1$, the parallel heat conduction loss hardly affects the operation of the proposed instability in the ionospheric E region. The characteristics of the instability, given by (2), (6), and (7), remain nearly unchanged except for a new factor, $[1 + (\Omega_e \Omega_i / v_e v_{in})(\lambda_{\perp} / \lambda_{\parallel})^2]$, appearing in (2') and the values of v_e therein representing the effective electron collision frequency that is approximately equal to the electron-neutral collision frequency in the E region.

For the excitation of modes with $\lambda_{\perp} \gg (2m/M)^{1/2} \pi v_i / \Omega_e \sim 4.7$ m, the threshold field of the instability is mainly determined by the collisional damping of the heat source; namely, (6) can be written as

$$|e e_{th} / m c| = 0.6 (\omega_0 / \omega_{pe}) k_{\perp} v_i (2m/M)^{1/2}$$

Hence, the instability with scale lengths of, for instance, 500 m, 2 km, and 5 km requires the threshold fields to be 2.5 V/m, 0.63 V/m, and 0.25 V/m, respectively, which are computed with $\omega_0/2\pi = 2.45$ GHz, $\omega_{pe}/2\pi = 3$ MHz, $M(\text{NO}^+)/m = 30 \times 1840$, and $v_i = 4.0 \times 10^4$ m/s. They are significantly less than the assumed incident microwave field intensity ~ 300 V/m corresponding approximately to a power density of 50 W/m² that is about one fifth of the maximum intensity at the beam center. The corresponding growth rates are 0.428 s^{-1} , 0.474 s^{-1} , and 0.50 s^{-1} and $(\delta B/B_0)/(\delta n/n_0) \sim 1.06 \times 10^{-3}$, 7.24×10^{-3} , and 1.12×10^{-2} for $\lambda_{\perp} = 500$ m, 2 km, and 5 km, respectively. As a function of the perpendicular scale length (λ_{\perp}), the threshold field (e_{th}), the growth rate (γ), and $(\delta B/B_0)/(\delta n/n_0)$ are plotted in Figure 3.

We note in (2') that when the factor $[1 + (\Omega_e \Omega_i / v_e v_{in})(\lambda_{\perp} / \lambda_{\parallel})^2]$ is much greater than unity for kilometer-scale (say, > 5 km) modes, $(\delta B/B_0)/(\delta n/n_0)$ reaches a constant value

of $(\gamma v_{in} / \Omega_e \Omega_i)(\lambda_{\parallel} \omega_{pe} / 2\pi c)^2 \sim 1.2 \times 10^{-2}$. That is, $\delta B/B_0$ is less than $\delta n/n_0$ by about two orders of magnitude in the case of microwave-ionosphere interaction. The earth's magnetic field perturbations can be quite significant even when $\delta B/B_0 \leq 10^{-2} \delta n/n_0$, which are associated with modes with scale lengths less than the beam size by about one order of magnitude. For example, $\delta B = 5.3$ and 36.2 gammas for $\lambda_{\perp} = 500$ m and 2 km, respectively, assuming that $\delta n/n_0 = 10\%$. They are comparable to the intensities (typically, tens of gammas) of geomagnetic field fluctuations during magnetospheric substorms.

4. DISCUSSION AND CONCLUSIONS

In summary, our theoretical model originally developed for a uniform medium has been modified for application to the study of microwave-ionosphere interaction. The inhomogeneity effect of the background plasma density on the thermal instability considered by Perkins and Valeo [1974] has not been generally treated in our model. Nevertheless, the stringent inhomogeneity effect imposed by the microwave beam, i.e., the heat conduction loss along the geomagnetic field, has been taken into account. This effect enhances the threshold fields of the instability and inhibits the operation of the instability in the F region but not in the E region.

Earth's magnetic field can be significantly perturbed locally by the conceptualized solar power satellite (SPS) that transmits a microwave beam at 2.45 GHz with power density of 230 W/m² at the center of the beam. The earth's magnetic field fluctuations caused by powerful microwaves via the thermal filamentation instability are a transient phenomenon. This fact can be seen from equation (2), or generally equation (2'), which requires $\delta B/B_0 = 0$ when $\gamma = 0$ for the equilibrium condition either before the onset or after the saturation of the instability. During the linear stage of the instability (i.e., γ a positive constant), $\delta B/B_0$ and $\delta n/n_0$ are related in (2') and significant magnetic field fluctuations can be produced. The duration of this transient phenomenon may be estimated from the growth rate of the instability. If we roughly define it to be the period for achieving the seven e folds of magnitude above the thermal fluctuation level, viz., $7\gamma^{-1}$, then it is of the order of 20 s.

The simultaneous excitation of earth's magnetic field fluctuations and ionospheric density irregularities is achievable within a minute by the thermal filamentation instability with scale lengths exceeding a few hundreds of meters. The ratio of $(\delta B/B_0)$ to $(\delta n/n_0)$ reaches a constant value of

$$(\gamma v_{in} / \Omega_e \Omega_i)(\lambda_{\parallel} \omega_{pe} / 2\pi c)^2 \sim 1.2 \times 10^{-2}$$

for kilometer-scale modes, indicating that $(\delta B/B_0)$ is less than $(\delta n/n_0)$ by about two orders of magnitude in the microwave-ionosphere interaction of interest. Earth's magnetic field perturbations with magnitudes (\sim a few tens of gammas) comparable to those in the magnetospheric substorms are predicted. It is expected that such perturbations can affect the orbits of charged particles to cause particle precipitation and airglow effects. Our present work adds the earth's magnetic field perturbations as an additional effect to those such as ionospheric density irregularities, plasma heating, etc., that should be assessed as the possible environmental impacts of the conceptualized solar power satellite program.

Acknowledgments. This work was supported by AFGL contract F19628-83-K-0024 at Regis College Research Center and jointly in part by NSF grant ATM-8315322 and in part by AFOSR grant AFOSR-83-0001 at Polytechnic Institute of New York. The two referees' comments are greatly appreciated.

The editor thanks the two referees for their assistance in evaluating this paper.

REFERENCES

- Glaser, P., Solar power from satellites, *Phys. Today*, 30, 30, 1977.
- Gordon, W. E., and L. M. Duncan, Ionosphere/microwave beam interaction study, *Rep. DRL 701349*, William Marsh Rice Univ., Houston, Tex., 1978.
- Gordon, W. E., and L. M. Duncan, Solar power satellites and telecommunications, *Radio Sci.*, 18, 291, 1983.
- Kuo, S. P., and M. C. Lee, Earth magnetic field fluctuations produced by filamentation instabilities of electromagnetic heater waves, *Geophys. Res. Lett.*, 10, 979, 1983.
- Lee, M. C., and S. P. Kuo, Excitation of magnetostatic fluctuations by filamentation of whistlers, *J. Geophys. Res.*, 89, 2289, 1984.
- Perkins, F. W., and M. V. Goldman, Self-focusing of radio waves in an underdense ionosphere, *J. Geophys. Res.*, 86, 600, 1981.
- Perkins, F. W., and R. G. Roble, Ionospheric heating by radio waves: Predictions for Arecibo and the satellite power station, *J. Geophys. Res.*, 83, 1611, 1978.
- Perkins, F. W., and E. J. Valeo, Thermal self focusing of electromagnetic waves in plasmas, *Phys. Rev. Lett.*, 32, 1234, 1974.
- Rush, C. M., SPS simulated effects of ionospheric heating on the performance of telecommunication systems: A review of experimental results, *Space Sol. Power Rev.*, 2, 355, 1981.
- S. P. Kuo, Polytechnic Institute of New York, Long Island Center, Farmingdale, NY 11735.
- M. C. Lee, Regis College Research Center, 235 Wellesley Street, Weston, MA 02193.

(Received June 7, 1984;
revised July 23, 1984;
accepted August 8, 1984.)

Modulational instability of lower hybrid waves

S.P. Kuo

Polytechnic Institute of New York, Long Island Center,
Farmlandale, N.Y. 11735, U.S.A.

M.C. Lee

Regis College Research Center, Weston, Mass. 02193, U.S.A.

Abstract. We investigate the excitation of a purely growing modulational mode together with two lower hybrid sidebands by a lower hybrid pump. The condition, $|k_{\perp}/k_{\parallel}| < \omega_{pe}/\omega_e$, needs to be satisfied for the instability, where $|k_{\perp}/k_{\parallel}|$ is the ratio of the perpendicular to the parallel scale lengths of the lower hybrid pump. The growth rate of the instability is found to be quite large for the power densities employed in the lower hybrid heating experiments in large tokamaks.

1. Introduction

The need of supplementary plasma heating in magnetic fusion devices has been generally recognized for achieving the operational temperatures for fusion power production. Among various RF heating schemes, lower hybrid waves have received much attention not only for plasma heating (e.g., Forklab, 1977) but also for plasma confinement (e.g., Fisch, 1978) purposes. The effectiveness of these processes relies on the penetration of RF wave energy into the interior of the plasmas. Hence, the self-modulational effects on the lower hybrid wave propagation are believed to be important on this aspect (e.g., Morales and Lee, 1975). In this paper, we perform a linear stability analysis of the modulational instability whereby a purely growing modulational mode together with two lower hybrid sidebands are excited by a lower hybrid pump wave.

2. Coupled mode equations

We consider the propagation of a lower hybrid pump wave $\phi = \tilde{\phi}_0 \exp[i(k_{\perp} \cdot r - \omega_0 t)]$ in a uniform, collisionless plasma embedded in a constant magnetic field $B_0 = B_0 \hat{z}$. Here, ϕ_0 is the lower hybrid wave field potential; $k_{\perp} (= \sqrt{k_{\perp 1}^2 + k_{\perp 2}^2})$ and ω_0 are respectively, the wave vector and the angular wave frequency of the lower hybrid pump that satisfies the dispersion relation: $\omega_0 = \omega_{LH} [1 - (M/m)(k_{\perp}/k_{\perp 1})^2]^{1/2}$, where $\omega_{LH} = \omega_{pe}/(1 + \omega_{pe}^2/\omega_e^2)^{1/2}$ is the lower hybrid resonance frequency.

The parameters, M/m , ω_{pe}/ω_e , and Ω_e are the ratio of ion to electron masses, the ion(electron) plasma frequency, and the electron gyro-frequency, respectively.

The process under consideration is a modulational instability whereby the lower hybrid pump wave (ω_0, k_0) excites two lower hybrid sidebands (ω_{\pm}, k_{\pm}) and a purely growing modulational mode (ω, k). This process can be described by the following frequency and wave vector matching relations: $\omega_{\pm} - \omega_0 = \omega = \omega_{\pm} + \omega$ and $k_{\pm} = k_0 \pm k$, where $k \parallel k_0$. The lower hybrid sidebands are excited through the beating current density driven by the lower hybrid pump field on the density perturbations, $n_{\pm} = \tilde{n}_{\pm} \exp[i(k_{\pm} \cdot r - \omega_{\pm} t)]$, of the zero-frequency modulational mode.

From the Poisson's equation, $k_{\perp}^2 \phi_0 = 4\pi e(\delta n_{\perp 1} - \delta n_{\perp 2})$, where the ion and electron density perturbations ($\delta n_{\perp 1}$ and $\delta n_{\perp 2}$) associated with the lower hybrid sidebands are given, respectively, by $\delta n_{\perp 1} = (n_0/\omega_{pe}^2) k_{\perp 1}^2 [\phi_0 + (k_{\perp 1}/k_{\perp 2})(\omega_0/\omega_{\pm})\phi_0(n_{\pm 2}/n_0)]$ and $\delta n_{\perp 2} = (n_0/\omega_{pe}^2) (1 - k_{\perp 1}^2/\Omega_e^2) k_{\perp 2}^2 [\phi_0 + (k_{\perp 1}/k_{\perp 2})(\omega_0/\omega_{\pm})\phi_0(n_{\pm 2}/n_0)]$. The coupled mode equation for the lower hybrid sidebands is obtained as

$$\partial_{\pm} = (k_{\perp 1}/k_{\perp 2})(\omega_0/\omega_{\pm}) \{ (k_{\perp 1}^2/k_{\perp 2}^2) [1 - \omega_{pe}^2/\omega_e^2] \omega_{\pm} (\omega_{\pm} \pm 2\omega_0) \} \phi_0 (n_{\pm 2}/n_0) \quad (1)$$

where the relations $\omega_{\pm} = \omega_0 \pm \omega$ have been used.

The nonlinear effects responsible for the excitation of the purely growing modulational mode include the nonlinear beating current and the ponderomotive force appearing, respectively in the continuity equation and the momentum equation. Under the assumption of quasi-neutrality, the coupled mode equation for the purely growing mode is derived from the continuity and the momentum equations of electrons and ions and has the following form:

$$\begin{aligned} & [1 - (1 + k_{\perp}^2/\Omega_e^2)] (n_0/n_0) + \omega_{pe}^2 (\delta v_{ey}^{NL} + \frac{e}{H} \delta v_{ly}^{NL}) \\ & - \omega_{pe}^2 (\delta v_{ex}^{NL} + \frac{e}{H} \delta v_{lx}^{NL}) + k_{\perp} \frac{\omega_{pe}}{\Omega_e} \left(-\frac{F_{1x}}{H} - \frac{F_{2x}}{H} \right) + ik_{\perp} \frac{\omega_{pe}}{\Omega_e} \left(\frac{F_{1y}}{H} + \frac{F_{2y}}{H} \right) \\ & F_{1x} + F_{2x} = -k_{\perp} \frac{1}{H} (F_{1x} + F_{2x}) \end{aligned} \quad (2)$$

where $C_0 = [(T_e + T_i)/m]^{1/2}$ is the ion acoustic velocity. The nonlinear heating current density $n_0 v_{ex}^{NL}$ and the ponderomotive force F_{ex} are given, respectively, by

$$n_0 v_{ex}^{NL} = \delta n_{\perp 1} \frac{\partial v_{ex}^{NL}}{\partial \omega_{\perp 1}} + \delta n_{\perp 2} \frac{\partial v_{ex}^{NL}}{\partial \omega_{\perp 2}} + \delta n_{\perp 1} \frac{\partial v_{ex}^{NL}}{\partial \omega_{\perp 1}} + \delta n_{\perp 2} \frac{\partial v_{ex}^{NL}}{\partial \omega_{\perp 2}}$$

$$\text{and } F_{ex} = -in_{\perp 1} \left(\frac{k_{\perp 1}}{\omega_{\perp 1}} \frac{\partial v_{ex}^{NL}}{\partial \omega_{\perp 1}} - \frac{k_{\perp 2}}{\omega_{\perp 2}} \frac{\partial v_{ex}^{NL}}{\partial \omega_{\perp 2}} \right) - in_{\perp 2} \left(\frac{k_{\perp 1}}{\omega_{\perp 1}} \frac{\partial v_{ex}^{NL}}{\partial \omega_{\perp 1}} - \frac{k_{\perp 2}}{\omega_{\perp 2}} \frac{\partial v_{ex}^{NL}}{\partial \omega_{\perp 2}} \right)$$

$$\text{where } \frac{\partial v_{ex}^{NL}}{\partial \omega_{\perp 1}} = -ik_{\perp 1} \left[\frac{1}{\omega_{\perp 1}} + \frac{1}{\omega_{\perp 2}} \left(\frac{\omega_0}{\omega_{\perp 1}} \right) - \frac{1}{\omega_{\perp 2}} \left(\frac{k_{\perp 1}}{k_{\perp 2}} \frac{\omega_0}{\omega_{\perp 1}} \right) \right] (e_0/\omega_{\perp 1}),$$

$$\omega = 0 \text{ or } \pm, \quad (3)$$

$$\frac{\partial v_{ex}^{NL}}{\partial \omega_{\perp 2}} = ik_{\perp 2} \left[\frac{1}{\omega_{\perp 1}} \left(\frac{\omega_0}{\omega_{\perp 2}} \right) - \frac{1}{\omega_{\perp 1}} \left(\frac{k_{\perp 1}}{k_{\perp 2}} \frac{\omega_0}{\omega_{\perp 2}} \right) \right] (e_0/\omega_{\perp 2}), \quad (4)$$

$$\frac{\partial v_{ex}^{NL}}{\partial \omega_{\perp 1}} = ik_{\perp 1} \left[\frac{1}{\omega_{\perp 1}} \left(\frac{\omega_0}{\omega_{\perp 1}} \right) - \frac{1}{\omega_{\perp 2}} \left(\frac{k_{\perp 1}}{k_{\perp 2}} \frac{\omega_0}{\omega_{\perp 1}} \right) \right] (e_0/\omega_{\perp 1}), \quad (5)$$

$$\delta n_{\perp 1} = n_0 k_{\perp 1}^2 (1 - k_{\perp 1}^2/\Omega_e^2) (e_0/\omega_{\perp 1}), \quad (6)$$

$$\delta n_{\perp 2} = n_0 k_{\perp 2}^2 (e_0/\omega_{\perp 2}). \quad (7)$$

With the aid of (3) - (7), two things have been noted from the RHS of (2): firstly, the ion-nonlinearity terms are relatively insignificant compared to the electron-nonlinearity terms; Secondly, the nonlinear beating current effect is partially cancelled by the ponderomotive force effect. Therefore, the electron-nonlinearity term that remains on the RHS of (2) is $-\omega_{pe}^2 \delta v_{ex}^{NL}$, contributed from the induced nonlinear beating current flowing along the imposed magnetic field.

Eliminating n_{\pm} and ϕ_0 from Equations (1) and (2) leads to the dispersion relation

$$\begin{aligned} & \omega^2 = k_{\perp}^2 \left[C_0^2 - \left((1 - k_{\perp 1}^2/\Omega_e^2) k_{\perp 1}^2 / (1 + M^2/\omega_{pe}^2) \right) (\Omega_e^2 + \omega_{pe}^2) \right] \\ & \cdot |v_{\perp}|^2 / (1 + k_{\perp}^2/\Omega_e^2) \end{aligned} \quad (8)$$

where $v_{\perp} = k_{\perp} \phi_0 / \omega_{\perp 1}$. For a purely growing mode (i.e., $\omega = i\gamma$), the growth rate obtained from (8) is given by

$$\gamma = k_{\perp} \left\{ \left[(1 - k_{\perp 1}^2/\Omega_e^2) k_{\perp 1}^2 / (1 + M^2/\omega_{pe}^2) \right] (\Omega_e^2 + \omega_{pe}^2) |v_{\perp}|^2 - C_0^2 \right\}^{1/2} / (1 + k_{\perp}^2/\Omega_e^2)^{1/2} \quad (9)$$

Since γ has to be positive for instability to occur, it is clear from (9) that (I) $|k_{\perp}/k_{\parallel}| < \omega_{pe}/\Omega_e$.

namely, the ratio of the perpendicular to the parallel scale lengths of the lower hybrid pump wave has to be less than the ratio of the ion plasma frequency to the electron gyrofrequency, (II) $|v_{\perp}| > |\tilde{v}_{\perp}| = (m/e)(\Omega_e^2 + \omega_{pe}^2)^{1/2} (C_0/k_0) (1 + M^2/\omega_{pe}^2)^{1/2} / (1 - \Omega_e^2/\omega_{pe}^2)^{1/2}$

namely, the pump field intensity represented by $|v_{\perp}|$ has to be greater than a threshold defined by $|\tilde{v}_{\perp}|$.

The growth rate has a minimum when $k_{\perp 1}^2/\Omega_e^2 = (1 - |\tilde{v}_{\perp}|^2/|\tilde{v}_{\perp}|^2) / (2 - |\tilde{v}_{\perp}|^2/|\tilde{v}_{\perp}|^2)$. In this optimum case and for a strong lower hybrid pump wave, (9) may be expressed as

$$\gamma \approx k_{\perp} |v_{\perp}| \Omega_e^2 / (2\Omega_e^2 + \omega_{pe}^2)^{1/2} (1 + k_{\perp}^2/\Omega_e^2)^{1/2} \quad (12)$$

which is proportional to the wave length of the modulational instability.

4. Summary and conclusions

The condition and the threshold power have been derived for the modulational instability of lower hybrid waves as shown, respectively, in (10) and (11). The nonlinearity for the excitation of purely growing modes is provided by the nonoscillatory beating current in the direction of the imposed magnetic field. For the power densities commonly used in the lower hybrid heating experiments in large tokamaks, the growth rate given in (12) is found to be quite large and it covers a broad spectrum. However, it should be stressed that the spatial modulation on the lower hybrid pump wave as discussed here only occurs in the resonance region where the condition, $|k_{\perp}/k_{\parallel}| < \omega_{pe}/\Omega_e$, can be satisfied.

References

- Fisch, N.J., Phys. Rev. Lett. **41**, 873, 1978.
Morales, G.J., and Y.C. Lee, Phys. Rev. Lett., **35**, 930, 1975.
Forklab, M., Phys. Fluids, **20**, 2058, 1977.

Acknowledgments. This work was supported jointly in part by the NSF grant ATM-8315322 and in part by the AFOSR grant AFOSR-83-0001 at Polytechnic Institute of New York and by AFGL contract F19628-83-K-0024 at Regis College Research Center.

Ionospheric and magnetospheric modifications caused by the injected VLF waves

M.C. Lee

Aegis College Research Center, Boston, Mass. 02193, U.S.A.

S.P. Kuo

Polytechnic Institute of New York, Long Island Center,
Farminale, N.Y. 11735, U.S.A.

Abstract. The ionosphere and the magnetosphere may be significantly modified by the injected VLF waves via the thermal filamentation instability and the excitation of lower hybrid waves.

1. Introduction

In VLF wave injection experiments performed, for example, at Siple, Antarctica, the ground-based transmitters are usually operated in a pulsed-wave mode with durations of a few seconds. These VLF wave pulses have been used to study coherent wave-particle interactions in the magnetosphere such as the wave amplification, the triggering of wave emissions, the induced particle precipitation etc. (see, e.g., Nelliwell, 1963). We show in this paper that if the transmitters are operated continuously for a few minutes, significant ionospheric and magnetospheric disturbances can be caused by the following two processes. One is the thermal filamentation of the pump wave and the other one is the excitation of lower hybrid waves.

2. Thermal filamentation of whistlers

Monochromatic VLF waves have been observed to change from linear into circular polarization (i.e., a whistler mode) on their path through the neutral atmosphere and into the ionosphere. If the pump waves are intense enough, the filamentation instability of whistlers can be excited. This instability yields a whistler sideband and zero-frequency modes that are associated with the simultaneous excitation of both plasma density fluctuations (δn) and magnetic field fluctuations (δB). The source of these magnetostatic fluctuations stems from the wave-induced quasi-DC electric current due to the electron $\mathbf{E} \times \mathbf{B}$ drift motion under the influence of the differential Ohmic heating force.

The plasma density fluctuations (δn) and the magnetostatic fluctuations (δB) are found to be related as

$$\delta n / n_0 = [1 + (v_e / v_i)(c^2 / \omega_p^2)] (\delta B / B_0) \quad (1)$$

where f_p , v_e , n_0 , B_0 , γ , and k are, respectively, the electron plasma frequency, the electron-ion collision frequency, the background plasma density, the earth's magnetic field, the growth rate of the instability, and the scale lengths of the excited modes. It is clear from (1) that significant magnetostatic fluctuations are associated with the excitation of large scale modes.

Although the whistler waves have a broad propagation regime: $|\mathbf{k}_\perp| \ll \omega_p / v_e$, the excitation of the filamentation instability is restricted to whistlers with frequencies (ω) satisfying the following condition:

$$1 - \omega_p^2 / (\omega^2 - \omega_{pe}^2) > 0 \quad (2)$$

where ω_p , $|\mathbf{k}_\perp|$, $|\mathbf{k}_\parallel|$, ω_{pe} , and k are the angular electron plasma frequency, the electron (ion) gyrofrequency, the angular whistler wave frequency, and the wave number of the excited modes, respectively. The inequality (2) demands that $\omega > |\mathbf{k}_\perp|/2$ for the excitation of large scale modes. Since $|\mathbf{k}_\perp| \sim 1.4$ Mhz (13.6 KHz) in the ionospheric F region (in the magnetosphere at $L = 4.0$), this result indicates that the thermal filamentation of whistlers can occur in the ionosphere (in the magnetosphere at $L = 4.0$) when the wave frequencies are within the frequency range: 1.4 Mhz $> \omega / 2 > 0.7$ Mhz (13.6 KHz $> \omega / 2 > 6.8$ KHz).

The threshold of this instability has been found to be

$$|\mathbf{E}_0| / \text{mV/m} \sim 1.5 \frac{\omega_p^2}{\omega^2} \left(\frac{\omega_c}{\omega} - \frac{|\mathbf{k}_\perp|^2}{\omega^2} \right)^{-1} (4 - a - ab)^{-1} \quad (3)$$

where $a = k^2 c^2 / (\omega_p^2 - \omega_{pe}^2) / \omega_p^2$, $b = \omega_c^2 / (\omega_c^2 - |\mathbf{k}_\perp|^2)$, and ω_c is the ion thermal velocity. The threshold fields thus calculated are of the order of a few mV/m (a few mV/m) for exciting modes with tens of kilometers (tens of meters) and larger scales in the magnetosphere at $L = 4.0$ (in the ionospheric F region), that are achievable whistler wave field intensities with available facilities. However,

whistler waves with much higher intensities are required to ensure the excitation of the thermal filamentation instability in the magnetosphere. This is because the growth rate of the instability is rather small if the whistler wave field intensities just barely exceed the threshold fields.

In terms of the threshold field (E_{th}), the growth rate of large scale modes (i.e., $\omega \gg c/v_e$) is given by

$$\gamma \sim (2\omega_p / \omega) \left(\frac{\omega_c}{\omega} - \frac{|\mathbf{k}_\perp|^2}{\omega^2} \right) \left(\frac{E_0}{E_{th}} \right) \quad (4)$$

that turns out to be independent of the scale lengths because as shown in (3), E_{th} is proportional to k . If $\omega_c / \omega \sim 0(1)$, γ is of the order of 10^{-3} Hz (10^{-3} Hz) in the magnetosphere at $L = 4.0$ (in the ionospheric F region). The Siple signals, propagating in the non-ducted whistler mode, have $\omega_c / \omega \sim 0(1)$ in the magnetosphere at $L = 4.0$. The probability for seeing the Siple signals in the ducted whistler mode is about 20%. The growth rate can be increased by two to three orders of magnitude in the ducted whistler propagation. Therefore, if the Siple transmitter is operated for a few minutes, the thermal filamentation instability can exist in the magnetosphere at $L = 4.0$ the plasma density fluctuations with scale lengths greater than tens of kilometers. This instability can also be excited in the ionospheric F region by the MF waves with frequencies close to but less than the local electron gyrofrequency.

3. Excitation of lower hybrid waves

The injected VLF waves can interact directly with the ionosphere through the excitation of lower hybrid waves and a field-aligned purely growing mode. This instability can be excited in a broad whistler frequency range in two domains. They are Domain 1: $\omega_{LH} [1 + (M/m)(v_e^2 / c^2)] (c^2 / \omega_p^2)^{1/2} < \omega < \omega_{pi}$ for the non-oscillatory beating current to be the dominant nonlinear effect, and Domain 2: $\omega_{pi} < \omega < |\mathbf{k}_\perp|$ for the thermal pressure force to be the dominant nonlinear effect, where ω_{LH} defined by $\omega_{LH}^2 / (1 + \omega_p^2 / \omega_{pe}^2)$ is the lower hybrid resonance frequency; $\omega_{pi}(\omega_e)$, $|\mathbf{k}_\perp|$, v_e , and (M/m) are the ion (electron) plasma frequency, the electron gyrofrequency, the electron thermal velocity, and the ratio of ion to electron masses, respectively.

The optimum threshold field for the instability is found to be $E_{th} \sim 1.2 (\omega_e / v_e) |\mathbf{k}_\perp|$ in frequency domain 1 and $E_{th} \sim 0.86 (k^2 v_e^2 / \omega_e) (\omega / c) [1 + (1 + 4\omega_p^2 \omega_{pe}^2 / \omega_e^2 v_e^2)^{1/2} / \omega_e]$ in frequency domain 2, where v_e and k are the electron-ion collision frequency and the wave number of the excited field-aligned mode, respectively; $n = [1 + (M/m)(\omega_e / k)^2] / [1 - (M/m)(\omega_e / k)^2 (\omega_e / \omega_p)^2]$, where ω_e / k is the ratio of the perpendicular to the parallel scale lengths of the excited lower hybrid waves.

The growth rate of the instability has the following expressions, $\gamma \sim 0.5 (\omega_e / v_e) (\omega_p^2 / \omega_e^2) (E_0^2 - 1)$ for $E_0^2 \ll 10$ and $\gamma \sim 1.4 (\omega_e / v_e) (\omega_p^2 / \omega_e^2) E_0$ for $E_0^2 \gg 10$, where E_0 is the ratio of the whistler field intensity (E_0) to the optimum threshold field intensity (E_{th}) of the instability. Since $\omega_{LH} \sim 6$ KHz in the ionosphere, the whistler wave frequencies have to be greater than 6 KHz for the excitation of lower hybrid waves. The threshold field has been estimated to be about 1 mV/m. If $E_0 \sim 0(10)$, the instability with dominant scale lengths near 10 meters can be excited with in a few seconds in the ionosphere. By contrast, kilometer-scale lower hybrid waves can be excited in the magnetosphere at $L = 4.0$ with much lower threshold field (\sim a few mV/m). The growth rate is, however, rather small for non-ducted whistler modes, where $E_0 \sim 0(1)$. Whereas, the ducted whistler modes can excite the instability with growth rates as large as 10^{-2} Hz. In other words, lower hybrid waves can be produced by ducted whistler waves in the magnetosphere within a few minutes. Electron precipitation is the ionospheric effects expected from the excitation of lower hybrid waves. Indeed, auroral effects have been observed in the Russian Juliana program (Chuvpov et al., 1976) to be associated with the VLF transmitter cycle.

References

- Chuvpov, V.M. et al., JETP Lett., **23**, 409, 1976.
Nelliwell, R.A., Radio Sci., **10**, 801, 1963.

Acknowledgments. This work was supported by AFGL contract F1962R-83-F-0024 at Aegis College Research Center and jointly in part by NSF grant ATM-8315322 and in part by the Air Force Office of Scientific Research grant AFOSR-83-0001 at Polytechnic Institute of New York.

ON THE SPREAD F ECHOES FROM THE IONOSPHERIC HEATED REGION

S.P. Kuo

Polytechnic Institute of New York, Long Island Center
Farmingdale, NY 11735

M.C. Lee

Regis College Research Center, Weston, MA 02193

ABSTRACT

Four invariants of the ray trajectory are derived for a ray propagating in a horizontally stratified ionosphere under the density perturbation of HF wave-induced field-aligned irregularities. The reflection height of the ray can then be determined with the aid of those invariants. The results show that the reflection height of the ray varies drastically (namely, strong spread F echoes) in the presence of irregularities that polarize in the magnetic meridian plane. By contrast, the reflection height is hardly affected (namely, no spread F echoes) by those irregularities that polarize in the direction perpendicular to the meridian plane.

I. INTRODUCTION

Spread F that refers to diffuse echoes on an ionogram from the ionospheric F region was observed in the ionospheric heating experiments conducted at Boulder, Colorado (Utlaut, 1971). This ionospheric phenomenon is generally believed to be caused by the excitation of large scale (a few hundreds of meters to kilometers), field-aligned ionospheric irregularities. However, spread F is a rare phenomenon in the experiments at Arecibo, Puerto Rico (Shoven and Kim, 1978) and it has not been observed at Tromsø, Norway since the new European heating facility has been in operation (Stubbe et al, 1982). Evidences, such as radio star scintillations and the anomalous absorption of the diagnostic waves through the ionospheric heated region, indicate that large-scale ionospheric irregularities have been excited by HF heater waves at Arecibo and Tromsø. A lack of spread F echoes does not imply the absence of heater wave-induced ionospheric irregularities. This may be due to the difference in the polarization directions of the HF wave-induced irregularities. In general, field-aligned irregularities may have two independent polarization directions. One lies in the meridian plane and the other one is in the direction perpendicular to the meridian plane. The theoretical results of filamentation instability in magneto-plasmas (Kuo and Schmidt, 1983) also show that the irregularities excited by the o-mode pump and by the x-mode pump have different polarization directions. The irregularities excited by the o-mode pump are field-aligned and are polarized in the direction perpendicular to the meridian plane. By contrast, the irregularities excited by the x-mode pump are polarized in the meridian plane and are, in general, not field-aligned. However, the field-aligned nature of the irregularities may be established to reduce the diffusion damping along the magnetic field.

In the present work, the relationship between the spread-F echoes and the HF wave-induced irregularities is studied. The primary purpose of this study is to determine the effect of the irregularity polarizations on the spread-F echo. In section II, the ray trajectory equations are analyzed to study the wave propagation in a horizontally stratified ionosphere under the density perturbation of the HF wave-induced field-aligned irregularities. Main results are illustrated in Figures. Conclusions are finally drawn in Section III.

II. MODEL AND ANALYSIS

We consider a horizontally stratified ionosphere having a scale length L . Thus, the unperturbed electron density is represented by $n_0(x) = n_0(1+x/L)$, where x is the vertical coordinate and $n_0 = n_0(0)$ is the electron density at the reference plane $x=0$ located at height H . When field-aligned irregularities are present, the background electron density distribution is perturbed. Thus, the total density is the sum of the unperturbed density and the fluctuating densities of the irregularities. For those irregularities which are field-aligned in the magnetic meridian plane, the total density perturbation is simply expressed in a form of $\delta n_1 \sin k_1(x \cos \theta_0 + z \sin \theta_0)$, where $2\pi/k_1 = \lambda_1$ is the average scale length of the irregularities, θ_0 is the magnetic dip angle, and z is the horizontal coordinate as shown in Fig. 1. Whereas, the density perturbation associated with the irregularities

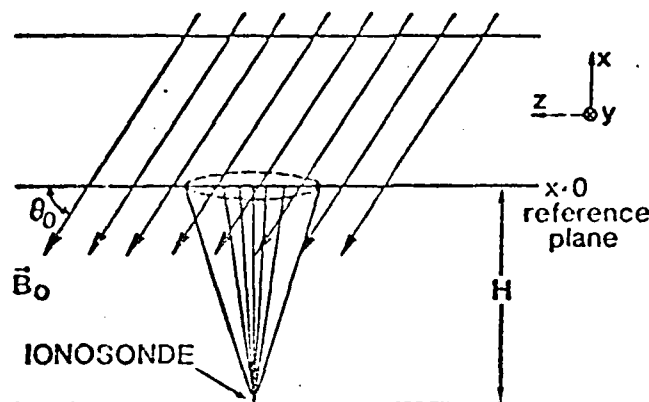


Fig. 1 Coordinates used in the analysis.

which are field-aligned in the direction perpendicular to the magnetic meridian plane is modelled as $\delta n_2 \sin(k_2 y + \phi)$, where $\lambda_2 = 2\pi/k_2$ is the averaged scale length; y is the coordinate perpendicular to the meridian plane, and ϕ is the arbitrary phase angle. In this model, the total electron density distribution, $n(x)$ is then composed of three components, viz.,

$$n(x) = n_0(1+x/L) + \delta n_1 \sin k_1(x \cos \theta_0 + z \sin \theta_0) + \delta n_2 \sin(k_2 y + \phi) \quad (1)$$

For simplicity, the effect of the geomagnetic field on wave propagation will be neglected in the following analyses. The dispersion relation for the wave propagation is thus given by

$$\omega^2 = \omega_{pe}^2 + k^2 c^2 \quad (2)$$

where ω and k are the wave frequency and the wave number respectively, and

$$\omega_{pe}^2 = \omega_{pe0}^2 [1 + x/L + (\delta n_1/n_0) \sin k_1(x \cos \theta_0 + z \sin \theta_0) + (\delta n_2/n_0) \sin(k_2 y + \phi)] \quad (3)$$

Since, in reality, the ionosonde antennas radiate radio wave beams with finite cross sections and spread angles, so it is more appropriate to consider the transmitted pulses to be composed of rays whose initial wave vectors and the horizontal locations on the reference plane $x=0$ are all different. The trajectory of each ray is then governed by the following set of characteristic equations:

$$\frac{d}{dt} x = k_x c^2 / \omega \quad (4)$$

$$\frac{d}{dt} y = k_y c^2 / \omega \quad (5)$$

$$\frac{d}{dt} z = k_z c^2 / \omega \quad (6)$$

$$\frac{d}{dt} k_x = - (\omega_{peo}^2 / 2\omega L) [1 + (\delta n_1 / n_o) (k_1 L \cos \theta_o) \cos k_1 (x \cos \theta_o + z \sin \theta_o)] \quad (7)$$

$$\frac{d}{dt} k_y = - (\omega_{peo}^2 / 2\omega) (\delta n_2 / n_o) k_2 \cos (k_2 y + \phi) \quad (8)$$

$$\frac{d}{dt} k_z = - \tan \theta_o (\omega_{peo}^2 / 2\omega L) (\delta n_1 / n_o) (k_1 L \cos \theta_o) \cos k_1 (x \cos \theta_o + z \sin \theta_o) \quad (9)$$

where Eqs. (5) and (8) form one set of coupled equations, and Eqs. (4), (6), (7) and (9) form the other set of coupled equations, but these two sets of equations do not couple to each other. However, those coupled equations can be separated by the invariants of the trajectory derived as follows. We first take the ratio of (5) and (8), which yields

$$\frac{dy}{dk_y} = - \frac{2k_y c^2}{\omega_{peo}^2 (\delta n_2 / n_o) k_2 \cos (k_2 y + \phi)} \quad (10)$$

Integrating this equation gives the first invariant of the trajectory

$$(\delta n_2 / n_o) \sin(k_2 y + \phi) + k_y^2 c^2 / \omega_{peo}^2 = \text{constant in time} = (\delta n_2 / n_o) \sin(k_2 y_o + \phi) + k_{yo}^2 c^2 / \omega_{peo}^2 \quad (11)$$

where the subscript o represents the initial value.

We next substitute (9) into (7) to yield

$$\frac{d}{dt} (k_x - \cot \theta_o k_z) = - \omega_{peo}^2 / 2\omega L \quad (12)$$

Integrating (12) from the initial height $x=0$ of the ray to the new height x at time t , leads to the second invariant relation

$$k_x - \cot \theta_o k_z + (\omega_{peo}^2 / 2\omega L) t = \text{const. in time} = k_{xo} - \cot \theta_o k_{zo} \quad (13)$$

We now construct an equation by first multiplying (4) and (6) by $\cos \theta_o$ and $\sin \theta_o$ respectively, and then summing them up. The result is

$$\frac{d}{dt} (x \cos \theta_o + z \sin \theta_o) = (c^2 / \omega) (k_x \cos \theta_o + k_z \sin \theta_o) \quad (14)$$

Two additional invariants will be derived as follows. From the ratio of (14) and (7), we obtain

$$\frac{d(x \cos \theta_o + z \sin \theta_o)}{dk_x} = - \frac{2c^2 L}{\omega_{peo}^2} \frac{k_x \cos \theta_o + k_z \sin \theta_o}{1 + (\delta n_1 / n_o) (k_1 L \cos \theta_o) \cos k_1 (x \cos \theta_o + z \sin \theta_o)} \quad (15)$$

With the aid of (13) and (14), (15) is integrated to obtain the third invariant

$$\begin{aligned} x + (\tan 2\theta_o / 2) z + (\delta n_1 / n_o) L (\cos^2 \theta_o / \cos 2\theta_o) \sin k_1 (x \cos \theta_o + z \sin \theta_o) + (c^2 L / \omega_{peo}^2) \\ (k_x^2 + \tan 2\theta_o k_x k_z) = \text{const. in time} = (\tan 2\theta_o / 2) z_o + (\delta n_1 / n_o) L (\cos^2 \theta_o / \cos 2\theta_o) \\ \sin(k_1 z_o \sin \theta_o) + (c^2 L / \omega_{peo}^2) (k_{xo}^2 + \tan 2\theta_o k_{xo} k_{zo}) \end{aligned} \quad (16)$$

The fourth invariant is obtained from integrating the resultant equation defined by the ratio of (14) and (9). It is

$$\begin{aligned}
& (\tan 2\theta_0/2)z + (\delta\eta_1/\eta_0)L(\sin^2\theta_0/\cos 2\theta_0)\sin k_1(x\cos\theta_0 + z\sin\theta_0) + (c^2L/\omega_{peo}^2) \\
& (-k_z^2 + \tan 2\theta_0 k_x k_z) = \text{const. in time} = (\tan 2\theta_0/2)z_0 + (\delta\eta_1/\eta_0)L(\sin^2\theta_0/\cos 2\theta_0)\sin \\
& (k_1 z_0 \sin\theta_0) + (c^2L/\omega_{peo}^2)(-k_{zo}^2 + \tan 2\theta_0 k_{xo} k_{zo})
\end{aligned} \tag{17}$$

However, the sum and the difference of (16) and (17) give much simpler forms of the invariants.

$$\begin{aligned}
& x + (\delta\eta_1/\eta_0)L \sin k_1(x\cos\theta_0 + z\sin\theta_0) + (k_x^2 c^2 L/\omega_{peo}^2) = (\delta\eta_1/\eta_0)L \sin(k_1 z_0 \sin\theta_0) + \\
& k_{zo}^2 c^2 L/\omega_{peo}^2
\end{aligned} \tag{18}$$

and

$$\begin{aligned}
& x\cos 2\theta_0 + z\sin 2\theta_0 + (\delta\eta_1/\eta_0)L \sin k_1(x\cos\theta_0 + z\sin\theta_0) + (c^2L/\omega_{peo}^2)[(k_x^2 - k_z^2)\cos 2\theta_0 \\
& + 2k_x k_z \sin 2\theta_0] = z_0 \sin 2\theta_0 + (\delta\eta_1/\eta_0)L \sin(k_1 z_0 \sin\theta_0) + (c^2L/\omega_{peo}^2)[(k_{xo}^2 - k_{zo}^2)\cos 2\theta_0 \\
& + 2k_{xo} k_{zo} \sin 2\theta_0]
\end{aligned} \tag{19}$$

We have shown that the trajectory of each ray is governed by four invariant relations (11), (13), (18) and (19) that are derived from two sets of coupled differential equations (4)-(9). Hence, the temporal evolution of any one of the four variables x , z , k_x and k_z , and either one of the two variables y and k_y , can be determined, with the aid of these invariants, by the corresponding rate equations, viz., Equations (4)-(9). The elapsed time for each ray traveling from the reference height to the reflection light can in principle be determined by integrating (7) from $k_x = k_{xo}$ to $k_x = 0$, with the prescribed initial conditions: $x(0) = 0$, $z(0) = z_0$ and $k_z(0) = k_{zo}$. Since the density perturbation $\delta\eta_2$ produced by the irregularities oriented in the direction perpendicular to the magnetic meridian plane does not appear in Eq. (7), the reflection height of each ray is thus not expected to be modified by the irregularities oriented in the direction perpendicular to the meridian plane. However, the density perturbation $\delta\eta_1$ produced by the irregularities that are oriented within the meridian plane can affect the reflection height of the ray as seen in Eq. (7). One way to show this effect is to integrate Eq. (7) numerically. Nevertheless, the main purpose of the present work is to give a physical interpretation of the spread-F echoes, our model will be further simplified to minimize the numerical analyses. It is assumed that $k_{zo} = 0$ and the temporal variations of k_z and z can be neglected. Therefore, only Eq. (18) remains for further analysis. It becomes

$$x + (\delta\eta_1/\eta_0)L \sin(k_1 x \cos\theta_0 + \phi_1) + k_x^2 c^2 L/\omega_{peo}^2 = (\delta\eta_1/\eta_0)L \sin\phi_1 + k_{xo}^2 c^2 L/\omega_{peo}^2 \tag{20}$$

where $\phi_1 = k_1 z_0 \sin\theta_0$.

At the reflection height, we have $k_x = 0$ and $x = x_r$ in Eq. (20), where x_r is determined by the equation

$$x_r + (\delta\eta_1/\eta_0)L \sin(k_1 x_r \cos\theta_0 + \phi_1) = (\delta\eta_1/\eta_0)L \sin\phi_1 + k_{xo}^2 c^2 L/\omega_{peo}^2 \tag{21}$$

Equation (21) shows that the reflection height of each ray varies with (1) its initial location z_0 on the reference plane, (2) the intensity $(\delta\eta_1/\eta_0)$ and the averaged scale length $(2\pi k_1^{-1})$ of the irregularities, and (3) the magnetic dip angle θ_0 . Therefore, if the ionosonde radiation beam is modelled by many rays having different initial locations on a reference plane, the spread-F echo can then be interpreted to be caused by the different reflection height of each ray. The virtual height spread is thus proportional to the maximum difference of these reflection heights.

We now employ the following parameters to analyze (21): $L = 50\text{km}$, $\lambda_1 = 1\text{km}$ and $k_{xo}^2 c^2 / \omega_{peo}^2 = 1$, and ϕ_1 varying from 0 to 2π in the determination of the normalized maximum difference $\Delta x_{r\text{max}}/L$ in the reflection heights of the rays. The calculated $\Delta x_{r\text{max}}/L$ vs the magnetic dip angle θ_0 for $\delta\eta_1/\eta_0 = .005$, .01, and .05 and 0.1 are presented in Figs. 2(a)-(d). Shown in Figs. 3(a)-(c) are $\Delta x_{r\text{max}}$ vs the irregularity intensity $\delta\eta_1/\eta_0$ for $\theta_0 = 50^\circ$, 68° and 78° that correspond to magnetic dip angles at Arecibo, Boulder and Tromsø, respectively.

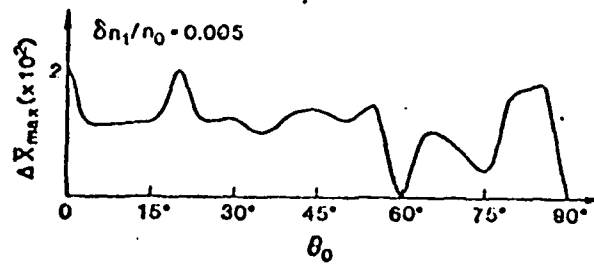


Fig. 2a Maximum deviation of the reflection height of a diagnostic beam vs the magnetic dip angle θ_0 for $\delta n_1/n_0 = 0.005$, where $\Delta \bar{x}_{\max} = \Delta x_{\max}/L$.

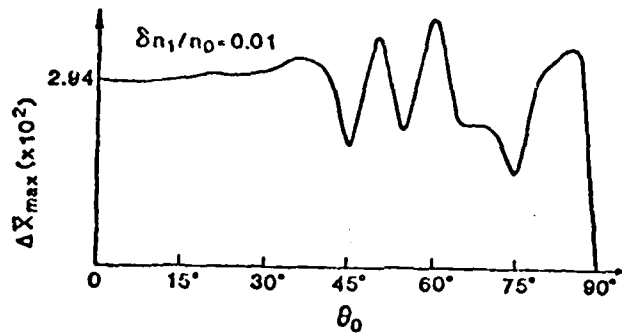


Fig. 2b

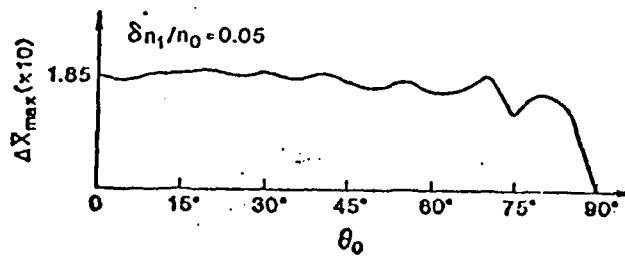


Fig. 2c

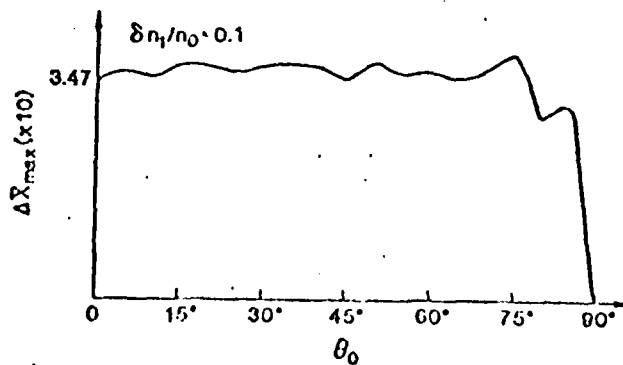


Fig. 2d

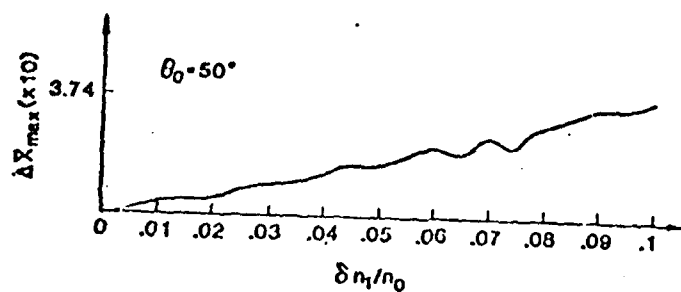


Fig. 3a Δx_{\max} vs $\delta n_1/n_0$ for $\theta_0 = 50^\circ$.

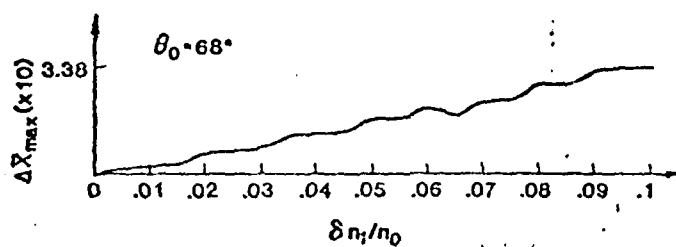


Fig. 3b

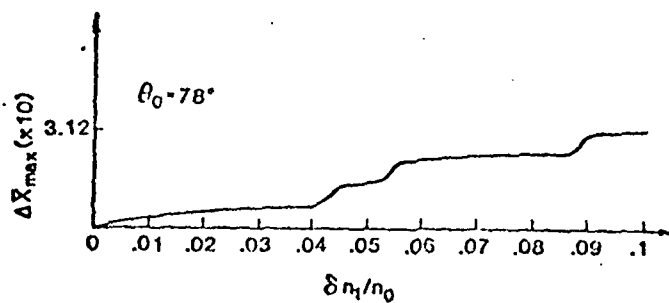


Fig. 3c

III. DISCUSSION AND CONCLUSIONS

Magnetic dip angle (θ), as indicated in Figures 2(a) and 2(b), can have a significant effect on the ionospheric echoes of ionosonde signals when the irregularity intensity is low (e.g., $\delta n_1/n_0 = 0.001$). As the irregularity intensity increases (e.g., $\delta n_1/n_0 = 0.01, 0.05$), only moderate dependence of spread F on θ is seen in Figures 2(c) and 2(d). A nearly linear increasing of virtual height spread with the irregularity intensity is found in Figures 3(a), 3(b), and 3(c) for $\theta = 50^\circ, 68^\circ$, and 78° that are, respectively, the magnetic dip angles at Arecibo, Boulder, and Tromsø. These results show that spread F is quite insensitive to the magnetic dip angle, namely, that spread F should not depend upon the locations of ionosondes. We conclude that spread F echoes on the ionograms are introduced by the irregularities with polarization directions within the meridian plane but not by those whose polarization directions are perpendicular to the meridian plane.

The different occurrence frequencies of artificial spread F noticed at Arecibo, Boulder, and Tromsø are most probably due to the excitation of different types of irregularities. The o mode and x mode pump waves transmitted from the Boulder heating facilities cannot be separated as easily as those from the Arecibo or the Tromsø facilities. This fact can be evidenced by the measurements of HF wave-induced short-scale irregularities at Boulder (Fialer, 1974) showing that x mode can still excite short-scale irregularities though not as efficiently as o mode wave. The heater wave (either o mode or x mode) induced irregularities at Tromsø are expected to be oriented in the directions perpendicular to the meridian plane. This may explain why spread F has never been observed since the Tromsø facilities were operated a few years ago. We note that when the heater is operated in o mode at Arecibo, no spread F or change of reflection heights can be seen (L.M. Duncan, private communication, 1984). This agrees with the theoretical prediction of the generation of large-scale irregularities by the filamentation instability (Kuo and Schmidt, 1983) and supports the proposed model of spread F mechanism.

REFERENCES

- Fialer, P.A., Field-Aligned Scattering from a Heated Region of the Ionosphere - Observation at HF and VHF, Radio Sci., 9, 923-940, 1974.
- Kuo, S.P. and G. Schmidt, Filamentation Instability in Magneto Plasmas, Phys. Fluids 26, 2529-2536, 1983.
- Shoven, R.L. and D.M. Kim, Time Variations of HF-Induced Plasma Waves, J. Geophys. Res. 83, 623-628, 1978.
- Stubbe, P. et.al., Ionospheric Modification Experiments in Northern Scandinavia, JATP 44, 1025-1041, 1982.
- Utlaut, W.F., A Survey of Ionospheric Modification Effects Produced by High-Power HF Radio Waves, AGARD Conf. Proc., 138, 3-1-3-16, 1973.

ACKNOWLEDGEMENTS

This work was supported jointly in part by the NSF Grant ATM-8315322 and in part by the AFOSR Grant No. AFOSR-83-0001 at Polytechnic Institute of New York and by AFGL contract F19628-83-K-0024 at Regis College Research Center.

ARTIFICIAL IONOSPHERIC DISTURBANCES CAUSED BY POWERFUL RADIO WAVES

M.C. Lee

Regis College Research Center, Weston, Mass. 02193

S.P. Kuo

Polytechnic Institute of New York, Long Island Center
Farmingdale, N.Y. 11735

ABSTRACT

Artificial ionospheric disturbances evidenced as fluctuations in plasma density and geomagnetic field can be caused by powerful radio waves with a broad frequency band ranging from a few KHz to several GHz. The filamentation instability of radio waves can produce both large-scale plasma density fluctuations and large-scale geomagnetic field fluctuations simultaneously. The excitation of this instability is examined in the VLF wave injection experiments, the envisioned MF ionospheric heating experiments, the HF ionospheric heating experiments and the conceptualized Solar Power Satellite project. Significant geomagnetic field fluctuations with magnitudes even comparable to those observed in magnetospheric (sub)storms can be excited in all of the cases investigated. Particle precipitation and airglow enhancement are expected to be the concomitant ionospheric effects associated with the wave-induced geomagnetic field fluctuations.

I. INTRODUCTION

Manifest ionospheric disturbances may be produced by powerful radio waves such as fluctuations in ionospheric density, plasma temperature, and the earth's magnetic field (see e.g., Fejer, 1979; Stubbe et al., 1982). Among them, we single out for discussion the excitation of ionospheric density irregularities and the geomagnetic field fluctuations. The interesting finding in our theoretical analyses is that the geomagnetic field fluctuations may be excited simultaneously with large-scale field-aligned ionospheric irregularities by radio heater waves. The frequencies of radio heater waves may be as low as in the VLF band and as high as in the SHF band.

Unexpectedly large perturbations in the earth's magnetic field ($\sim 10.8\gamma$) were observed in the Tromsø HF ionospheric heating experiments (Stubbe and Kopka, 1981; Kuo and Lee, 1983). Transmitters operated at frequencies close to but less than the local electron gyrofrequency are expected to cause both plasma density fluctuations and geomagnetic field fluctuations in the ionosphere if MF signals are transmitted or in the magnetosphere if VLF signals are injected, instead (Lee and Kuo, 1984). Microwave transmissions at the conceptualized power density (230 W/m^2) from the Solar Power Satellite (SPS) are also expected to perturb the earth's magnetic field significantly in the ionosphere along the beam path. Our studies, therefore, add an additional effect to those that should be assessed as the possible environmental impact of the SPS program.

The formulation of the theory is first presented in Section I. In the subsequent four sections (i.e., Sections III-VI), we discuss the excitation of the instability in the VLF wave injection experiments, the envisioned MF ionospheric heating experiments, the Tromsø HF ionospheric heating experiments, and the conceptualized Solar Power Satellite program, respectively. The conclusions are finally drawn in Section VII with a brief discussion.

II. THEORY

For simplicity, radio waves are assumed to be circularly polarized propagating along the earth's magnetic field. This is a reasonable assumption for the VLF wave injection experiments and the Tromsø HF ionospheric heating experiments. As for the microwave propagation, the geomagnetic field imposes a relatively immaterial effect. If the positive z axis of a rectangular coordinate system represents the wave propagation direction and is taken to be parallel to the geomagnetic field, the monochromatic radio wave with frequency, ω_0 , and wave vector, k_0 , can be represented by $E_0(r,t) = \epsilon_0(\hat{x} \pm i\hat{y}) \exp[i(k_0 z - \omega_0 t)] + \text{C.C.}$ where the wave field amplitude, ϵ_0 , is assumed to be a constant;

the \pm signs designate the right-hand and the left-hand circular polarizations, respectively.

Since the wave field interacts with the charged-particles, the plasmas experience a radiation pressure force (i.e., the nonlinear Lorentz force) and a thermal pressure force. The latter force results from the collisional dissipation of wave energy in plasmas. If the wave field is intense enough, a sideband mode (ϵ_1) can be excited together with zero-frequency modes via the filamentation instability, this is similar to the self-focusing instability of a radio wave beam. This high-frequency sideband is a quasi-mode, satisfying the Fourier transform wave equation

$$[k_0^2 + k^2 - \frac{\omega_0^2}{c^2}] \epsilon_1 - k_0^2 \frac{\hat{A}}{zz} - k^2 \frac{\hat{A}}{xx} + ik_0 \frac{\partial}{\partial x} (\frac{\hat{A}}{xz} + \frac{\hat{A}}{zx}) \cdot \epsilon_1 = i \frac{4\pi\omega_0}{c^2} (J_L + J_N) \quad (1)$$

where $\epsilon_1 = (\tilde{\epsilon}_{11} \cos kx + \frac{1}{2} \tilde{\epsilon}_{1z} \sin kx) \exp(\gamma t)$ is the wave field perturbation with the growth rate, γ , and the filamentation wave vector, $k = \hat{k}k$; J_L and J_N represent the induced linear and nonlinear electric current densities. While J_L given by $-en_0 \tilde{V}_1$ results from the linear response of electrons to the sideband field (ϵ_1), J_N includes two parts, $-en_0 \tilde{V}_M$ and $-c\delta n''_0$, that are nonlinear beating currents caused by the nonlinear coupling between the purely growing mode (δn and δB) and the incident wave field (ϵ_0). The electron velocity perturbations denoted by \tilde{V}_0 , \tilde{V}_1 , and \tilde{V}_M , have the following expressions:

$$\tilde{V}_j = -i \frac{e}{m} \frac{\omega_0}{(\omega_0^2 - \Omega_e^2)} [\epsilon_{j1} + \frac{1}{2} (1 - \frac{\Omega_e^2}{\omega_0^2}) \epsilon_{jz} + i \frac{\Omega_e}{\omega_0} \frac{\hat{A}}{zx} \epsilon_j]$$

where $j = 0, 1$ represents the response of electrons to the incident wave field (ϵ_0) and the sideband field (ϵ_1) respectively;

$$\tilde{V}_M = -i \frac{e}{mc} \frac{\omega_0}{(\omega_0^2 - \Omega_e^2)} [\tilde{V}_0 \times \frac{\hat{A}}{z} + i \frac{\Omega_e}{\omega_0} \tilde{V}_0] \delta B$$
 is the electron velocity perturbation induced by

the $\tilde{V}_0 \times \delta B$ Lorentz force, where M , Ω_e , e , and c have their conventional meanings as the electron mass, the electron gyrofrequency, the electric charge, and the speed of light in vacuum, respectively. Because of the large inertia, the corresponding ion responses have been ignored.

The purely growing mode has the general form of $\delta P = \delta \tilde{P} (\cos kx) \exp(\gamma t)$, that is associated with the excitation of both the plasma density fluctuations (i.e., $\delta \tilde{P} = \delta \tilde{n}$) and the geomagnetic field fluctuations (i.e., $\delta \tilde{P} = \frac{1}{2} \delta B$). It is the wave-induced quasi-DC current that gives rise to the magnetostatic fluctuations. This can be seen in the Maxwell equation

$$(k^2 + \frac{1}{c^2} \frac{\partial^2}{\partial t^2}) \delta \tilde{A} = \frac{4\pi}{c} e N_0 (\delta \tilde{V}_1 - \delta \tilde{V}_e)_y = \frac{4\pi}{c} \delta J_y \quad (2)$$

where $\delta \tilde{A}$ is the vector potential defined by $\nabla \times \delta \tilde{A} = \delta B$ and the Coulomb gauge $\nabla \cdot \delta \tilde{A} = 0$ has been chosen in (2). The wave-induced quasi-DC current, $\delta J_y = en (\delta \tilde{V}_1 - \delta \tilde{V}_e)_y$, and a relation between δn and δB can be derived from Equation (2), the continuity equation and the momentum equation for both electrons and ions. They are

$$\delta J_y = \frac{en_0}{\Omega_1} \{ \frac{F_{ex}}{M} + \frac{\partial}{\partial x} (\frac{\delta T_e}{M}) - [\frac{\gamma (\gamma + \nu_{in})}{k} + kc_s^2] (\frac{\delta n}{n_0}) \} \quad (3)$$

$$\text{and } \frac{\delta n}{n_0} = [1 + (1 + \frac{\nu_e}{\gamma}) (\frac{k^2 c^2 + \gamma^2}{\omega_{pe}^2})] (\frac{\delta B}{B_0}) \quad (4)$$

where M , Ω_1 , ω_{pe} , c_s , ν_e , and ν_{in} are, respectively, the ion mass, the ion gyrofrequency, the electron plasma frequency, the ion acoustic velocity, the electron-ion collision frequency, and the ion-neutral collision frequency; δT_e is the electron temperature perturbation caused by the collisional dissipation of the radio pump and the excited sideband; and F_{ex} is the x component of the nonlinear Lorentz force

$$F_{ex} = m \nabla (V_0^* \cdot \tilde{V}_1 + V_0 \cdot \tilde{V}_1^*) + i \frac{e}{\omega_0} m \{ -ik_0 (\tilde{V}_1^* V_0 + \tilde{V}_1 V_0^*) \times \frac{\hat{A}}{z} + \frac{V_0^* \times [V \times (\tilde{V}_1 \times \frac{\hat{A}}{z})] - V_0 \times [V \times (\tilde{V}_1^* \times \frac{\hat{A}}{z})]}{\omega_{pe}^2} \}$$

It is seen from (3) that the wave-induced quasi-DC current is primarily caused by the $F \times B$ drift motion of electrons under the influence of the thermal pressure force, $n_0 (\partial/\partial x) \delta T_e$, and the nonlinear Lorentz force, $n_0 F_{ex}$. The electron temperature perturbation (δT_e) obtained from the

electron energy equation is found to be

$$\delta T_e = \frac{2}{3} \frac{Q_e + \gamma T_o \delta n}{n_o \bar{\gamma}} \quad (5)$$

where $Q_e = 2v_e n_o m (\bar{V}_o^* \cdot \bar{V}_1 + \bar{V}_o \cdot \bar{V}_1^*)$ is the wave energy dissipation rate in the electron gas due to the differential Ohmic loss of the incident wave and the excited sidebands, and $\bar{\gamma} = \gamma + 2v_e (m/M) + v_e k^2 V_t^2 / \Omega_e^2$, where V_t is the electron thermal velocity.

Equation (4) shows that the simultaneously excited δn and δB are proportional to each other. In all cases under study, $v_e \gg \gamma$ and $k^2 c^2 \gg \gamma^2$. Therefore, Equation (4) can be reduced to

$$\frac{\delta n}{n_o} = [1 + (\frac{v_e}{\gamma}) (\frac{k^2 c^2}{\omega_{pe}^2})] (\frac{\delta B}{B_o}) \quad (4')$$

indicating that if $(v_e/\gamma)(k^2 c^2/\omega_{pe}^2)$ is much greater than unity, the magnetostatic fluctuations $(\delta B/B_o)$ is much less than the plasma density fluctuations $(\delta n/n_o)$. It is thus expected that significant magnetic field fluctuations are associated with the excitation of large-scale (i.e., small k) modes.

The coupled mode equation for the purely growing mode that can be obtained from (2) and (3) with the aid of (5) has the expression of

$$((\gamma^2 + k^2 c^2) [1 + \frac{m}{M} (1 + \frac{v_e}{\gamma}) f + \omega_{pe}^2 f] \delta B = \frac{8\pi e c k}{3m\Omega_e \bar{\gamma}} \frac{\partial}{\partial x} Q_e \quad (6)$$

where $f = (\gamma \bar{v}_{in} + k^2 c_s^2 + 2 \gamma k^2 V_s^2 / 3 \bar{\gamma})$; $\bar{v}_{in} = \gamma + v_{in}$; ω_{pi} and V_s are the ion plasma frequency and the ion thermal velocity. It should be mentioned that the nonlinear Lorentz force term (F_e) has been neglected in (6) because it is negligibly small compared to the differential Ohmic heating force term (Q_e). Substituting (4') into (6) and eliminating δn from (1) and (6) yields the dispersion relation

$$\begin{aligned} & k^2 c^2 (\gamma + \frac{m}{M} \bar{v}_e f) + \gamma \omega_{pi}^2 f \\ & = 2 (\frac{\omega_o}{\Omega_e}) (\frac{\omega_{pe}}{\omega_o \mp \Omega_e})^4 (\frac{e c}{m c})^2 [(\frac{\omega_o}{\Omega_e} \mp 1) \bar{v}_e \frac{k^2 c^2}{\omega_{pe}^2} + \gamma \frac{\omega_o}{\Omega_e}] [\\ & \frac{4}{3} (\frac{v_e}{\bar{\gamma}}) \frac{(4 - q_+ - P_+ q_+)}{(1 + P_+ - P_+ q_+)}] \end{aligned} \quad (7)$$

$$\text{where } \bar{v}_e = \gamma + v_e; P_{\pm} = \frac{\omega_o (\omega_o^2 - \omega_{pe}^2 \mp \omega_o \Omega_e)}{(\omega_o \mp \Omega_e) (\omega_o^2 - \omega_{pe}^2 - k^2 c^2)} \quad (8a)$$

$$\text{and } q_{\pm} = \pm \frac{k^2 c^2 (\omega_o^2 - \Omega_e^2)}{\omega_o \Omega_e \omega_{pe}^2}; \quad (8b)$$

$P_+(P_-)$ and $q_+(q_-)$ correspond to the right - (left -) hand circularly polarized wave. The threshold field (e_{th}) of the instability is determined from (7) by taking $\gamma = 0$, namely,

$$|\frac{e c_{th}}{m c}|^2 = 0.75 \frac{(\omega_o \mp \Omega_e)^3}{\omega_o \omega_{pe}^2} \frac{k^2 V_t^2 (2 \frac{m}{M} + \frac{k^2 V_t^2}{\Omega_e^2}) (1 + P_{\pm} - P_{\pm} q_{\pm})}{(4 - q_{\pm} - P_{\pm} q_{\pm})} \quad (9)$$

These characteristics of the instability are discussed separately for different wave frequency regimes of the incident radio waves as follows.

III. VLF VE INJECTION EXPERIMENTS

The VLF signals transmitted from the Siple circular polarization (i.e., whistler modes) on

their paths through the neutral atmosphere and into the ionosphere (Kintner et al., 1983). The whistler waves are assumed to satisfy the cold plasma dispersion relation

$$1 - \frac{\omega_{pe}^2}{\omega_o(\omega_o - |\Omega_e|)} = \frac{k_o^2 c^2}{\omega_o^2}$$

in the wave propagation regime: $|\Omega_e| \ll \omega_o < |\Omega_e|$. Since the positive z axis represents the wave propagation direction and has been taken to be parallel to the geomagnetic field, $\Omega_e > (<) 0$ for the right- (left-) hand circularly polarized wave and thus

$$P_+ = P_- = \omega_o (\omega_o^2 - \omega_{pe}^2 - \omega_o |\Omega_e|) / (\omega_o - |\Omega_e|) (\omega_o^2 - \omega_{pe}^2 - k^2 c^2) \text{ and } q_+ = q_- = k^2 c^2 (\omega_o^2 - \Omega_e^2) /$$

$$\omega_o |\Omega_e| \omega_{pe}^2 \text{ for a whistler mode.}$$

In the upper atmosphere, the electron plasma frequency is much greater than the electron cyclotron frequency, viz., $\omega_{pe}^2 \gg \Omega_e^2 > \omega_o^2$. Therefore, $P \approx -\omega_o \omega_{pe}^2 / (|\Omega_e| - \Omega_o) (\omega_{pe}^2 + k^2 c^2) < 0$ and

$q = -k^2 c^2 (\Omega_e^2 - \omega_o^2) / \omega_o |\Omega_e| \omega_{pe}^2 < 0$. The positive RHS of (8) thus requires the factor, $(1 + P - q)$, to be negative, namely,

$$1 - \frac{\omega_o \omega_{pe}}{(|\Omega_e| - \omega_o) (\omega_{pe}^2 + k^2 c^2)} - \frac{k^2 c^2 (|\Omega_e| + \omega_o)}{(\omega_{pe}^2 + k^2 c^2) |\Omega_e|} < 0. \quad (10)$$

For the excitation of large-scale modes (i.e., $\omega_{pe}^2 \gg k^2 c^2$), the above inequality leads to $\omega_o > |\Omega_e|/2$. In other words, the filamentation instability of whistler waves that generate both plasma density fluctuations and geomagnetic field fluctuations can only be excited within the narrow frequency range:

$$|\Omega_e| > \omega_o > |\Omega_e|/2 \quad (11)$$

Since $|\Omega_e| \sim 1.4$ MHz in the ionosphere (e.g., the F region) and $|\Omega_e| \sim 13.65$ MHz in the magnetosphere at $L = 4.0$, the condition for the instability shown in (11) leads to the following conclusions. The frequencies of VLF signals that are injected in the active VLF wave experiments typically range from a few KHz to a few tens of KHz (<30 KHz). These signals are not expected to cause ionospheric disturbances via the filamentation instability. But those with frequencies larger than 6.83 KHz but less than 13.65 KHz can excite the instability in the magnetosphere at $L = 4.0$. It is predicted from (11) that ionospheric disturbances caused by the filamentation instability of whistler waves are possible if the wave frequencies are less than $|\Omega_e| \sim 1.4$ MHz but greater than $|\Omega_e|/2 \sim 0.7$ MHz, namely, whistler waves in the MF band can cause large-scale ionospheric density irregularities and geomagnetic field fluctuations in the ionosphere. Quantitative analyses of these two cases are illustrated as follows.

The relevant magnetospheric parameters used in this work include $|\Omega_e|/2\pi = 13.65$ KHz (i.e., $B_o \sim 500$ G), $\omega_{pe}/2\pi = 179$ KHz, $T_o = 0.4$ eV, and $M(H^+)/m = 1840$. If the VLF wave frequency is 10.9 KHz, i.e., $\omega_o/|\Omega_e| = 0.8$, the threshold field (ϵ_{th}) calculated from (9) are e.g., 12 μ V/m and 2 μ V/m for the excitation of modes with scale lengths of 10 Km and 100 Km, respectively. These threshold fields can be exceeded by the injected VLF waves from the Siple station even in the "non-ducted" whistler propagation mode. The growth rates of the instability expressed in terms of the threshold field is obtained from (7) as

$$k^2 c^2 (\gamma + \frac{m}{M} \bar{v}_e f) + \gamma \omega_{p1}^2 f = k^2 v_e^2 (2 \frac{m}{M} + k^2 \frac{v_e^2}{\Omega_e^2}) \frac{2}{|\Omega_e|} \frac{\omega_{pe}^2}{(\omega_o - |\Omega_e|)} \left| \frac{\epsilon_o}{\epsilon_{th}} \right|^2 \left(\frac{\omega_o - |\Omega_e|}{|\Omega_e|} \right) \frac{v_e}{\omega_{pe}^2} \cdot k^2 c^2 + \gamma \frac{\omega_o}{|\Omega_e|} \frac{v_e}{\gamma}.$$

This equation can be easily solved for γ under the following assumptions: $v_e \gg \gamma$, $k^2 c_s^2 \gg \gamma \bar{v}_{in}$, and $m/M \gg k^2 v_e^2 / \Omega_e^2$ that can be confirmed. For large-scale modes, $\omega_{pe}^2 \gg k^2 c^2$ (i.e., $\lambda \gg 1.7$ Km), the growth rate is found to have the following simple expression $\gamma \sim (2v_e k v_s / |\Omega_e|) (\epsilon_o / \epsilon_{th})$. This growth rate turns out to be independent of the scale lengths because as shown in (9), $\epsilon_{th} \propto k$. Although the threshold of the instability can be exceeded by the "non-ducted" whistler mode in the

magnetosphere at $L = 4.0$, the growth rate is rather small ($\sim 10^{-3}$ Hz) if $\epsilon_0/\epsilon_{th} \sim 0(1)$ because of the small electron-ion collision frequency (~ 0.1 Hz). However, the ϵ_0/ϵ_{th} of the "ducted" whistler mode may be increased by two to three orders of magnitude though only 20% of the injected VLF waves are found to propagate in the "ducted" whistler mode (Carpenter and Miller, 1976). The growth rate of ducted whistler waves can be as high as ($10^{-3} - 10^{-2}$) Hz, namely, the instability can be excited by the ducted mode within a few minutes.

For modes with scale lengths > 10 Km, $(\delta n/n_0) \approx (\delta B/B_0)$ from (4'). Presumably, a few percents of magnetospheric density fluctuations are able to be generated. Then, a few percents of geomagnetic field fluctuations in the magnetosphere at $L = 4.0$ is of the order of 10 γ (c.f. the background magnetic field ~ 500 γ), that may significantly affect the orbits of charged particles. The scintillations of the Siple signals received at Roberval, Canada (Inan et al., 1977), may be attributable to the excitation of large-scale plasma density fluctuations in the magnetosphere by the injected VLF waves via the filamentation instability.

IV. ENVISIONED MF IONOSPHERIC HEATING EXPERIMENTS

The ionospheric heating facilities located at, for example, Arecibo (Puerto Rico), Boulder (Colorado), and Tromsø (Norway) are currently operated at lowest frequencies on the order of 3 MHz. The transmission of signals at frequencies close to the electron gyrofrequency (≤ 1.4 MHz) would require a major antenna and transmitter change. In our "envisioned" MF ionospheric heating experiments, we adopt the typical ionospheric parameters: $|\Omega_e|/2\pi = 1.4$ MHz (i.e., $B_0 = 5 \times 10^4$ γ), $\omega_{pe}/2\pi = 6$ MHz, and $M(0+)/m = 16 \times 1840$. The threshold fields of the instability excited by the incident MF wave at 1.12 MHz (i.e., $\omega/|\Omega_e| = 0.8$) are found from (9) to be 6 mV/m and 0.4 mV/m for the excitation of modes with scale lengths of 100 m and 1 Km, respectively. If we assume that $\epsilon_0 = 0.3$ V/m, the growth rate of the instability for large-scale modes (i.e., $\omega_{pe}^2 \gg k^2 c^2$ or $\lambda \gg 50$ m) is about 1 Hz. Under the illumination of powerful MF radio waves, large-scale ionospheric disturbances can be produced in seconds.

It is obtained from (4') that $(\delta n/n_0) \approx 2.3 (\delta B/B_0)$ (e.g., $\lambda = 1$ Km) for modes with $\lambda \gg 50$ m. The excitation of a few percents of ionospheric density fluctuations are accompanied by the concomitant excitation of geomagnetic field fluctuations of the order of 500 γ , that is comparable to the perturbation in a severe magnetospheric (sub)storm.

V. HF IONOSPHERIC HEATING EXPERIMENTS

The HF radio waves transmitted in ionospheric heating (or modification) experiments have frequencies greater than the electron gyrofrequency ($\omega_0 \gg \Omega_e$) but less than FOF2 in the ionosphere. Ordinary (O) or extraordinary (X) modes have been employed. At the Tromsø facilities, these modes can be represented by two circularly polarized waves propagating along the geomagnetic field. Since the wave propagation direction is antiparallel to the geomagnetic field, the X and O modes correspond to a left-hand and a right-hand circularly polarized wave, respectively, and satisfy the dispersion relations:

$$1 - \frac{\omega_{pe}^2}{\omega_0(\omega_0 \mp |\Omega_e|)} = \frac{k^2 c^2}{\omega_0^2} \quad (12)$$

where the \mp signs denote the left- and right-hand circularly polarized waves, respectively.

Near the reflection heights of these pump waves (i.e., $k_0 \rightarrow 0$), it is from (12) that $\omega_{pe}^2 = \omega_0(\omega_0 \mp |\Omega_e|)$. In this case, P_{\pm} given by (8a) approximately vanish and $q_{\pm} \approx k^2 c^2 (\omega_0 \pm |\Omega_e|) / \omega_0^2 |\Omega_e|$ from (8b). Expression (9) then reduces to

$$\left| \frac{e \epsilon_{th}}{mc} \right|^2 = 0.75 \frac{(\omega_0 \mp |\Omega_e|)^2}{\omega_0^2 (4 - q_{\pm})} k^2 v_t^2 \left(2 \frac{m}{M} + \frac{k^2 v_t^2}{\Omega_e^2} \right) \quad (13)$$

where q_{\pm} (q_{\pm}) is for the right- (left-) hand circularly polarized wave. While the factor, $(4 - q_{\pm})$, is positive, a positive $(4 - q_{\pm})$ requires that $q_{\pm} < 4$, viz., $\lambda > (\pi c / \omega_0) [(\omega_0 \pm |\Omega_e|) / |\Omega_e|]^2$ (14) that can thus ensure the positive RHS of (13). If we take $|\Omega_e|/2\pi = 1.4$ MHz, $v_t = 1.3 \times 10^5$ m/sec, $M(0+)/m = 16 \times 1840$, $\omega_0/2\pi = 4.04$ MHz, the scale lengths of the modes that are excited by the X mode cannot be less than 70 meters according to (14). By contrast no minimum scale length is found in the case of O mode heating.

The threshold fields of kilometer-scale instability excited by either X or O mode are a few mV/m calculated from (13) that are quite small compared with the incident power densities (~ 1 V/m) of the Tromsø signals. Although the growth rate of the instability is generally a function of scale lengths, it has an asymptotic value found to be

$$\sim 2.5 \times 10^{10} \frac{v_e \omega_o^2 |\epsilon_o|^2}{\Omega_e^2 (\omega_o - |\Omega_e|)} \sim 3.4 \times 10 \text{ Hz for x - mode heating}$$

$$\sim 3.0 \times 10^{-2} \text{ Hz for O - mode heating}$$

when the scale lengths exceed a few hundreds of meters. It thus takes a few minutes for the instability to be excited in agreement with the observations that HF wave-induced geomagnetic field fluctuations needs a few minutes for development (Stubbe and Kopka, 1981). Substituting $v_e = 500$ Hz, $\gamma = 3.4 \times 10^{-2}$ Hz, $\lambda = 1$ Km, $\omega_{pe}/2\pi = 3.4$ MHz and $B_o = 5 \times 10^4$ γ into (4'), we have $\delta B = 4.4 \times 10^2$ ($\delta n/n_o = (4.4 - 44) \gamma$ for $(\delta n/n_o) = (1 - 10)\%$ also in agreement with the Stubbe and Kopka's experiments.

VI. CONCEPTUALIZED SOLAR POWER SATELLITE (SPS) PROJECT

The conversion of solar energy into microwaves is the basic idea behind the conceptualized Solar Power Satellite (SPS) project. The microwave energy would be transmitted from the satellite to the surface of the earth at a frequency of 2.45 GHz, that is much greater than the electron gyro-frequency ($|\Omega_e|$). The cross section of the microwave beam has been estimated to have a linear dimension of 10 Km in the ionosphere, and the incident power density at the center of the beam would be as high as 230 W/m^2 (i.e., the wave field intensity is about 640 V/m).

The formulation outlined above for the excitation of both plasma density fluctuations and geomagnetic field fluctuations can be also applied to the case of SPS project after some modifications. First of all, the microwave beam does not necessarily propagate along the geomagnetic field. Therefore, the positive z axis taken as the wave propagation direction is generally not in the direction of the geomagnetic field in this case. The polarization of the microwave is assumed to be within a meridian plane (i.e., the assumption of an ordinary mode) for efficiently exciting the field-aligned modes. Hence, the geomagnetic field perturbations (δB) are still in the direction of the background earth's magnetic field.

Since $\omega_o \gg |\Omega_e|$, we then have $P_{\pm} \approx 1$ from (8a) and $q_{\pm} \rightarrow \infty$ from (8b) by taking $|\Omega_e| \rightarrow 0$ (i.e., equivalent to an unmagnetized plasma case). The threshold field given by (9) then reduces to

$$\left| \frac{e \epsilon_{th}}{mc} \right|^2 = 0.38 \frac{\omega_o^2}{\omega_{pe}^2} k^2 v_t^2 \left(2 \frac{m}{M} + k^2 \frac{v_t^2}{\Omega_e^2} \right). \quad (15)$$

Using $\omega_o/2\pi = 2.45$ GHz, $\omega_{pe}/2\pi = 6$ MHz, $v_t = 1.3 \times 10^5$ m/sec, $|\Omega_e|/2\pi = 1.4$ MHz, and $m/M(0+) = 3.4 \times 10^{-5}$ in (15), we obtain $\epsilon_{th} = 2.89 \times 10^3/\lambda$. For instance, 2.89 V/m (2.89 V/m) for the excitation of the modes with a scale length of 100 m (1 Km). The growth rate derived from (7) has the approximate form

$$\gamma \sim 2v_e \left(\frac{m}{M} c_s \frac{\omega_o}{\Omega_e} \frac{\epsilon_o}{\epsilon_{th}} \right)^2 \quad (16)$$

In spite that the power density of the microwave beam is not uniform, we assume a constant value of 20 W/m^2 ($\sim 60 \text{ V/m}$), that is about one tenth of the maximum intensity at the beam center, for the calculation of the growth rate. Then, if v_e is taken to be 500 Hz, $\gamma \sim 5$ Hz for the excitation of one kilometer scale modes, namely, it takes a few seconds for the filamentation instability of microwaves to be excited.

The percentage of the geomagnetic field fluctuations is estimated from (4') as $(\delta B/B_o) \approx 0.4$ ($\delta n/n_o$), that has a comparable magnitude to that of ionospheric density fluctuations. For the 1% of $(\delta n/n_o)$, the geomagnetic field fluctuations (δB) can be as large as 200 γ . Such large geomagnetic field fluctuations are expected to significantly perturb the orbits of charged particles and, consequently, to cause particle precipitation and airglow effects. These ionospheric effects introduced by the powerful microwave beams should be taken into account in the evaluation of environmental impacts of the conceptualized Solar Power Satellite program.

VII. CONCLUSION AND DISCUSSION

Ionospheric and magnetospheric disturbances evidenced as fluctuations in plasma density and geomagnetic field can be generated by powerful radio waves with frequencies as low as a few KHz and as high as several GHz. Depending on the incident power density of radio waves, ionospheric (or magnetospheric) plasma density fluctuations and geomagnetic field fluctuations can be excited simultaneously by the filamentation instability of radio waves within a few seconds or minutes. This instability typically has kilometeric scale lengths in the ionosphere and tens of kilometeric scale lengths in the magnetosphere.

Radio waves with frequencies less than the electron gyrofrequency may propagate in a whistler mode. The excitation of the filamentation instability is only possible for those with frequencies greater than half the local electron gyrofrequency. This criterion for the instability leads to the conclusions that the injected VLF signals can produce magnetospheric rather than ionospheric disturbances. It is, however, predicted that ionospheric disturbances can be induced by MF signals whose frequencies are less than 1.4 MHz but larger than 0.7 MHz.

In the HF ionospheric heating experiments ($\omega_i^2 \gg \Omega^2$), both the ordinary and the extraordinary modes have been used. The scale lengths of the instability are found to have a cut-off in the case of extraordinary wave heating. The microwave beams that are transmitted from the conceptualized Solar Power Satellite to the surface of the earth are also expected to cause large ionospheric disturbances in their ordinary mode propagation. The geomagnetic field fluctuations caused by the filamentation instability of radio waves are very significant in all of the cases discussed in this paper. Their magnitudes may even become comparable to those seen in the magnetospheric (sub)storms.

It is interesting to note from (9) that the threshold field of the instability is inversely proportional to the electron plasma frequency. Therefore, ionospheric disturbances excited by radio waves should be most noticeable in the F region. Finally, it should be pointed out that the nonlinearity for the mode coupling is dominantly provided by the thermal pressure force due to the collisional dissipation of the pump wave field and the excited high-frequency sideband field in the electron gas. To emphasize this outstanding feature, the instability may be adequately termed the thermal filamentation instability of radio waves.

REFERENCES

- Carpenter, D.L., and T.R. Miller, Ducted magnetospheric propagation of signals from the Siple, Antarctica, VLF transmitter, *J. Geophys. Res.*, 81, 2692, 1976.
- Fejer, J.A., Ionospheric modification and parametric instabilities, *Rev. Geophys. Space Phys.*, 17, 135, 1979.
- Inan, U.S., T.F. Bell, D.L. Carpenter, and R.R. Anderson, Explorer 45 and Imp 6 Observations in the magnetosphere of injected waves from the Siple Station VLF transmitter, *J. Geophys. Res.*, 82, 1177, 1977.
- Kintner, P.M., R. Brittain, M.C. Kelley, D.L. Carpenter, and M.J. Rycroft, In situ measurements of trans-ionospheric VLF wave injection, *J. Geophys. Res.*, 83, 3235, 1978.
- Kuo, S.P., and M.C. Lee, Earth magnetic field fluctuations produced by filamentation instabilities of electromagnetic heater waves, *Geophys. Res. Lett.*, 10, 979, 1983.
- Lee, M.C., and S.P. Kuo, Excitation of magnetostatic fluctuations by filamentation of whistlers, to be published in the April issue of *Journal of Geophysical Research (Space Physics)*, 1984.
- Stubbe, P., and H. Kopka, Modification of the polar electrojet by powerful HF waves, *J. Geophys. Res.*, 82, 2319, 1977.
- Stubbe, P., H. Kopka, M.T. Rietveld, and R.L. Dowden, ELF and VLF wave operation by modulated HF heating of the current carrying lower ionosphere, *J. Atmos. Terr. Phys.*, 44, 1123, 1982.

ACKNOWLEDGMENTS

This work was supported by AFGL contract F19628-83-K-C024 at Regis College Research Center and jointly in part by the NSF grant ATM-8315322 and in part by the AFOSR grant AFOSR-83-0001 at Polytechnic Institute of New York.

A Theoretical Model of Artificial Spread F Echoes

S.P. Kuo
Polytechnic Institute of New York, Long Island Center
Farmingdale, NY 11735

M.C. Lee
Regis College Research Center, Weston, MA 02193

Steven C. Kuo
Polytechnic Institute of New York, Long Island Center
Farmingdale, NY 11735

ABSTRACT

Four invariants of the ray trajectory are found for a ray propagating in a horizontally stratified ionosphere under the density perturbation of HF wave-induced field-aligned irregularities. The reflection height of the ray can then be determined with the aid of those invariants. The results show that the reflection height of the ray varies drastically (namely, strong spread F echoes) in the presence of irregularities that polarize in the magnetic meridian plane. By contrast, the reflection height is not affected (namely, no spread F echoes) by those irregularities that polarize in the direction perpendicular to the meridian plane. Spread F is quite insensitive to the magnetic dip angle θ_0 in the region from 20° to 70° . The dependence of spread F on the scale length of the irregularity has also been examined for the case $\theta_0 = 50^\circ$. It is found that spread F is not caused by irregularity with scale length less than about 100 meters.

I. INTRODUCTION

Spread F that refers to diffuse echoes on an ionogram from the ionospheric F region was observed in the ionospheric heating experiments conducted at Boulder, Colorado [Utlaut, 1971]. This ionospheric phenomenon is generally believed to be caused by the excitation of large scale (a few hundreds of meters to kilometers), field-aligned ionospheric irregularities. However, spread F is a rare phenomenon in the experiments at Arecibo, Puerto Rico [Shoven and Kim, 1978] and it has not been observed at Tromsø, Norway since the new European heating facility has been in operation [Stubbe et al., 1982]. Evidences, such as radio star scintillations and the anomalous absorption of the diagnostic waves through the ionospheric heated region, indicate that large-scale ionospheric irregularities have been excited by HF heater waves at Arecibo and Tromsø. Hence, a lack of spread F echoes does not imply the absence of heater wave-induced ionospheric irregularities. This may be due to the difference in the polarization directions of the HF wave-induced irregularities. In general, field-aligned irregularities can have two independent polarization directions. One lies in the meridian plane and the other one is in the direction perpendicular to the meridian plane. The theoretical results of filamentation instability in magneto-plasmas [Kuo and Schmidt, 1983] also show that the irregularities excited by the o-mode pump and by the x-mode pump have different polarization directions. The irregularities excited by the o-mode pump are field-aligned and are polarized in the direction perpendicular to the meridian plane. By contrast, the irregularities excited by the x-mode pump are polarized in the meridian plane and are, in general, not field-aligned. However, the field-aligned nature of the irregularities may be established to reduce the diffusion damping along the magnetic field.

In the present work, the relationship between the spread-F echoes and the HF wave-induced irregularities is studied. The primary purpose of this study is to determine the effects of the irregularity polarizations, scale length, and the magnetic dipangle on the spread F-echo. In section II, the ray trajectory equations are analyzed to study the wave propagation in a horizontally stratified ionosphere under the density perturbation of the HF wave-induced field-aligned irregularities. Four invariants of the ray trajectory are found. Main results are illustrated in Figures. Conclusions are finally drawn in Section III.

II. MODEL AND ANALYSIS

We consider a horizontally stratified ionosphere having a scale length L . Thus, the unperturbed electron density is represented by $n_0(x) = n_0(1 + x/L)$, where x is the vertical coordinate and $n_0 = n_0(0)$ is the electron density at the reference plane $x=0$ located at height H . When field-aligned irregularities are present, the background electron density distribution is perturbed. Thus, the total density is the sum of the unperturbed density and the fluctuating densities of the irregularities. For those irregularities which are field-aligned in the magnetic meridian plane, the total density perturbation is simply expressed in a form of $\delta n_1 \sin k_1(x \cos \theta_0 + z \sin \theta_0)$, where $2\pi/k_1 = \lambda_1$ is the average scale length of the irregularities, θ_0 is the magnetic dip angle, and z is the horizontal coordinate as shown in Fig. 1. Whereas, the density perturbation associated with the irregularities which are field-aligned in the direction perpendicular to the magnetic meridian plane is modelled as $\delta n_2 \sin(k_2 y + \phi)$, where $\lambda_2 = 2\pi/k_2$ is the averaged scale length, y is the coordinate perpendicular to the meridian plane, and ϕ is the arbitrary phase angle. In this model, the total electron density distribution, $n(x)$ is then composed of three components, viz.,

$$n(x, z) = n_0(1 + x/L) + \delta n_1 \sin k_1(x \cos \theta_0 + z \sin \theta_0) + \delta n_2 \sin(k_2 y + \phi) \quad (1)$$

For simplicity, the effect of the geomagnetic field on wave propagation will be neglected in the following analyses. The dispersion relation for the wave propagation is thus given by

$$\omega^2 = \omega_{pe}^2 + k^2 c^2 \quad (2)$$

where ω and k are the wave frequency and the wave number respectively, and

$$\omega_{pe}^2 = \omega_{pe0}^2 [1 + x/L + (\delta n_1/n_0) \sin k_1(x \cos \theta_0 + z \sin \theta_0) + (\delta n_2/n_0) \sin(k_2 y + \phi)] \quad (3)$$

Since, in reality, the ionosonde antennas radiate radio wave beams with finite cross sections and spread angles, so it is more appropriate to consider the transmitted pulses to be composed of rays whose initial wave vectors and the horizontal locations on the reference plane $x=0$ are all different. The trajectory of each ray is then governed by the following set of characteristic equations:

$$\frac{d}{dt} x = k_x c^2 / \omega \quad (4)$$

$$\frac{d}{dt} y = k_y c^2 / \omega \quad (5)$$

$$\frac{d}{dt} z = k_z c^2 / \omega \quad (6)$$

$$\frac{d}{dt} k_x = - (\omega_{peo}^2 / 2\omega L) [1 + (\delta n_1 / n_o) (k_1 L \cos \theta_o) \cos k_1 (x \cos \theta_o + z \sin \theta_o)] \quad (7)$$

$$\frac{d}{dt} k_y = - (\omega_{peo}^2 / 2\omega) (\delta n_2 / n_o) k_2 \cos (k_2 y + \phi) \quad (8)$$

$$\frac{d}{dt} k_z = - \tan \theta_o (\omega_{peo}^2 / 2\omega L) (\delta n_1 / n_o) (k_1 L \cos \theta_o) \cos k_1 (x \cos \theta_o + z \sin \theta_o) \quad (9)$$

where Eqs. (5) and (8) form one set of coupled equations, and Eqs. (4), (6), (7) and (9) form the other set of coupled equations, but these two sets of equations do not couple to each other. However, those coupled equations can be separated by the invariants of the trajectory derived as follows. We first take the ratio of (5) and (8), which yields

$$\frac{dy}{dk_y} = - \frac{2k_y c^2}{\omega_{peo}^2 (\delta n_2 / n_o) k_2 \cos (k_2 y + \phi)} \quad (10)$$

Integrating this equation gives the first invariant of the trajectory

$$(\delta n_2 / n_o) \sin(k_2 y + \phi) + k_y^2 c^2 / \omega_{peo}^2 = \text{constant in time} = (\delta n_2 / n_o) \sin(k_2 y_o + \phi) + k_{yo}^2 c^2 / \omega_{peo}^2 \quad (11)$$

where the subscript o represents the initial value.

We next substitute (9) into (7) to yield

$$\frac{d}{dt} (k_x - \cot \theta_o k_z) = - \omega_{peo}^2 / 2\omega L \quad (12)$$

Integrating (12) from the initial height $x=0$ of the ray to the new height x at time t , leads to the second invariant relation

$$k_x - \cot \theta_0 k_z + (\omega_{peo}^2 / 2\omega L)t = \text{const. in time} = k_{x0} - \cot \theta_0 k_{z0} \quad (13)$$

We now construct an equation by first multiplying (4) and (6) by $\cos \theta_0$ and $\sin \theta_0$ respectively, and then summing them up. The result is

$$\frac{d}{dt} (x \cos \theta_0 + z \sin \theta_0) = (c^2 / \omega) (k_x \cos \theta_0 + k_z \sin \theta_0) \quad (14)$$

Two additional invariants will be derived as follows. From the ratio of (14) and (7), we obtain

$$\frac{d(x \cos \theta_0 + z \sin \theta_0)}{d k_x} = - \frac{2c^2 L}{\omega_{peo}^2} \frac{k_x \cos \theta_0 + k_z \sin \theta_0}{1 + (\delta n_1 / n_0) (k_1 L \cos \theta_0) \cos k_1 (x \cos \theta_0 + z \sin \theta_0)} \quad (15)$$

With the aid of (13), (14) and (4), (15) is integrated to obtain the third invariant

$$\begin{aligned} & x + (\tan 2\theta_0 / 2)z + (\delta n_1 / n_0)L(\cos^2 \theta_0 / \cos 2\theta_0) \sin k_1 (x \cos \theta_0 + z \sin \theta_0) + \\ & (c^2 L / \omega_{peo}^2) (k_x^2 + \tan 2\theta_0 k_x k_z) = \text{const. in time} = (\tan 2\theta_0 / 2)z_0 + (\delta n_1 / n_0) \\ & L(\cos^2 \theta_0 / \cos 2\theta_0) \sin(k_1 z_0 \sin \theta_0) + (c^2 L / \omega_{peo}^2) (k_{x0}^2 + \tan 2\theta_0 k_{x0} k_{z0}) \end{aligned} \quad (16)$$

The fourth invariant is obtained from integrating the resultant equation defined by the ratio of (14) and (9). It is

$$\begin{aligned} & (\tan 2\theta_0 / 2)z + (\delta n_1 / n_0)L(\sin^2 \theta_0 / \cos 2\theta_0) \sin k_1 (x \cos \theta_0 + z \sin \theta_0) + (c^2 L / \omega_{peo}^2) \\ & (-k_z^2 + \tan 2\theta_0 k_x k_z) = \text{const. in time} = (\tan 2\theta_0 / 2)z_0 + (\delta n_1 / n_0)L(\sin^2 \theta_0 / \cos 2\theta_0) \sin \\ & (k_1 z_0 \sin \theta_0) + (c^2 L / \omega_{peo}^2) (-k_{z0}^2 + \tan 2\theta_0 k_{x0} k_{z0}) \end{aligned} \quad (17)$$

However, (16) and (17) can be rearranged to reduce to much simpler forms. We first take the difference of (16) and (17) to yield

$$\begin{aligned} x + (\delta n_1/n_0)L \sin k_1 (x \cos \theta_0 + z \sin \theta_0) + (k_0^2 c^2 L / \omega_{peo}^2) \\ = (\delta n_1/n_0)L \sin (k_1 z_0 \sin \theta_0) + k_0^2 c^2 L / \omega_{peo}^2 \end{aligned} \quad (18)$$

where $k_0 = k(o)$. We next multiply (16) by $\sin^2 \theta_0$ and (17) by $\cos^2 \theta_0$ and then take their difference. The result is

$$\begin{aligned} x - z \cot \theta_0 + (c^2 L / \omega_{peo}^2) (k_x - k_z \cot \theta_0)^2 = -z_0 \cot \theta_0 \\ + (c^2 L / \omega_{peo}^2) (k_{x0} - k_{z0} \cot \theta_0)^2 \end{aligned} \quad (19)$$

We have shown that the trajectory of each ray is governed by four invariant relations (11), (13), (18) and (19) that are derived from two sets of coupled differential equations (4)-(9). Hence, the temporal evolution of any one of the four variables x, z, k_x and k_z , and either one of the two variables y and k_y , can be determined, with the aid of these invariants, by the corresponding rate equations, viz., equations (4)-(9). The elapsed time for each ray traveling from the reference height to the reflection height can in principle be determined by integrating (7) from $k_x = k_{x0}$ to $k_x = 0$, with the prescribed initial conditions: $x(o) = 0$, $z(o) = z_0$ and $k_z(o) = k_{z0}$. Since the density perturbation δn_2 produced by the irregularities oriented in the direction perpendicular to the magnetic meridian plane does not appear in Eq. (7), the reflection height of each ray is thus not expected to be modified by the irregularities oriented in the direction perpendicular to the meridian plane. However, the density perturbation δn_1 produced by the irregularities that are oriented within the meridian plane can affect the reflection height of the ray as seen in Eq. (7). One way to show this effect is to integrate Eq. (7) numerically. This equation can be integrated with the aid of the invariant relations (13), (18) and (19). If we assume that each ray of the antenna radiation beam has a straight trajectory from the ionosonde to the reference plane as shown in Fig. 1, then the initial conditions for ray trajectory starting from the reference plane can be defined as $x = x_0$, $k_{x0} = k_0 H / (H^2 + z_0^2)^{1/2}$, and $k_{z0} = k_0 z_0 / (H^2 + z_0^2)^{1/2}$, where z_0 is a free parameter characterizing the ray. By varying z_0 within the cross sectional range of the beam, a set of trajectories for the rays of the

beam can be determined. However, not all the rays can be reflected back to the ionosonde. Only the rays which can return to the ionosonde are responsible for the observed diffuse echoes on the ionogram, and hence the intensity of spread F is proportional to the maximum difference of the reflection heights of those rays. The boundary conditions at $x=0$ for a downgoing ray which can propagate straightly from the reference plane back to the ionosonde are defined to be $k_x = -k_o H / (H^2 + z_f^2)^{1/2}$ and $k_z = -k_o z_f / (H^2 + z_f^2)^{1/2}$, where z_f is the z coordinate of the ray on the reference plane. Those conditions can be satisfied only by rays with appropriate z_o . In other words, the conditions at $x=0$ for the upgoing rays which can be received later by the ionosonde can not be predefined. Instead, z_o and z_f have to be determined simultaneously.

Presented in Fig. 2 are the two distinctive trajectories for two different groups of rays in the beam. The rays which follow these trajectories can return to the ionosonde. It is shown that if the ionosonde transmitting beam is modelled by many rays having different initial locations on a reference plane, the spread F echoes can indeed be interpreted to be caused by the difference in the reflection heights of the returned signals. The virtual height spread is thus proportional to the maximum difference of these reflection heights.

We now employ the following parameters to analyze the system of Eqs. (7), (13), (18), and (19): $L = 50$ km, $\lambda_1 = 1$ km and $k_o^2 c^2 / \omega_{peo}^2 = 1$. z_o is allowed to vary for determining the trajectories of the rays. Only taken into account are the trajectories of the rays detectable to the ionosonde for determining the maximum difference Δx_{\max} from the reflection heights of these rays. Δx_{\max} vs the magnetic dip angle θ_o as calculated for $\alpha (= n_1/n_o) = .005, .01, .05$ and 0.1 and presented in Figs. 3(a)-(d). Shown in Figs. 4(a)-(c) are Δx_{\max} vs the irregularity intensity α for $\theta_o = 50^\circ, 68^\circ$, and 78° that correspond to magnetic dip angles at Arecibo, Boulder and Tromsø, respectively. The dependence of spread F on the scale length of the irregularity has also been examined for the case $\theta_o = 50^\circ$ and $\alpha = 0.05$. The result is presented in Fig. 5 showing that spread F can only be caused by irregularities with scale lengths larger than about 106 meters.

III. DISCUSSION AND CONCLUSIONS

A theoretical model of spread F echoes has been developed for determining the effects of the magnetic dip angle, irregularity intensity, and the polarization direction and the scale length of irregularity on the occurrence frequency and the intensity of spread F. We first show that irregularities polarized perpendicular to the meridian plane do not cause spread F. Therefore, only irregularities polarized within the meridian plane have been considered in the analyses for evaluating the afore-mentioned effects.

As shown in Figs. (3a)-(3d), spread F becomes prominent as the magnetic dip angle exceeds about 5° . The reflection height spread Δx_{\max} first increases rapidly to a maximum at about $\theta_o = 8^\circ$ (except for very low irregularity intensity, e.g., $\alpha = 0.001$, where the peak appears at $\theta_o \approx 20^\circ$) and then decreases monotonically to zero at $\theta_o = 90^\circ$. However, Δx_{\max} is quite flat in the region from 20° to 70° (30° to 80° for $\alpha = 0.001$). Furthermore, Δx_{\max} increases monotonically with the irregularity intensity as seen in Figs. (4a), (4b) and (4c) for $\theta_o = 59^\circ$, 68° , and 78° corresponding, respectively, to the magnetic dip angles at Arecibo, Boulder, and Tromsø. While a near linear dependence is found in the $\theta_o = 50^\circ$ and 68° cases, Δx_{\max} starts to approach a maximum at $\alpha = 0.02$ for $\theta_o = 78^\circ$. The dependence of spread F on the scale length λ_1 of irregularities has been examined for $\theta_o = 50^\circ$ and $\alpha = 0.05$. The result shown in Fig. 5 indicates that spread F appears only when $\lambda_1 > 106$ m. The reflection height spread remains a fairly constant value from 106m to about 500m. This value then increases monotonically by 35% at $\lambda_1 = 1$ km which is the largest scale length employed in the analyses. Our model shows that spread F is quite insensitive to the magnetic dip angle. As long as the irregularity with the polarization within the meridian plane exists, significant spread F should be observed over a wide range of latitude including Arecibo, Boulder, and even Tromsø. In other words, the appearance of spread F should not depend upon the locations of the ionosondes. We, therefore, conclude that spread F echoes on the ionograms are caused by the irregularities with polarization directions within the meridian plane and the scale lengths greater than about 100m. By contrast, irregularities with polarization directions perpendicular to the meridian plane do not give rise to spread F echoes.

The different occurrence frequencies of artificial spread F noticed at Arecibo, Boulder, and Tromsø are most probably due to the excitation of different types of irregularities. The o mode and x mode pump waves transmitted from the Boulder heating facilities cannot be separated as easily as those from the Arecibo or the Tromsø facilities. This fact can be evidenced by the measurements of HF wave-induced short-scale irregularities at Boulder [Fialer, 1974] showing that x mode can still excite short-scale irregularities though not as efficiently as o mode wave. The heater wave (either o mode or x mode) induced irregularities at Tromsø are expected to be oriented in the directions perpendicular to the meridian plane. This may explain why spread F has never been observed since the Tromsø facilities were operated a few years ago. We note that when the heater is operated in o mode at Arecibo, no spread F or change of reflection heights can be seen [L.M. Duncan, private communication, 1984]. This agrees with the theoretical prediction of the generation of large-scale irregularities by the filamentation instability [Kuo and Schmidt, 1983] and supports the proposed model of spread F mechanism.

ACKNOWLEDGEMENTS

This work was supported jointly in part by the NSF Grant ATM-8315322 and in part by the AFOSR Grant No. AFOSR-83-0001 at Polytechnic Institute of New York and by AFGL Contract F19628-83-K-0024 at Regis College Research Center.

REFERENCES

- Fialer, P.A. (1974), Field-Aligned Scattering from a Heated Region of the Ionosphere - Observation at HF and VHF, *Radio Sci.*, 9, 923-940.
- Kuo, S.P. and C.Schmidt (1983), Filamentation Instability in Magneto Plasmas, *Phys. Fluids* 26, 2529-2536.
- Shoven, R.L. and D.M. Kim (1978), Time Variations of HF-Induced Plasma Waves, *J. Geophys. Res.* 83, 623-628.
- Stubbe, P., H. Kopka, H. lauche, M.T. Rietveld, A. Brekke, O. Holt, T.B. Jones, T. Robinson, A. Hedberg, B. Thide, M. Crochet and H.J. Lotz (1982), Ionospheric Modification Experiments in Northern Scandinavia, *J. Atmos. Terr. Phys.* 44, 1025-1041.
- Utlaut, W.F. (1973), A Survey of Ionospheric Modification Effects Produced by High-Power HF Radio Waves, *AGARD Conf. Proc.*, 138, 3-1-3-16.

Figure Captions:

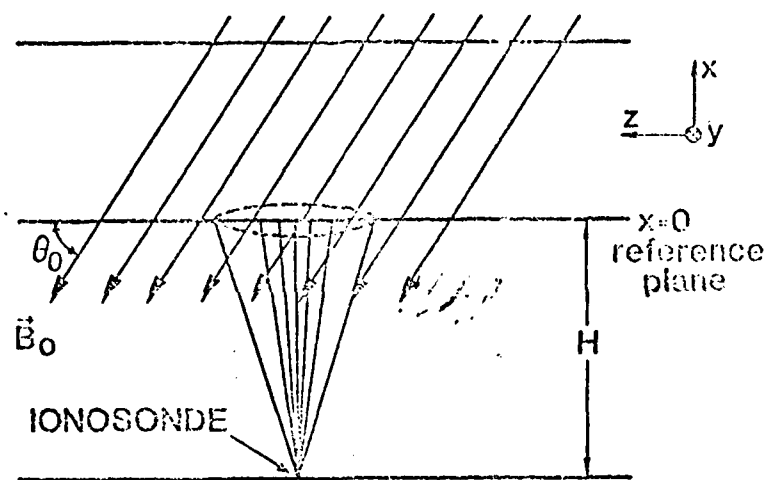
Fig. 1 - Coordinates used in the analysis.

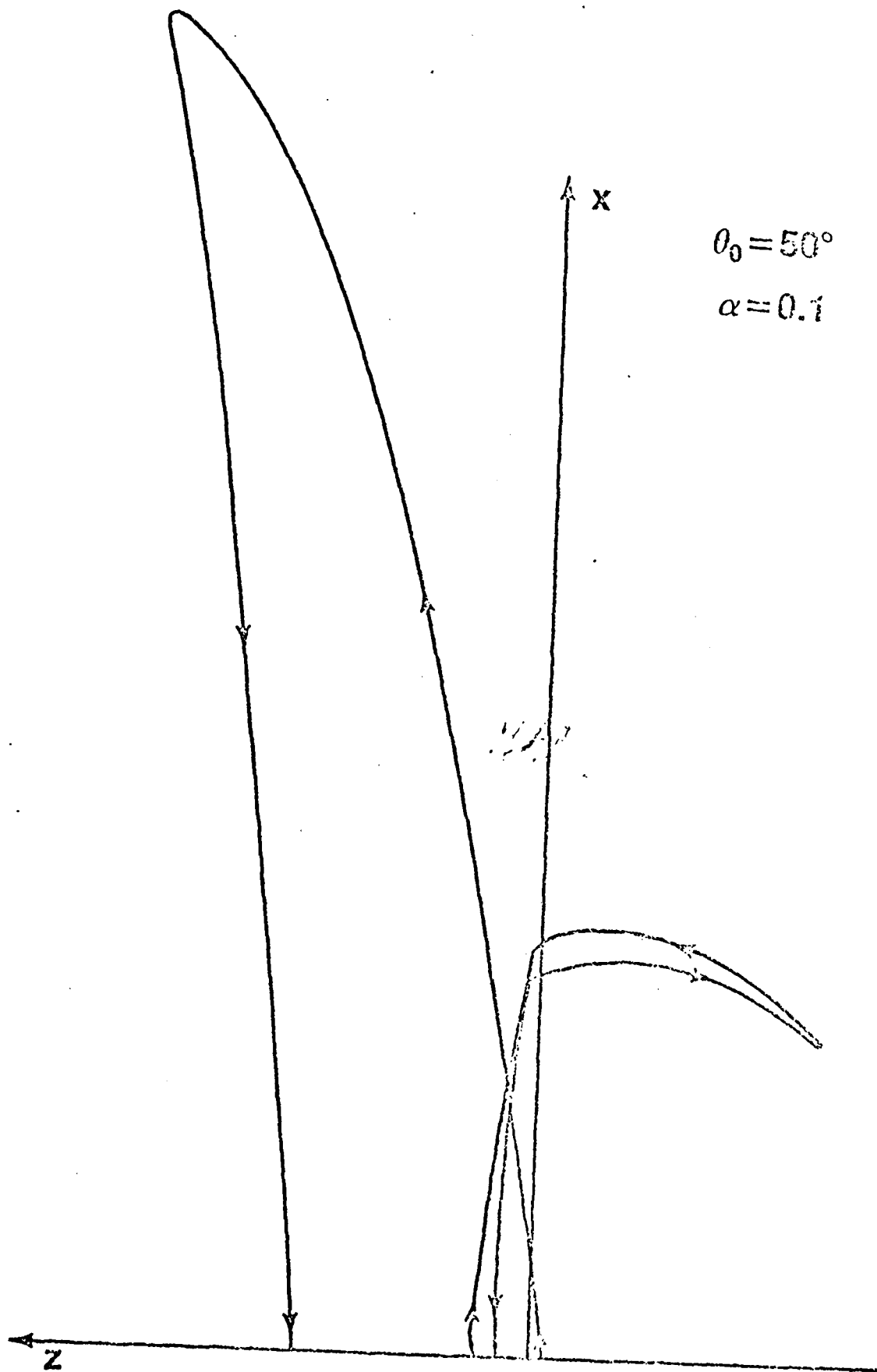
Fig. 2 - Example of the appropriate trajectories of the rays detectable to the ionosonde. The parameters used in the calculation are $\theta_0 = 50^\circ$, $L = 50\text{km}$, $\lambda_1 = 1\text{km}$, $k_0^2 c^2 / \omega_{\text{peo}} = 1$ and $\delta n_1 / n_0 = 0.1$.

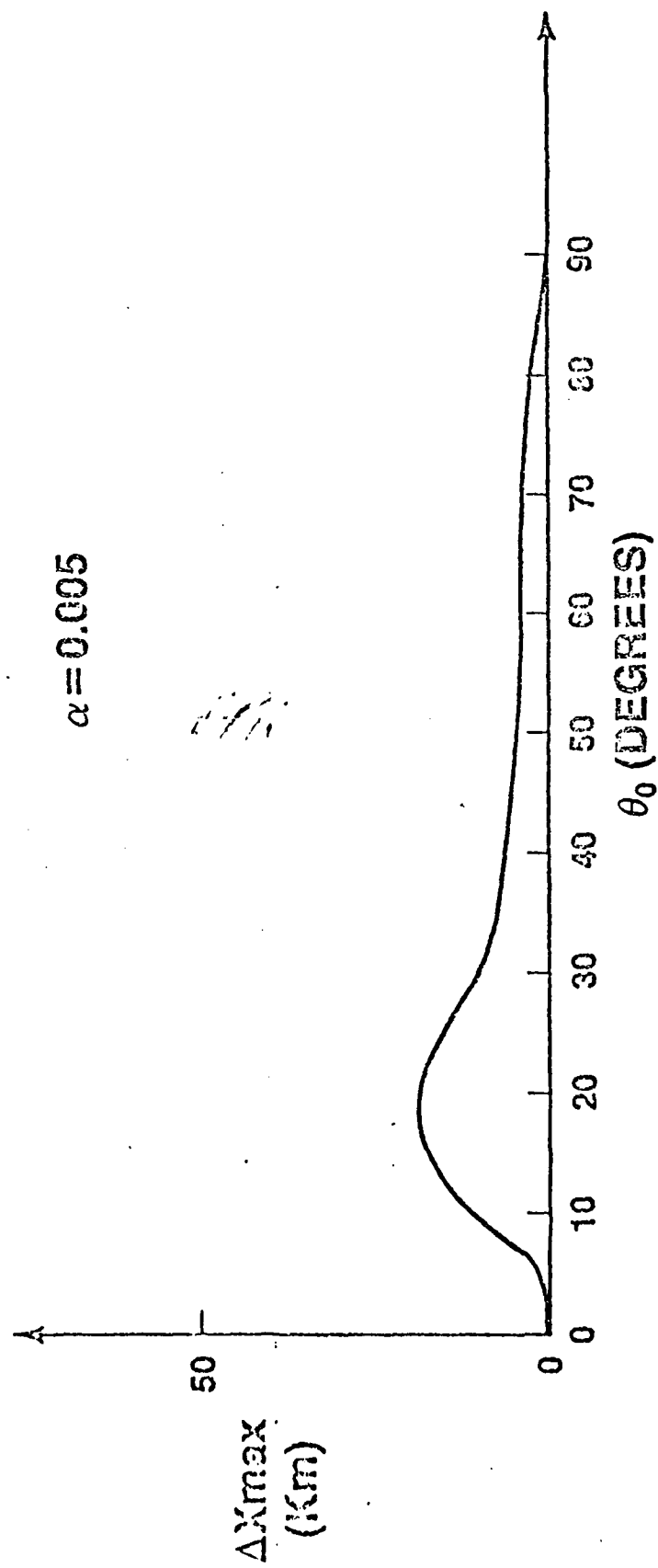
Fig. 3 - The functional dependence of the reflection height spread Δx_{max} of a diagnostic beam on the magnetic dip angle θ_0 for $\delta n_1 / n_0 =$ (a) 0.005, (b) 0.01, (c) 0.05, and (d) 0.1.

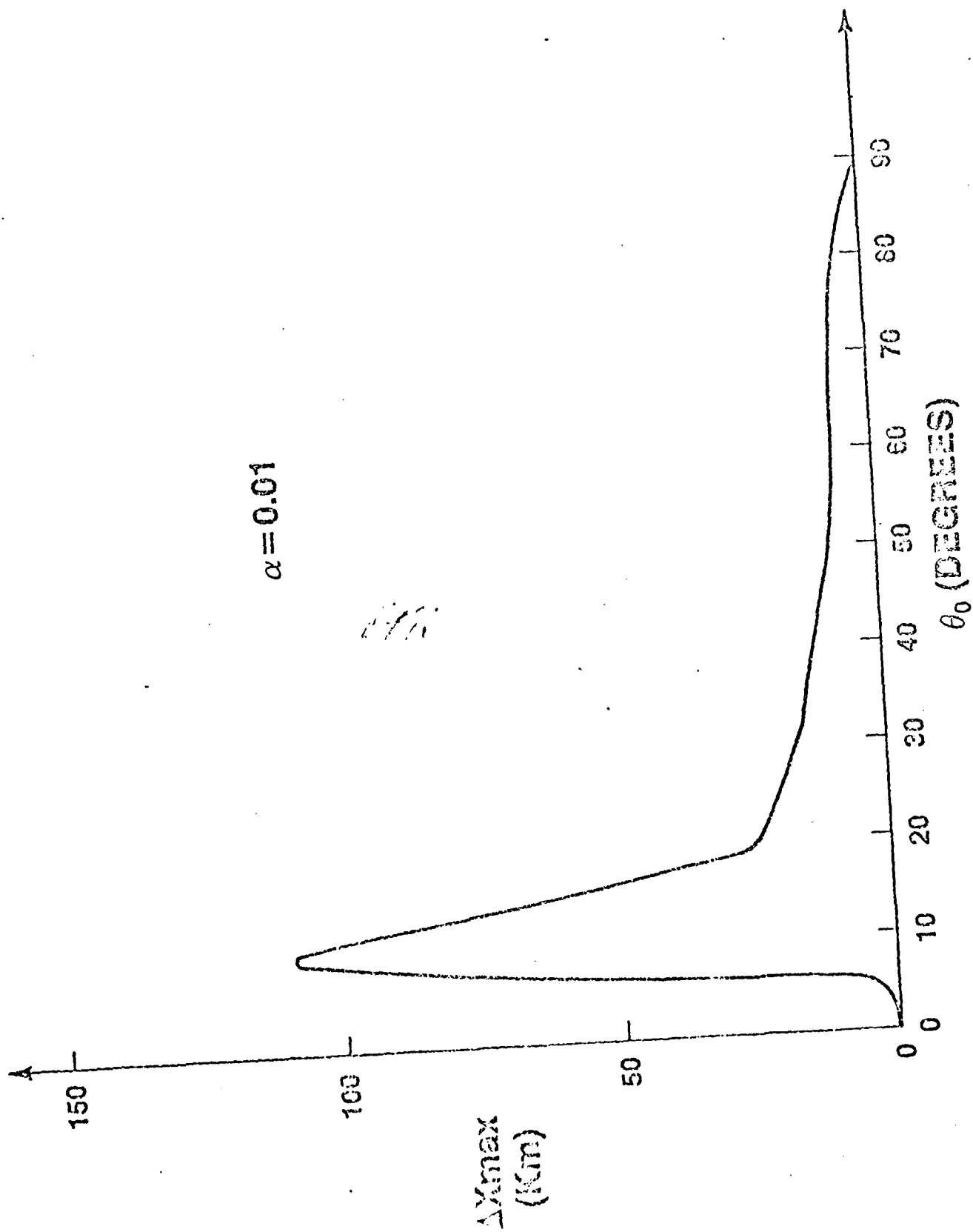
Fig. 4 - Δx_{max} vs α for $\theta_0 =$ (a) 50° , (b) 68° , and (c) 78° , where $\alpha = \delta n_1 / n_0$.

Fig. 5 - The dependence of the spread F on the scale length λ_1 of the irregularity, where $\theta_0 = 50^\circ$ and $\alpha = 0.05$.

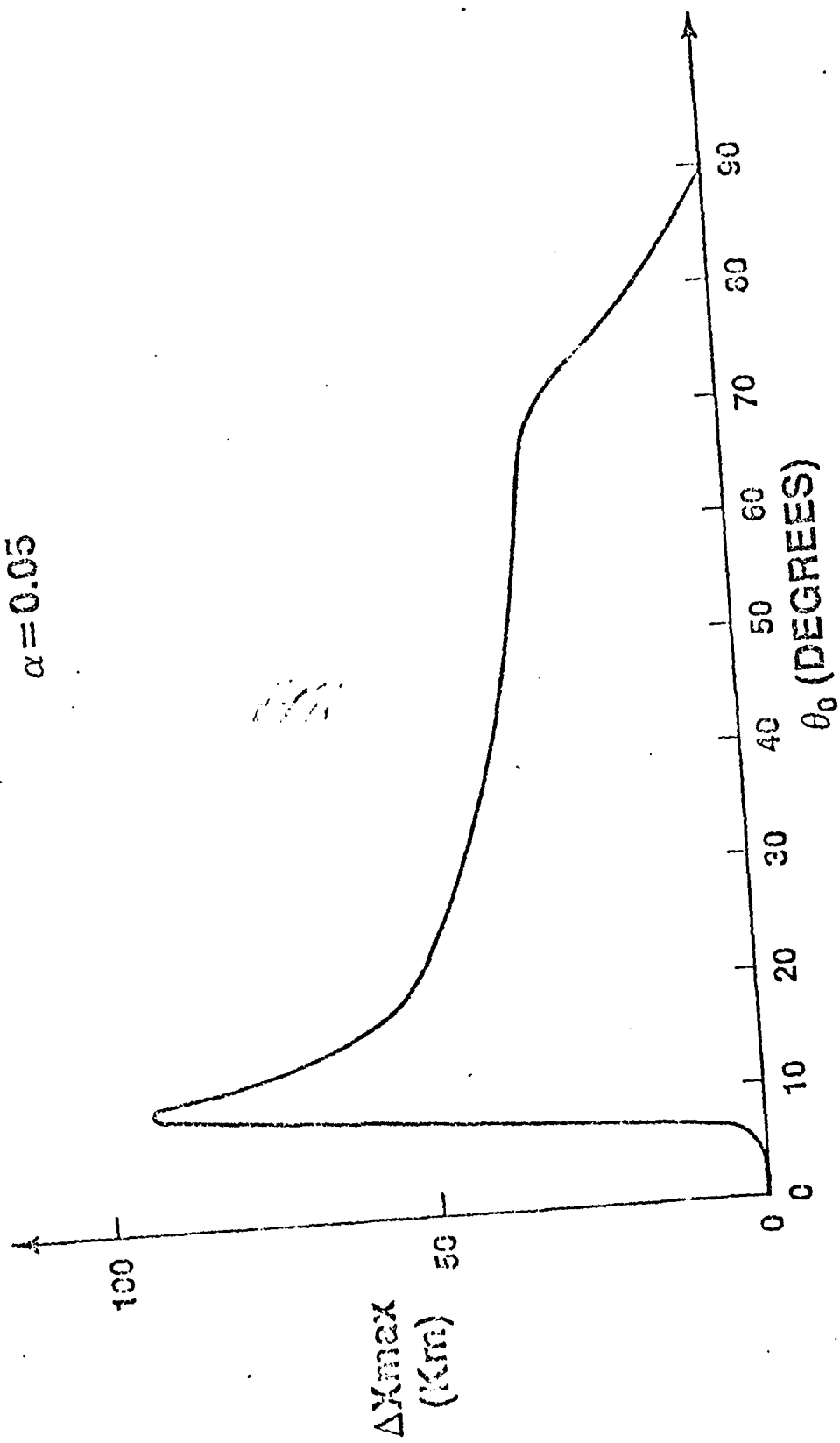








$\alpha = 0.05$



AD-A153 980

MILLIMETER WAVE GENERATION BY RELATIVISTIC ELECTRON
BEAMS(U) POLYTECHNIC INST OF NEW YORK FARMINGDALE DEPT
OF ELECTRICAL E. S P KUO ET AL. 01 DEC 84 POLY-84-007

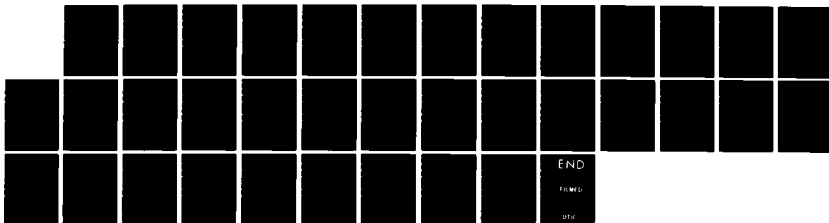
2/2

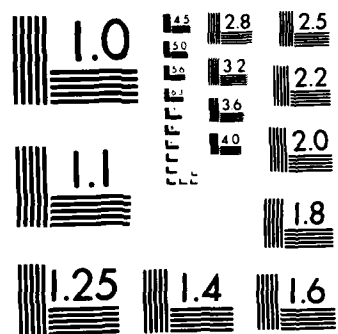
UNCLASSIFIED

AFOSR-TR-85-0342 AFOSR-83-0001

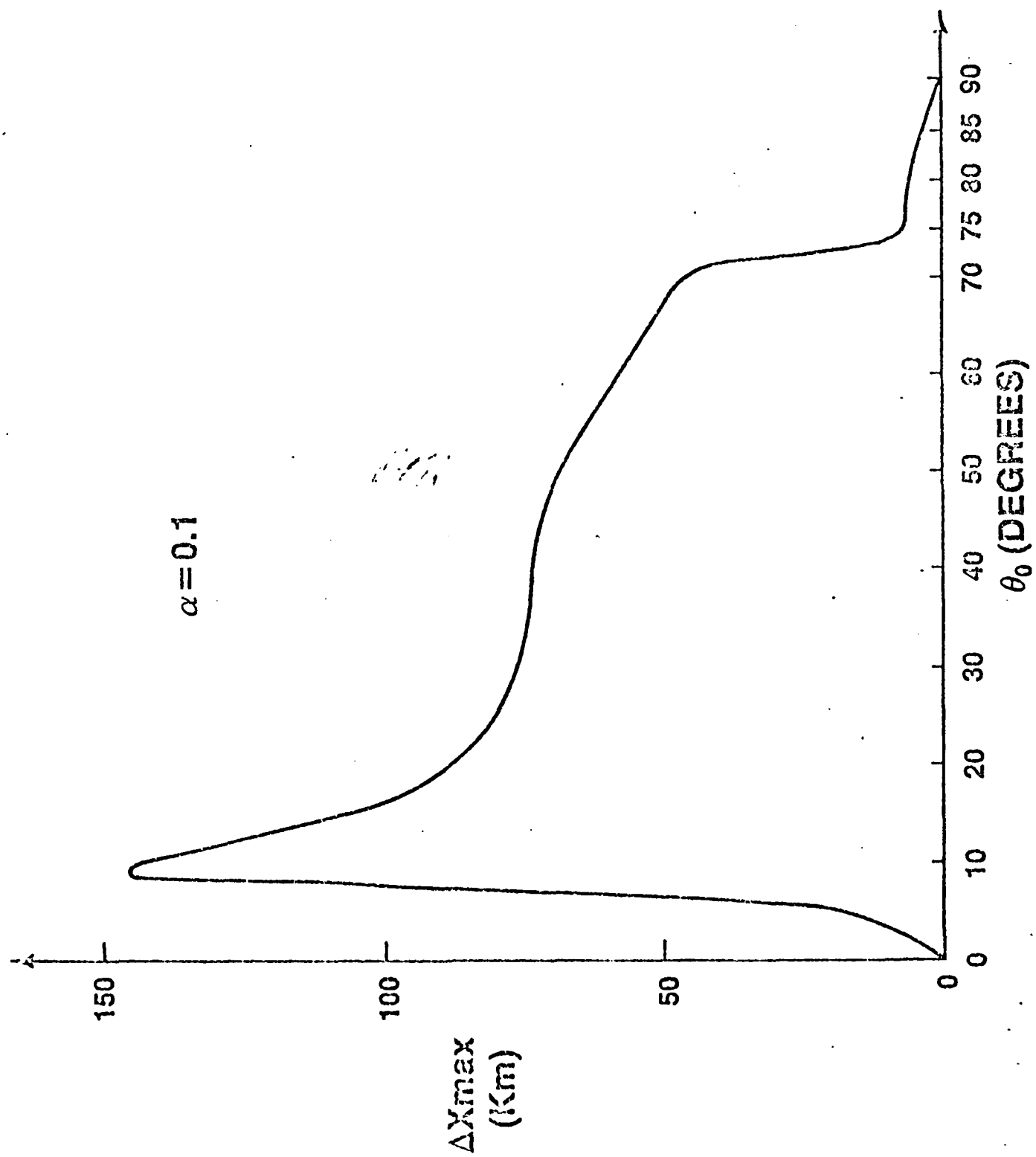
F/G 20/9

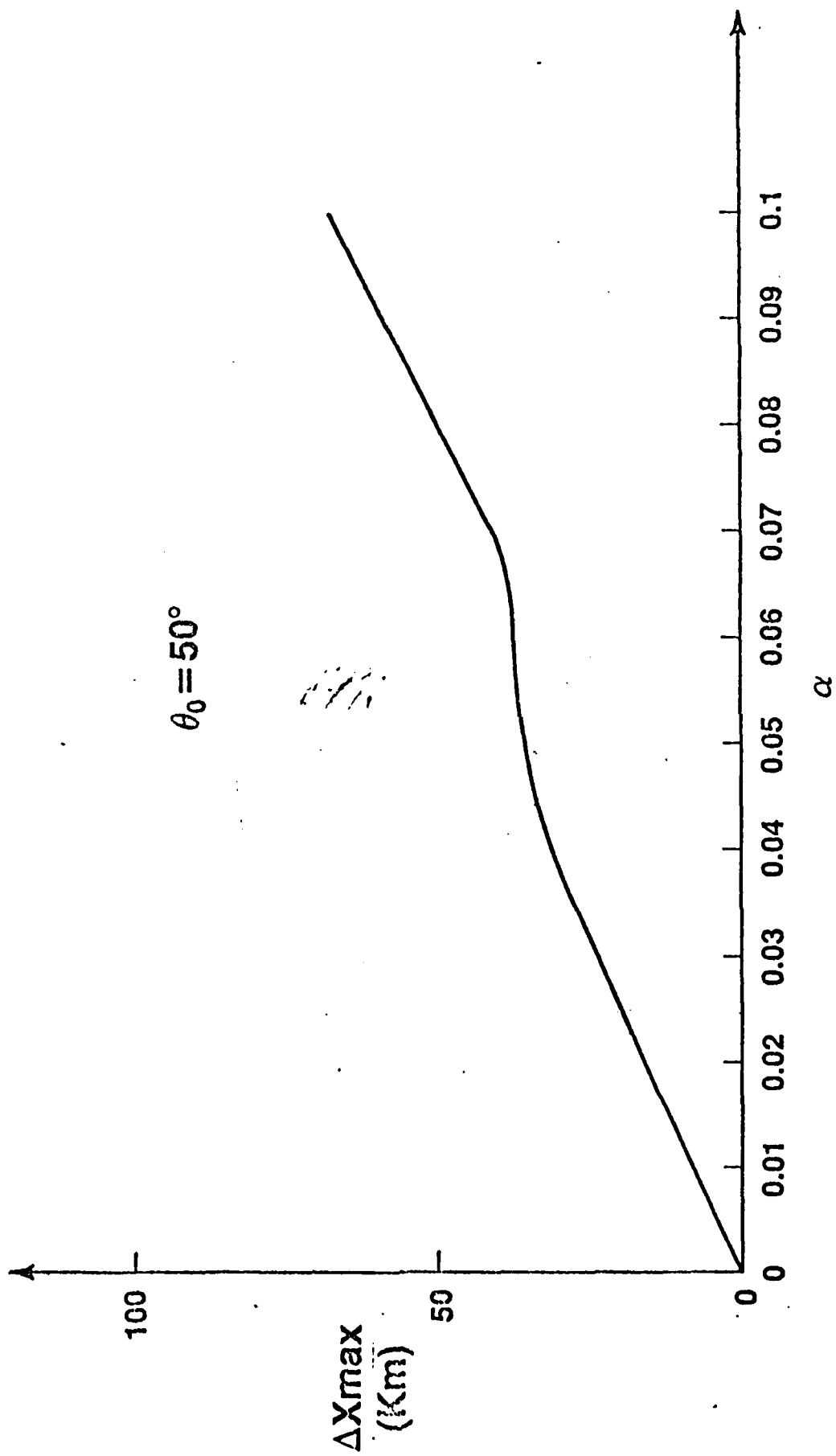
NL

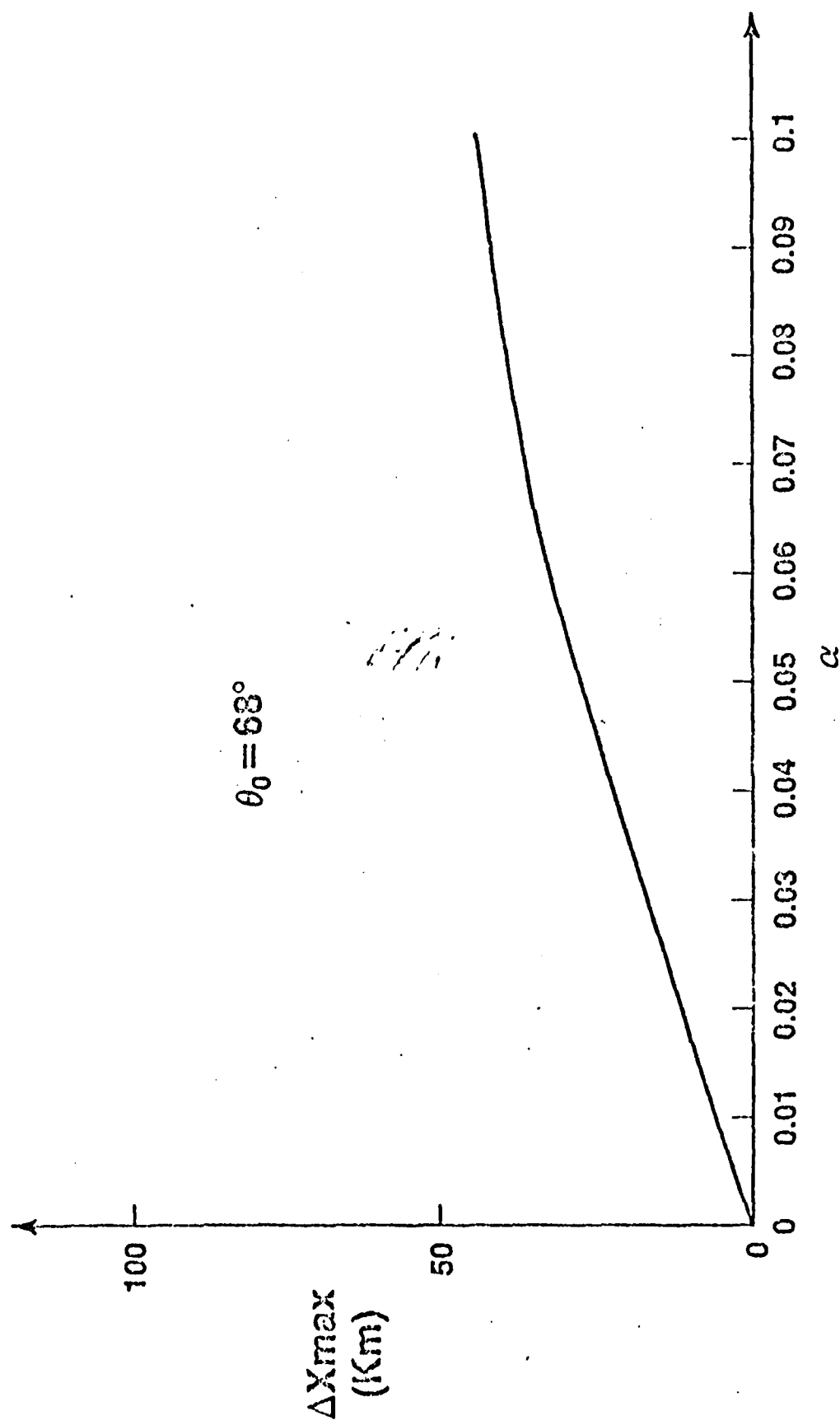


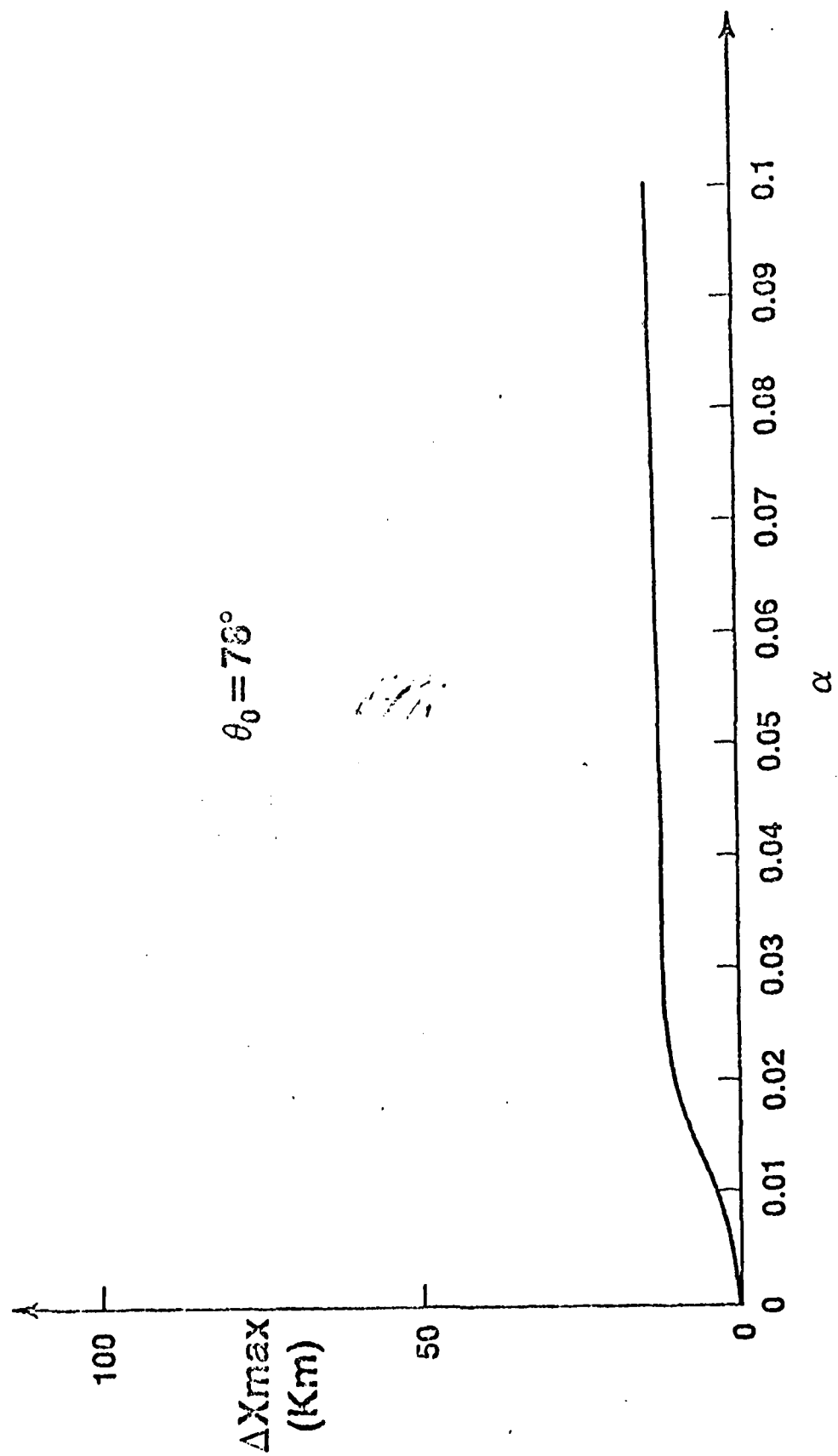


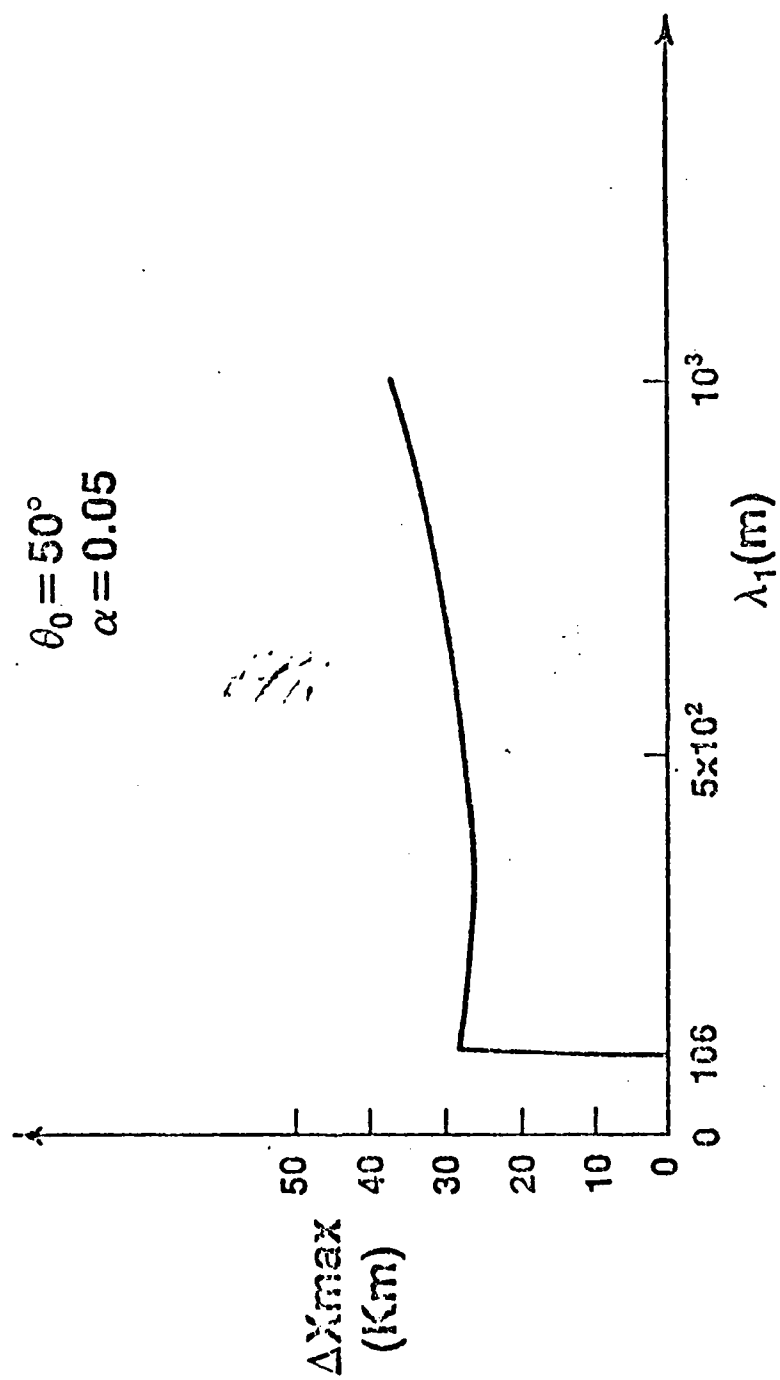
MICROCOPY RESOLUTION TEST CHART
NATIONAL BUREAU OF STANDARDS-1963-A











Simultaneous Excitation of Earth's Magnetic Field Fluctuations
and Plasma Density Irregularities by Powerful Radio Waves
From VLF to SHF Bands

M.C. Lee

Regis College Research Center, Weston, Mass. 02193

S.P. Kuo

Polytechnic Institute of New York, Long Island Center
Farmingdale, N.Y. 11735

Submitted to Radio Science

Abstract

Ionospheric disturbances evidenced as fluctuations in plasma density and geomagnetic field can be caused by powerful radio waves with a broad frequency band ranging from a few KHz to several GHz. The filamentation instability of radio waves can produce both large-scale plasma density fluctuations and large-scale geomagnetic field fluctuations simultaneously. The excitation of this instability is examined in the VLF wave injection experiments, the envisioned MF ionospheric heating experiments, the HF ionospheric heating experiments and the conceptualized Solar Power Satellite project. Significant geomagnetic field fluctuations can be excited in all of the cases investigated. Particle precipitation and airglow enhancement are expected to be the concomitant ionospheric effects associated with the wave-induced geomagnetic field fluctuations.

I. Introduction

Manifest ionospheric disturbances can be produced by powerful HF radio waves such as fluctuations in ionospheric density, plasma temperature, and the earth's magnetic field [see e.g., Gurevich, 1978; Fejer, 1979; Stubbe et al., 1982; Lee and Kuo, 1983 a]. In this paper, we discuss the excitation of ionospheric density irregularities and geomagnetic field fluctuations. The interesting finding in our theoretical analyses is that the geomagnetic field fluctuations may be excited simultaneously with large-scale field-aligned ionospheric irregularities by radio waves via the filamentation instability. The frequencies of radio waves may be as low as in the VLF band and as high as in the SHF band.

Unexpectedly large perturbations in the earth's magnetic field ($\sim 10.8\gamma$) were observed in the Tromsø HF ionospheric heating experiments [Stubbe and Kopka, 1981; Kuo and Lee, 1983]. Transmitters operated at frequencies close to but less than the local electron gyrofrequency are expected to cause both plasma density irregularities and geomagnetic field fluctuations in the ionosphere if MF signals are transmitted, or in the magnetosphere if VLF signals are injected, instead [Lee and Kuo, 1984 a]. Microwave transmissions at 2.45 GHz with the conceptualized power density (230 W/m^2) from the Solar Power Satellite (SPS) are also expected to perturb the earth's magnetic field significantly in the ionosphere along the beam [Lee and Kuo, 1984 b]. Our study, therefore, adds an additional effect to

those that should be assessed as the possible environmental impact of the SPS program.

The general formulation of the theory is first presented in Section I. In the subsequent four sections (i.e., Sections III-VI), we discuss the excitation of the filamentation instability in a uniform plasma in the VLF wave injection experiments, the envisioned MF ionospheric heating experiments, the Tromsø HF ionospheric heating experiments, and the conceptualized Solar Power Satellite program, respectively. The conclusions are finally drawn in Section VII with a brief discussion.

II. Theory

For simplicity, radio waves are assumed to be circularly polarized and propagate along the earth's magnetic field. This is a reasonable assumption for the VLF wave injection experiments and the Tromsø HF ionospheric heating experiments. As for the Solar Power Satellite case, the geomagnetic field imposes a relatively immaterial effect on the microwave propagation. If the positive z axis of a rectangular coordinate system represents the wave propagation direction and is taken to be parallel to the geomagnetic field, the monochromatic radio wave with frequency, ω_0 , and the wave vector \mathbf{k}_0 , can be represented by $\mathbf{E}_0(\mathbf{r}, t) = \epsilon_0 (\hat{x} \pm i\hat{y}) \exp[i(\mathbf{k}_0 \cdot \mathbf{r} - \omega_0 t)] = \text{C.C.}$ where the wave field amplitude, ϵ_0 , is assumed to be a constant; the \pm signs designate the right-hand and the left-hand circular polarizations, respectively.

Since the wave field interacts with the charged-particles, the plasmas experience a radiation pressure force (i.e., the nonlinear Lorentz force) and a thermal pressure force. The latter force results from the collisional dissipation of wave energy in plasmas. If the wave field is intense enough, a sideband mode (ϵ_1) can be excited together with zero-frequency modes via the filamentation instability, this is similar to the self-focusing instability of a radio wave beam. This high-frequency sideband is a quasi-mode, satisfying the Fourier transform wave equation

$$\begin{aligned} & [(k_0^2 + k^2 - \frac{\omega_0^2}{c^2}) \tilde{\epsilon}_1 - k_0^2 \hat{z}\hat{z} - k^2 \hat{x}\hat{x} + ik_0' \frac{\partial}{\partial x} (\hat{x}\hat{z} + \hat{z}\hat{x})] \cdot \tilde{\epsilon}_1 \\ & = i \frac{4\pi\omega_0}{c^2} (\tilde{J}_l + \tilde{J}_n) \end{aligned} \quad (1)$$

where $\tilde{\epsilon}_1 = (\tilde{\epsilon}_{11} \cos kx + \hat{z} \tilde{\epsilon}_{12} \sin kx) \exp(\gamma t)$ is the wave field perturbation with the growth rate, γ , and the filamentation wave vector, $\tilde{k} = \hat{x}k$; \tilde{J}_l and \tilde{J}_n represent the induced linear and nonlinear electric current densities. While \tilde{J}_l given by $-en_o \tilde{V}_1$ results from the linear response of electrons to the sideband field (ϵ_1), \tilde{J}_n includes two parts, $-en_o \tilde{V}_M$ and $-e\delta n \tilde{V}_o$, that are nonlinear beating currents caused by the nonlinear coupling between the purely growing mode (δn and δB) and the incident wave field (ϵ_o). The electron velocity perturbations denoted by \tilde{V}_o , \tilde{V}_1 , and \tilde{V}_M , have the following expressions:

$$\tilde{v}_j = -i \frac{e}{m} \frac{\omega_0}{(\omega_0^2 - \Omega_e^2)} \left[\tilde{\epsilon}_{j1} + \hat{z} \left(1 - \frac{\Omega_e^2}{\omega_0^2} \right) \cdot \tilde{\epsilon}_{jz} + i \frac{\Omega_e}{\omega_0} \hat{z} \times \tilde{\epsilon}_j \right]$$

where $j = 0, 1$ represent the response of electrons to the incident wave field ($\tilde{\epsilon}_0$) and the sideband field ($\tilde{\epsilon}_1$) respectively:

$$\tilde{v}_M = -\frac{e}{mc} \frac{\omega_0}{(\omega_0^2 - \Omega_e^2)} \left[\tilde{v}_0 \times \hat{z} + i \frac{\Omega_e}{\omega_0} \tilde{v}_0 \right] \delta B$$

is the electron velocity

perturbation induced by the $\tilde{v}_0 \times \delta B$ Lorentz force, where M , Ω_e , e , and c have their conventional meanings as the electron mass, the electron gyrofrequency, the electric charge, and the speed of light in vacuum, respectively. Because of the large inertia, the corresponding ion responses have been ignored.

The purely growing mode has the general form of $\delta P = \delta \tilde{P} (\cos kx) \cdot \exp(\gamma t)$, that is associated with the excitation of both the plasma density fluctuations (i.e., $\delta \tilde{P} = \delta \tilde{n}$) and the geomagnetic field fluctuations (i.e., $\delta \tilde{P} = \hat{z} \delta \tilde{B}$). It is the wave induced quasi-DC current that gives rise to the magnetostatic fluctuations. This can be seen in the Maxwell equation

$$\left(k^2 + \frac{1}{c^2} \frac{\partial^2}{\partial t^2} \right) \delta \tilde{A} = \frac{4\pi}{c} e n_0 (\delta \tilde{v}_i - \delta \tilde{v}_e)_y = \frac{4\pi}{c} \delta \tilde{J}_y \quad (2)$$

where $\delta \tilde{A}$ is the vector potential defined by $\nabla \times \delta \tilde{A} = \delta \tilde{B}$ and $\delta \tilde{J}_y = e n_0 (\delta \tilde{v}_i - \delta \tilde{v}_e)_y$ is the wave-induced quasi-DC current. The Coulomb gauge $\nabla \cdot \delta \tilde{A} = 0$ has been chosen in (2). From (2) and the continuity equations and the momentum equations for both electrons and ions,

we obtain

$$\delta J_y = \frac{en_o}{\Omega_i} \left\{ \frac{F_{ex}}{M} + \frac{\partial}{\partial x} \left(\frac{\delta T_e}{M} \right) - \left[\frac{\gamma(\gamma + v_{in})}{k} + kC_s^2 \right] \cdot \left(\frac{\delta n}{n_o} \right) \right\} \quad (3)$$

and a relation between δn and δB , viz.,

$$\frac{\delta n}{n_o} = \left[1 + \left(1 + \frac{v_e}{\gamma} \right) \left(\frac{k^2 c^2 + \gamma^2}{\omega_{pe}^2} \right) \right] \left(\frac{\delta B}{B_o} \right) \quad (4)$$

where M , Ω_i , ω_{pe} , C_s , v_e , and v_{in} , are respectively, the ion mass, the ion gyrofrequency, the electron plasma frequency, the ion acoustic velocity, the electron-ion collision frequency, and the ion-neutral collision frequency; δT_e is the electron temperature perturbation caused by the collisional dissipation of the radio pump and the excited sideband; and F_{ex} is the x component of the nonlinear Lorentz force

$$\begin{aligned} \tilde{F}_e = m \nabla (\tilde{V}_o^* \cdot \tilde{V}_1 + \tilde{V}_o \cdot \tilde{V}_1^*) + i \frac{\Omega_e}{\omega_o} m \{ -ik_o (\tilde{V}_o^* \tilde{V}_1 + \tilde{V}_o \tilde{V}_1^*) \times \hat{z} \\ + \tilde{V}_o^* \times [\nabla \times (\tilde{V}_1 \times \hat{z})] - \tilde{V}_o \times [\nabla \times (\tilde{V}_1^* \times \hat{z})] \}. \end{aligned}$$

It is seen from (3) that the wave-induced quasi-DC current is primarily caused by the $F \times B$ drift motion of the electrons under the influence of the thermal pressure force, $n_o (\partial/\partial x) \delta T_e$, and the nonlinear Lorentz force, $n_o F_{ex}$. The nonlinear Lorentz force term

can be neglected, because its contribution in generating field-aligned modes turns out to be much smaller than that of the thermal pressure force by a factor of $k^2 r_e^2$ for modes with scale lengths ($2\pi k^{-1}$) less than $\pi r_e (2M/m)^{1/2}$ (~ 15 m in the ionosphere) and by a factor of (m/M) ($\sim 3.4 \times 10^{-5}$) otherwise [Kuo et al., 1983; Lee and Kuo, 1983b]. The electron temperature perturbation (δT_e) obtained from the electron energy equation is found to be

$$\delta T_e = \frac{2}{3} \frac{Q_e + \gamma T_o \delta n}{n_o \bar{\gamma}} \quad (5)$$

where $Q_e = 2v_e r_o m (\vec{V}_o^* \cdot \vec{V}_1 + \vec{V}_o \cdot \vec{V}_1^*)$ is the wave energy dissipation rate in the electron gas due to the differential Ohmic loss of the incident wave and the excited sidebands, and $\bar{\gamma} = \gamma + 2v_e (m/M) + v_e k^2 \cdot v_t^2 / \Omega_e^2$, where v_t is the electron thermal velocity.

Equation (4) shows that the simultaneously excited δn and δB are proportional to each other. In all cases under study $v_e \gg \gamma$ and $k^2 c^2 \gg \gamma$. Therefore, Equation (4) can be reduced to

$$\frac{\delta n}{n_o} \simeq [1 + (\frac{v_e}{\gamma}) (\frac{k^2 c^2}{\omega_{pe}^2})] (\frac{\delta B}{B_o}) \quad (4')$$

indicating that if $(v_e/\gamma)(k^2 c^2/\omega_{pe}^2)$ is much less than unity, the magnetostatic fluctuations ($\delta B/B_o$) is comparable to the plasma density fluctuations ($\delta n/n_o$). It is thus expected that significant magnetic field fluctuations are associated with the excitation of large-scale (i.e., small k) modes.

The physical picture that illustrates the simultaneous excitation of earth's magnetic field fluctuations ($\delta\tilde{B}$) and plasma density irregularities ($\delta\tilde{N}$) is outlined in Figure 1. In the high-frequency wave fields (i.e., ϵ_0 and ϵ_1), electrons but not ions can be efficiently heated. If the electron temperature perturbations (δT_e) have a spatial variation across the earth's magnetic field ($\tilde{B}_0 = \hat{Z}B_0$) electrons experience a thermal pressure force, $\tilde{f}_T = -\hat{x}(\partial/\partial y)(N_0 \delta T_e)$, as indicated by the dotted arrow along the x axis. This force causes electron bunching, namely, electron density irregularities ($\delta\tilde{N}$). Charge separation thus formed gives rise to a self-consistent field ($\delta\tilde{E} = \hat{x} \delta E$) that is associated with the excitation of purely growing modes. In the presence of $\delta\tilde{E}$ and \tilde{f}_T , plasmas have the $\delta\tilde{E} \times \tilde{B}_0$ and $\tilde{f}_T \times \tilde{B}_0$ types of drift motion. While both electrons and ions move together in the $\delta\tilde{E} \times \tilde{B}_0$ drift, only electrons drift at the velocity of $-\tilde{f}_T \times \tilde{B}_0 / eB_0^2$ due to the thermal pressure force. The wave-induced quasi-DC electric current ($\delta\tilde{J} = \hat{y} \delta J$) or the vector potential ($\delta\tilde{A} = \hat{y} \delta A$), caused by the $\tilde{f}_T \times \tilde{B}_0$ drift, is responsible for the earth's magnetic field perturbations ($\delta\tilde{B} = \hat{Z} \delta B$) that orient along the background magnetic field ($\tilde{B}_0 = \hat{Z} B_0$) because of $\delta\tilde{B} = \nabla \times \delta\tilde{A}$.

The physical process of producing both $\delta\tilde{B}$ and $\delta\tilde{N}$ is reiterated with the aid of block diagrams in Figure 2 that displays a positive feedback loop for the filamentation instability of radio waves. There are two things to note: (1) since $\delta\tilde{N}$ and $\delta\tilde{J}$ (then $\delta\tilde{B}$) are

induced in proportion by f_T , one can expect that $\delta B \propto \delta N$ whose full expression given by (4) is indeed found in the formulation; (II) δn caused by the spatially varying δT_e reinforces the nonuniform electron heating that yields δT_e in turn.

The coupled mode equation for the purely growing mode that can be obtained from (2) and (3) with the aid of (5) has the expression of

$$\{(\gamma^2 + k^2 c^2)[1 + \frac{m}{M}(1 + \frac{v_e}{\gamma})f + \omega_{pe}^2 f]\delta B = \frac{8\pi e c k}{3m\Omega_e \gamma} \frac{\partial}{\partial x} Q_e \quad (6)$$

where $f = (\gamma \bar{v}_{in} + k^2 c^2 + 2 \gamma k^2 V_s^2 / 3\gamma)$; $\bar{v}_{in} = \gamma + v_{in}$; ω_{pi} and V_s are the ion plasma frequency and the ion thermal velocity. Substituting (4') into (6) and eliminating δn from (1) and (6) yields the dispersion relation

$$\begin{aligned} & k^2 c^2 (\gamma + \frac{m}{M} \bar{v}_e f) + \gamma \omega_{pi}^2 f \\ &= 2 \left(\frac{\omega_o}{\Omega_e} \right) \left(\frac{\omega_{pe}}{\omega_o \mp \Omega_e} \right)^4 \left(\frac{e \epsilon_o}{m c} \right)^2 \left[\left(\frac{\omega_o}{\Omega_e} \mp 1 \right) \bar{v}_e \frac{k^2 c^2}{\omega_{pe}^2} + \gamma \frac{\omega_o}{\Omega_e} \right] \left[\right. \\ & \left. \frac{4}{3} \left(\frac{v_e}{\gamma} \right) \frac{(4 - q_{\pm} - p_{\pm} q_{\pm})}{(1 + p_{\pm} - p_{\pm} q_{\pm})} \right] \quad (7) \end{aligned}$$

$$\text{where } \bar{v}_e = \gamma + v_e; p_{\pm} = \frac{\omega_o (\omega_o^2 - \omega_{pe}^2 \mp \omega_o \Omega_e)}{(\omega_o \mp \Omega_e) (\omega_o^2 - \omega_{pe}^2 - k^2 c^2)} \quad (8a)$$

$$\text{and } q_{\pm} = \pm \frac{k^2 c^2 (\omega_0^2 - \Omega_e^2)}{\omega_0 \Omega_e \omega_{pe}^2}; \quad (8b)$$

$p_+(p_-)$ and $q_+(q_-)$ correspond to the right - (left-) hand circularly polarized wave. The threshold field (ϵ_{th}) of the instability is determined from (7) by taking $\gamma = 0$, namely,

$$\left| \frac{e\epsilon_{th}}{mc} \right|^2 = 0.75 \frac{(\omega_0 \mp \Omega_e)^3}{\omega_0 \omega_{pe}^2} \frac{k^2 V_t^2 (2 \frac{m}{M} + \frac{k^2 V_t^2}{\Omega_e^2}) (1 + p_{\pm} - p_{\pm} q_{\pm})}{(4 - q_{\pm} - p_{\pm} q_{\pm})}. \quad (9)$$

It should be stressed that the filamentation instability has been so far formulated for a uniform plasma. The uniform-medium theory is considered to be adequate for the instability with scale lengths much less than the scale size of the plasma density gradient. The present form of our theory is applicable to all cases under consideration except the Solar Power Satellite Program (SPS). The theory is modified by including the parallel heat conduction loss that cannot be ignored in the SPS case wherein the microwave beam with a linear dimension of 10 Km in the ionosphere does not propagate along the earth's magnetic field. The characteristics of the filamentation instability are examined as follows for cases in different wave frequency regimes of the incident radio waves.

III. VLF WAVE INJECTION EXPERIMENTS

The VLF signals transmitted from the Siple Station were ob-

served to change from linear to circular polarization (i.e., whistler modes) on their paths through the neutral atmosphere and into the ionosphere [Kintner et al., 1983]. These whistler waves are assumed to satisfy the cold plasma dispersion relation

$$1 - \frac{\omega_{pe}^2}{\omega_o (\omega_o - |\Omega_e|)} = \frac{k^2 c^2}{\omega_o^2}$$

in the wave propagation regime: $|\Omega_e| \ll \omega_o < |\Omega_e|$. Since the positive z axis represents the wave propagation direction and has been taken to be parallel to the geomagnetic field, $\Omega_e > (<) 0$ for the right- (left-) hand circularly polarized wave and thus

$$p_+ = p = \omega_o (\omega_o^2 - \omega_{pe}^2 - \omega_o |\Omega_e|) / (\omega_o - |\Omega_e|) (\omega_o^2 - \omega_{pe}^2 - k^2 c^2)$$

$$\text{and } q_+ = q = k^2 c^2 (\omega_o^2 - \Omega_e^2) / \omega_o |\Omega_e| \omega_{pe}^2 \text{ for a whistler mode.}$$

In the upper atmosphere, the electron plasma frequency is much greater than the electron cyclotron frequency, viz., $\omega_{pe}^2 \gg \Omega_e^2 > \omega_o^2$. Therefore, $p \approx -\omega_o \omega_{pe}^2 / (|\Omega_e| - \omega_o) (\omega_{pe}^2 + k^2 c^2) < 0$ and $q = -k^2 c^2 (\Omega_e^2 - \omega_o^2) / \omega_o |\Omega_e| \omega_{pe}^2 < 0$. Since $p q$ has a value less than 2, the factor $(4 - q - p q)$ in (9) is positive.

$$1 - \frac{\omega_o \omega_{pe}}{(|\Omega_e| - \omega_o) (\omega_{pe}^2 + k^2 c^2)} - \frac{k^2 c^2 (|\Omega_e| + \omega_o)}{(\omega_{pe}^2 + k^2 c^2) |\Omega_e|} < 0. \quad (10)$$

For the excitation of large-scale modes (i.e., $\omega_{pe}^2 \gg k^2 c^2$), the above inequality leads to $\omega_0 > |\Omega_e|/2$. In other words, the filamentation instability of whistler waves that generate both plasma density fluctuations and geomagnetic field fluctuations can only excite within the narrow frequency range:

$$|\Omega_e| > \omega_0 > |\Omega_e|/2. \quad (11)$$

Since $|\Omega_e| \sim 1.4$ MHz in the ionosphere (e.g., the F region) and $|\Omega_e| \sim 13.65$ MHz in the magnetosphere at $L = 4.0$, the condition for the instability shown in (11) leads to the following conclusions. The frequencies of VLF signals that are injected in the active VLF wave experiments typically range from a few KHz to a few tens of KHz (< 30 KHz). These signals are not expected to cause ionospheric disturbances via the filamentation instability. But those with frequencies larger than 6.83 KHz but less than 13.65 KHz can excite the instability in the magnetosphere at $L = 4.0$. It is predicted from (11) that ionospheric disturbances caused by the filamentation instability of whistler waves are possible if the wave frequencies are less than $|\Omega_e| \sim 1.4$ MHz but greater than $|\Omega_e|/2 \sim 0.7$ MHz, namely, whistler waves in the MF band can cause large-scale ionospheric density irregularities and geomagnetic field fluctuations in the ionosphere. Quantitative analyses of these two cases are illustrated as follows.

The relevant magnetospheric parameters used in this work include $|\Omega_e|/2\pi = 13.65$ KHz (i.e., $B_0 \sim 500$ γ), $\omega_{pe}/2\pi = 179$ KHz, $T_0 = 0.4$

ev, and $M(H^+)/m = 1840$. If the VLF wave frequency is 10.9 KHz, i.e., $\omega_0/|\Omega_e| = 0.8$, the threshold field (ϵ_{th}) calculated from (9) are e.g., 12 μ V/m and 2 μ V/m for the excitation of modes with scale lengths of 10 Km and 100 Km, respectively. These threshold fields can be exceeded by the injected VLF waves from the Siple station even in the "non-ducted" whistler propagation mode. The growth rates of the instability expressed in terms of the threshold field is obtained from (7) as

$$\begin{aligned}
 & k^2 c^2 (\gamma + \frac{m}{M} v_e f) + \gamma \omega_{pe}^2 \\
 & = k^2 V_t^2 (2 \frac{m}{M} + k^2 \frac{V_t^2}{\Omega_e^2} \frac{2}{|\Omega_e|} \frac{\omega_{pe}^2}{(\omega_0 - |\Omega_e|)} \left| \frac{\epsilon_0}{\epsilon_{th}} \right|^2 \left[\frac{(\omega_0 - |\Omega_e|)}{|\Omega_e|} \right. \\
 & \left. \cdot \frac{v_e}{\omega_{pe}^2} \left(k^2 c^2 + \gamma \frac{\omega_0}{|\Omega_e|} \right) \frac{v_e}{\gamma} \right]
 \end{aligned}$$

This equation can easily be solved for γ under the following assumptions: $v_e \gg \gamma$, $k^2 c_s^2 \gg \gamma \bar{v}_{in}$, and $m/M \gg k^2 V_t^2 / \Omega_e^2$ that can be confirmed. For large scale-modes, $\omega_{pe}^2 \gg k^2 c^2$ (i.e., $\lambda \gg 1.7$ Km), the growth rate is found to have the following expression $\gamma \sim (2 v_e k V_s / |\Omega_e|) (\epsilon_0 / \epsilon_{th})$. This growth rate turns out to be independent of the scale lengths because as shown in (9): $\epsilon_{th} \propto k$. Although the threshold of the instability can be exceeded by the "non-ducted" whistler mode in the magnetosphere at $L = 4.0$, the growth rate is rather small ($\sim 10^{-5}$ Hz) if $\epsilon_0 / \epsilon_{th} \sim 0$ (1) because of the small electron-ion collision frequency (~ 0.1 Hz). However, the $\epsilon_0 / \epsilon_{th}$ of the "ducted" whistler mode may be increased by two to three orders of magnitude

though only 20% of the injected VLF waves are found to propagate in the "ducted" whistler mode [Carpenter and Miller, 1976]. The growth rate of ducted whistler waves can be as high as $(10^{-3} - 10^{-2})$ Hz, namely, the instability can be excited by the ducted mode within a few minutes.

For modes with scale lengths > 10 Km, $(\delta n/n_0) \approx (\delta B/B_0)$ from (4'). Presumably, a few percents of magnetospheric density fluctuations are able to be generated. Then, a few percents of geomagnetic field fluctuations in the magnetosphere at $L = 4.0$ is of the order of 10γ (c.f. the background magnetic field $\sim 500 \gamma$), that may significantly affect the orbits of charged particles. The scintillations of the Siple signals received at Roberval, Canada [Inan et al., 1977], may be attributable to the excitation of large-scale plasma density fluctuations in the magnetosphere by the injected VLF waves via the filamentation instability.

IV. ENVISIONED MF IONOSPHERIC HEATING EXPERIMENTS

The ionospheric heating facilities located at, for example, Arecibo (Puerto Rico), Boulder (Colorado), and Tromsø (Norway) are currently operated at lowest frequencies on the order of 3 MHz. The transmission of signals at frequencies close to the electron gyrofrequency (≈ 1.4 MHz) would require a major antenna and transmitter change. In our "envisioned" MF ionospheric heating experiments, we adopt the typical ionospheric parameters: $|\Omega_e|/2\pi = 1.4$ MHz (i.e., $B_0 = 5 \times 10^4 \gamma$), $\omega_{pe}/2\pi = 6$ MHz, and $M(0+)/m = 16 \times 1840$.

The threshold fields of the instability excited by the incident MF wave at 1.12 MHz (i.e., $\omega_0/|\Omega_e| = 0.8$) are found from (9) to be 6 mV/m and 0.4 mV/m for the excitation of modes with scale lengths of 100 m and 1 Km, respectively. If we assume that $\epsilon_0 = 0.3$ V/m, the growth rate of the instability for large-scale modes (i.e., $\omega_{pe}^2 \gg k^2 c^2$ or $\lambda \gg 50$ m) is about 1 Hz. Under the illumination of powerful MF radio waves, large-scale ionospheric disturbances can be produced in seconds.

It is obtained from (4') that $(\delta n/n_0) \approx 2.3 (\delta B/B_0)$ (e.g., $\lambda = 1$ Km) for modes with $\lambda \gg 50$ m. The excitation of a few percents of ionospheric density fluctuations are accompanied by the concomitant excitation of geomagnetic field fluctuations of the order of 500 γ , that is comparable to the perturbation in a severe magnetospheric (sub)storm.

V. HF IONOSPHERIC HEATING EXPERIMENTS

The HF radio waves transmitted in ionospheric heating (or modification) experiments have frequencies greater than the electron gyrofrequency ($\omega_0^2 \gg \Omega_e^2$) but less than FOF2 in the ionosphere. Ordinary (O) or extraordinary (X) modes have been employed. At the Tromsø facilities, these modes can be represented by two circularly polarized waves propagating along the geomagnetic field. Since the wave propagation direction is antiparallel to the geometric field, the X and O modes correspond to a left-hand and a right-hand circularly polarized wave, respectively, and satisfy the dispersion relations:

$$1 - \frac{\omega_{pe}^2}{\omega_0(\omega_0 \mp |\Omega_e|)} = \frac{k_0^2 c^2}{\omega_0^2} \quad (12)$$

where the \mp signs denote the left- and right-hand circularly polarized waves, respectively.

Near the reflection heights of these pump waves (i.e., $k_0 \rightarrow 0$), it is from (12) that $\omega_{pe}^2 \approx \omega_0(\omega_0 \mp |\Omega_e|)$. In this case, p_{\pm} given by (8a) approximately vanish and $q_{\pm} \approx \mp k^2 c^2 (\omega_0 \pm |\Omega_e|)/\omega_0^2 |\Omega_e|$ from (8b). Expression (9) then reduces to

$$|\frac{e^c}{mc} \text{th}|^2 = 0.75 \frac{(\omega_0 \mp |\Omega_e|)^2}{\omega_0^2 (4 - q_{\pm})} k v_t (2 \frac{m}{M} + \frac{k^2 v_t^2}{\Omega_e^2}) \quad (13)$$

where q_+ (q_-) is for the right- (left-) hand circularly polarized wave. While the factor, $(4 - q_+)$, is positive, a positive $(4 - q_-)$ requires that $q_- < 4$, viz.,

$$\lambda > (\pi c/\omega_0) [(\omega_0 + |\Omega_e|)/|\Omega_e|]^{\frac{1}{2}} \quad (14)$$

that can thus ensure the positive RHS of (13). If we take $|\Omega_e|/2\pi = 1.4$ MHz, $v_t = 1.3 \times 10^5$ m/sec, $M(0^+)/m = 16 \times 1840$, $\omega_0/2\pi = 4.04$ MHz, the scale lengths of the modes that are excited by the X mode cannot be less than 70 meters according to (14). By contrast no minimum scale length is found in the case of O mode heating.

The threshold fields of kilometer-scale instability excited by either X or O mode are a few mV/m calculated from (13) that are

quite small compared with the incident power densities (~ 1 V/m) of the Tromosø signals. Although the growth rate of the instability is generally a function of scale lengths, it has an asymptotic value found to be

$$\sim 2.5 \times 10^{-10} \frac{v_e \omega_0^2 |\epsilon_0|^2}{\Omega^2 (\omega_0 - |\Omega_e|)} \sim 3.4 \times 10^{-2} \text{ Hz for x - mode heating}$$

$$\sim 3.0 \times 10^{-2} \text{ Hz for O - mode heating}$$

when the scale lengths exceed a few hundreds of meters. It thus takes a few minutes for the instability to be excited in agreement with the observations that HF wave-induced geomagnetic field fluctuations needs a few minutes for development (Stubbe and Kopka, 1981). Substituting $v_e = 500$ Hz, $\gamma = 3.4 \times 10^{-2}$ Hz, $\lambda = 1$ Km, $\omega_{pe}/2\pi = 3.4$ MHz and $B_0 = 5 \times 10^4$ γ into (4'), we have $\delta B = 4.4 \times 10^2 (\delta n/n_0) = (4.4 - 44) \gamma$ for $(\delta n/n_0) = (1-10)\%$ also in agreement with the Stubbe and Kopka's experiments.

VI. CONCEPTUALIZED SOLAR POWER SATELLITE (SPS) PROJECT

The conversion of solar energy into microwaves on a geostationary satellite is the basic idea behind the conceptualized Solar Power Satellite (SPS) project [Glaser, 1977]. The microwave energy would be transmitted from the satellite toward the earth at a frequency of 2.45 GHz, that is much greater than the electron gyro-

frequency ($|\Omega_e|$). The cross section of the microwave beam has been estimated to have a linear dimension of 10 Km in the ionosphere, and the incident power density at the center of the beam would be as high as 230 W/m^2 (i.e., the wave field intensity is about 640 V/m).

The formulation outlined above for the excitation of both plasma density fluctuations and geomagnetic field fluctuations can be also applied to the case of SPS project after some modifications. First of all, the microwave beam does not propagate along the geomagnetic field, rather, with a propagation angle of, say, 45° with respect to the geomagnetic field. The inhomogeneity effect imposed by the microwave beam, i.e., the heat conduction along the geomagnetic field cannot be neglected in this case. Therefore, the parallel scale length ($\lambda_{||}$) has a given value of $L/\cos\theta = 10 \text{ Km}/\cos 45^\circ \sim 14 \text{ Km}$, where L and θ are the beam size and the beam wave propagation angle, respectively. The polarization of the microwave is assumed to be within a meridian plane (i.e., the assumption of an ordinary mode) for efficiently exciting the field-aligned modes. Hence, the geomagnetic field perturbations ($\delta\tilde{B}$) are still in the direction of the background earth's magnetic field.

With the inclusion of a non-zero parallel wave number ($k_{||} = 2\pi/\lambda_{||}$), (4') is modified as follows:

$$\frac{\delta n}{n_0} \simeq \left\{ 1 + \frac{v_e}{\gamma} \left(\frac{2\pi c}{\lambda_{\perp} \omega_{pe}} \right)^2 \left[1 + \frac{\Omega_e \Omega_i}{v_e v_{in}} \left(\frac{\lambda_{\perp}}{\lambda_{||}} \right)^2 \right] \right\} \left(-\frac{\delta B}{B_0} \right) \quad (15)$$

where λ_{\perp} and λ_{\parallel} are the perpendicular and the parallel scale lengths of the filamentation instability. Since the finite parallel wave number (k_{\parallel}) gives rise to a heat conduction loss along the earth's magnetic field, it introduces a new term in (9) for the threshold condition of the instability. The three terms in (9), $2m/M + k_{\perp}^2 V_t^2 / \Omega_e^2 + k_{\parallel}^2 V_t^2 / v_e^2$, correspond to the collisional damping of the heat source, the cross-field heat conduction loss, and the parallel heat conduction loss, respectively. The effect of ionospheric refringence on microwave propagation is relatively immaterial because the microwave frequency ($\omega_0 / 2\pi = 2.45$ GHz) is greater than the electron gyrofrequency ($\Omega_e / 2\pi \sim 1.4$ MHz) by three orders of magnitude. We then have $p_{\pm} \approx 1$ from (8a) and $q_{\pm} \rightarrow \infty$ from (8b). The threshold field given by (9) thus reduces to

$$|\frac{e \epsilon_{th}}{mc}| \approx 0.6 \frac{\omega_0}{\omega_{pe}} k_{\perp} V_t (2 \frac{m}{M} + \frac{k_{\perp}^2 V_t^2}{\Omega_e^2} + \frac{k_{\parallel}^2 V_t^2}{v_e^2})^{1/2}. \quad (16)$$

If the newly added factor in (15) is much greater than unity, viz., $(\Omega_e \Omega_i / v_e v_{in})(\lambda_{\perp} / \lambda_{\parallel})^2 \gg 1$, then the product of $(v_e / \gamma)(2\pi c / \lambda_{\perp} \omega_{pe})^2$ and $(\Omega_e \Omega_i / v_e v_{in})(\lambda_{\perp} / \lambda_{\parallel})^2$ can greatly exceed unity and consequently, the geomagnetic field fluctuations may become insignificant. This situation occurs in the ionospheric F region where $v_e v_i$ (~ 250) is rather small compared with $\Omega_e \Omega_i$ ($\sim 2.6 \times 10^9$). A detailed calculation shows that $\delta B / B_0 \sim 6.0 \times 10^{-7} (\delta n / n_0)$, namely, $\delta B \sim 3.0 \times 10^{-3}$ gammas for $\delta n / n_0 = 10\%$ (c.f. the background geomagnetic field,

$B_0 = 5 \times 10^4$ gammas) that is negligibly small. This result indicates that the large heat conduction loss along the geomagnetic field inhibits the filamentation instability from producing significant geomagnetic field perturbations in the F region.

However, the condition for the instability is quite different in the E region whose relevant parameters are taken to be $M(NO^+)/m = 30 \times 1840$, $V_t = 4.0 \times 10^4$ m/sec (i.e., $T_e \sim 200$ °K), $\omega_{pe}/2\pi \sim 3.0$ MHz, $\nu_{in} = 1.0 \times 10^3$ Hz and $\nu_{en} = 1.0 \times 10^4$ Hz. The factor, $(\Omega_e \Omega_i / \nu_e \nu_{in})(\lambda_\perp / \lambda_\parallel)^2$, is, for instance, 0.11 for $\lambda_\perp = 500$ m and 11.0 for $\lambda_\perp = 5$ Km. The parallel heat conduction loss $k_\parallel^2 V_t^2 / \nu_e^2 \sim 3.8 \times 10^{-8}$, is greater than the cross-field heat conduction loss, $k_\perp^2 V_t^2 / \Omega_e^2 \sim 3.3 \times 10^{-9}$ (for $\lambda_\perp = 500$ m) but very much less than the collisional damping of the heat source represented by $2m/M \sim 3.6 \times 10^{-5}$. These calculations show that the parallel heat conduction loss hardly affect the proposed instability with $\lambda_\perp / \lambda_\parallel \ll 1$ to operate in the ionospheric E region.

For the excitation of modes with $\lambda_\perp \gg (2M/m)^{1/2} \pi V_t / \Omega_e \sim 4.7$ m, the threshold field of the instability is mainly determined by the collisional damping of the heat source, namely, (16) can be approximated as $|e^{\epsilon} \text{th}/mc| \approx 0.6(\omega_0 / \omega_{pe}) k_\perp V_t (2m/M)^{1/2}$. For instance, the instability with $\lambda_\perp = 500$ m, 2 Km, and 5 Km requires $\epsilon_{th} = 2.5$, 0.63, and 0.25 V/m, respectively. They are significantly less than the incident microwave field intensity 640 V/m corresponding to the envisioned power density of 230 W/m^2 at the beam center. If we assume a uniform power density of 50 W/m^2 that is about one fifth of the

maximum beam intensity, the growth rates calculated from (7) are 0.43 sec^{-1} , 0.47 sec^{-1} , and 0.50 sec^{-1} and $(\delta B/B_0)/(\delta n/n_0)$ from (15) are 1.1×10^{-3} , 7.2×10^{-3} , and 1.1×10^{-2} for $\lambda_{\perp} = 500 \text{ m}$, 2 Km , and 5 Km , respectively.

We note that when the factor, $(\Omega_e \Omega_i / v_e v_{in})(\lambda_{\perp} / \lambda_{\parallel})^2$, is much greater than unity for kilometer-scale (say, $> 5 \text{ Km}$) modes, $(\delta B/B_0)/(\delta n/n_0)$ reaches a constant value of $(\gamma v_{in} / \Omega_e \Omega_i)(\lambda_{\parallel} \omega_{pe} / 2\pi c)^2 \sim 1.2 \times 10^{-2}$. That is, $\delta B/B_0$ is less than $\delta n/n_0$ by about two orders of magnitude in the case of microwave-ionosphere interaction. The earth's magnetic field can be significantly perturbed by modes with scale lengths less than the beam size by about one order of magnitude. For example, $\delta B = 5.3$ and 36.2 gammas for $\lambda_{\perp} = 500 \text{ m}$ and 2 Km , respectively, assuming that $\delta n/n_0 = 10\%$. They are comparable to the intensities (typically tens of gammas) of geomagnetic field fluctuations during magnetospheric substorms. Such large geomagnetic field fluctuations are expected to significantly perturb the orbits of charged particles and, consequently, to cause particle precipitation and airglow effects. These ionospheric effects introduced by the powerful microwave beams should be taken into account in the evaluation of environmental impacts of the conceptualized Solar Power Satellite program.

VIII. CONCLUSION AND DISCUSSION

Ionospheric and magnetospheric disturbances evidenced as

fluctuations in plasma density and geomagnetic field can be generated by powerful radio waves with frequencies as low as a few KHz and as high as several GHz. Depending on the incident power density of radio waves, ionospheric (or magnetospheric) plasma density irregularities and geomagnetic field fluctuations can be excited simultaneously by the filamentation instability of radio waves within a few seconds or minutes. This instability typically has kilometric scale lengths in the ionosphere and tens of kilometric scale lengths in the magnetosphere.

Radio waves with frequencies less than the electron gyrofrequency may propagate in a whistler mode. The excitation of the filamentation instability is only possible for those with frequencies greater than half the local electron gyrofrequency. This criterion for the instability leads to the conclusions that the injected VLF signals can produce magnetospheric rather than ionospheric disturbances. It is, however, predicted that ionospheric disturbances can be induced by MF signals whose frequencies are less than 1.4 MHz but larger than 0.7 MHz.

In the HF ionospheric heating experiments ($\omega_o^2 \gg \Omega_e^2$), both the ordinary and the extraordinary modes have been used. The scale lengths of the instability are found to have a cut-off in the case of extraordinary wave heating. The microwave beams that are transmitted from the conceptualized Solar Power Satellite to the surface of the earth are also expected to cause large ionospheric

disturbances in their ordinary mode propagation. The geomagnetic field fluctuations caused by the filamentation instability of radio waves are very significant in all the cases discussed in this paper. Their magnitudes may even become comparable to those seen in the magnetospheric (sub)storms. It is expected that such perturbations can affect the orbits of charged particles and cause particle precipitation and airglow effects.

The earth's magnetic field perturbations caused by powerful microwaves via the filamentation instability is a transient phenomenon. This fact can be seen from (4') that requires $\delta B/B_0 = 0$ when $\gamma = 0$ for the equilibrium condition either before the onset or after the saturation of the instability. During the linear stage of this instability (i.e., $\gamma = \text{a positive constant}$), $\delta B/B_0$ and $\delta n/n_0$ are related by (4') and significant geomagnetic field fluctuations can be produced. The duration of this transient phenomenon may be roughly defined as the period for achieving the seven e-folds of magnitude above the thermal fluctuation level, viz., $7\gamma^{-1}$. Then, it is either a few minutes or a few tens of minutes in all cases concerned.

It is interesting to note from (9) that the threshold field of the instability is inversely proportional to the electron plasma frequency. Therefore, ionospheric disturbances excited by radio waves should be most noticeable in the high plasma density environment. Finally, it should be pointed out that the non-linearity for the mode coupling is dominantly provided by the

thermal pressure force due to the collisional dissipation of both the pump wave field and the excited high-frequency sideband field in the electron gas. To emphasize this outstanding feature, the instability may be adequately termed the thermal filamentation instability of radio waves.

ACKNOWLEDGMENTS

This work was supported by AFGL contract F19628-83-K-0024 at Regis College Research Center and jointly in part by the NSF grant ATM-831-5322 and in part by the AFOSR grant AFOSR-83-0001 at Polytechnic Institute of New York.

REFERENCES

- Carpenter, D.L., and T.R. Miller, Ducted magnetospheric propagation of signals from the Siple, Antarctica, VLF transmitter, J. Geophys. Res., 81(16), 2692 - 2700, 1976.
- Fejer, J.A., Ionospheric modification and parametric instabilities, Rev. Geophys. Space Phys., 17(1), 135-153, 1979.
- Glaser, P.E., Solar power from satellites, Phys. Today, 30(2), 30-38, 1977.
- Gurevich, A.V., Nonlinear phenomena in the ionosphere (Physics and Chemistry in Space 10), Springer - Verlag, New York, 1978.
- Inan, U.S., T.F. Bell, D.L. Carpenter, and R.R. Anderson, Explorer 45 and Imp 6 Observations in the magnetosphere of injected

waves from the Siple Station VLF transmitter, J. Geophys. Res., 82(7), 1177-1187, 1977.

Kintner, P.M., R. Brittain, M.C. Kelley, D.L. Carpenter, and M.J. Rycroft, In situ measurements of trans-ionospheric VLF wave injection, J. Geophys. Res., 88(A9), 7065-7073, 1983.

Kuo, S.P., and M.C. Lee, Earth magnetic field fluctuations produced by filamentation instabilities of electromagnetic heater waves, Geophys. Res. Lett., 10(10), 979-981, 1983.

Kuo, S.P., B.R. Cheo, and M.C. Lee, The role of parametric decay instabilities in generating ionospheric irregularities, J. Geophys. Res., 88(A1), 417-423, 1983.

Lee, M.C., and S.P. Kuo, Ionospheric irregularities and geomagnetic field fluctuations due to ionospheric heating, Proceedings of International Symposium on Active Experiments in Space, Spec. Publ. 95, 81-89, European Space Agency, Neuilly, France, 1983a.

Lee, M.C., and S.P. Kuo, Excitation of upper hybrid waves by a thermal parametric instability, J. Plasma Phys., 30 (3), 463-478, 1983b.

Lee, M.C. and S.P. Kuo, Excitation of magnetostatic fluctuations by filamentation of whistlers, J. Geophys. Res., 89(A4), 2289-2294, 1984a.

Lee, M.C., and S.P. Kuo, Earth's magnetic field perturbations as the possible environmental impact of the conceptualized solar power satellite, accepted to be published in the Journal of Geophysical Research, 1984b.

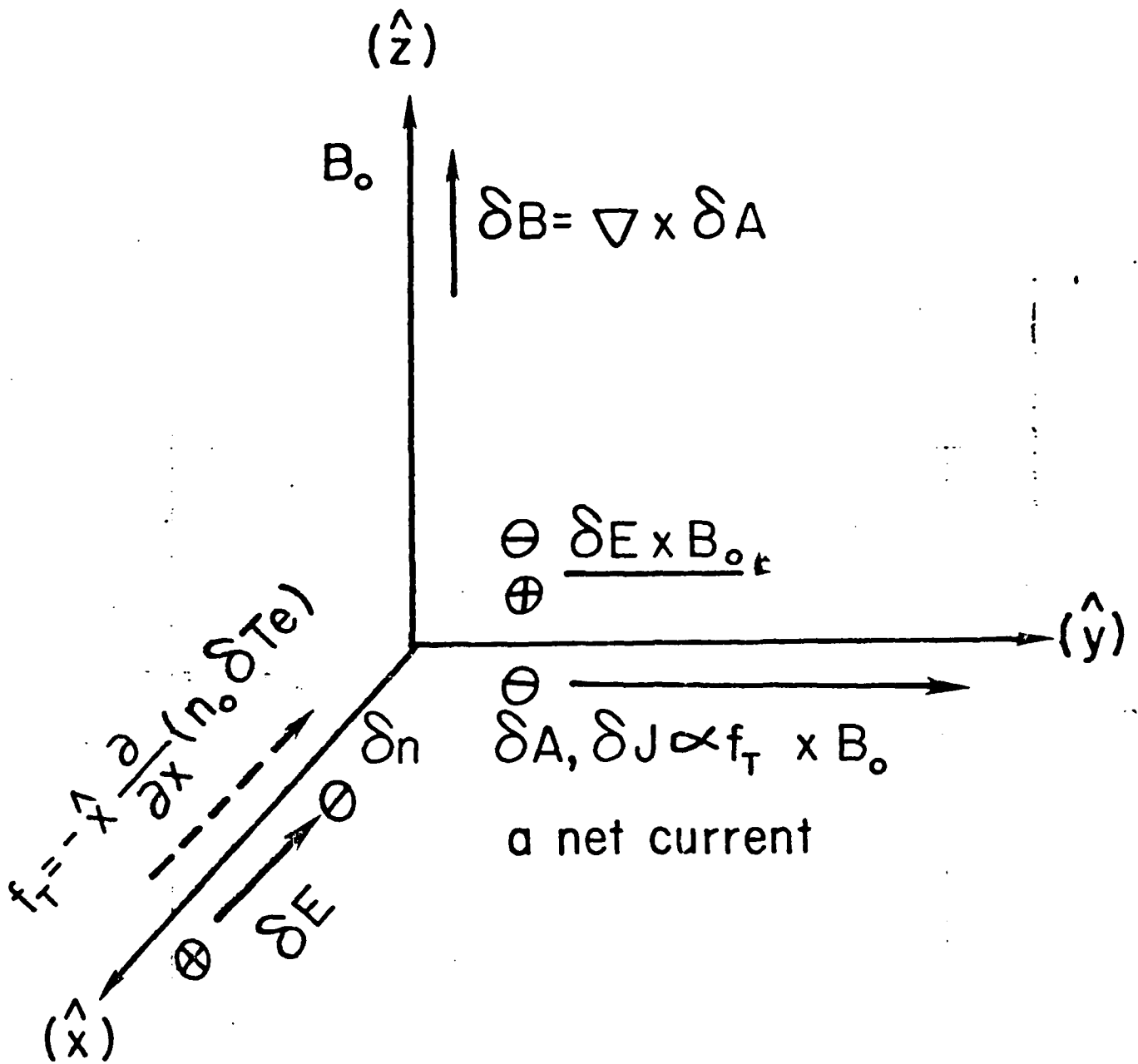
Stubbe, P., and H. Kopka, Modification of the polar electrojet by power HF waves, J. Geophys. Res., 82(16), 2319-2325, 1977.

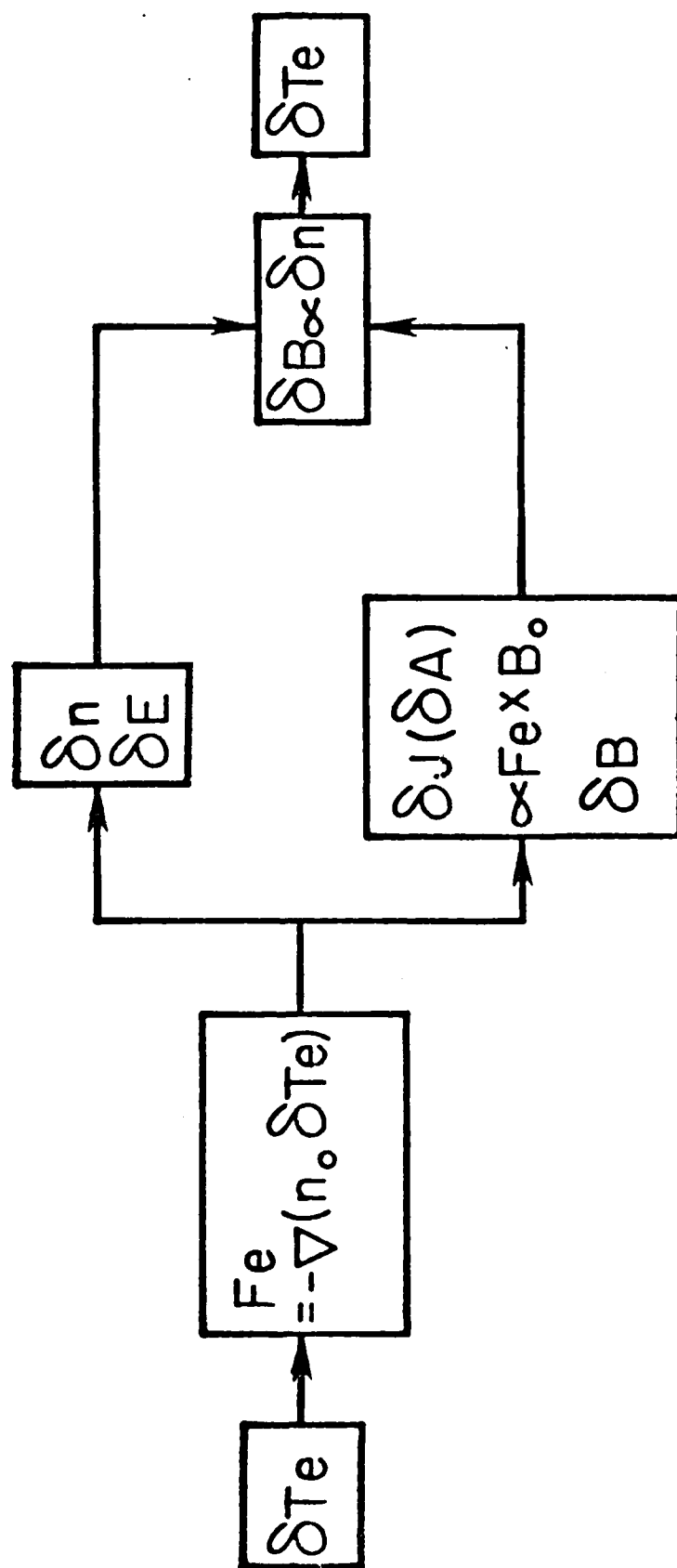
Stubbe, P., H. Kopka, M.T. Rietveld, and R.L. Dowden, ELF and VLF wave operation by modulated HF heating of the current carrying lower ionosphere, J. Atmos. Terr. Phys., 44(12), 1123-1135, 1982.

Figure Captions

Figure 1. The physical process leading to the simultaneous excitation of earth's magnetic field perturbations (δB) and plasma density irregularities (δn) by the filamentation instability of powerful radio waves.

Figure 2. A positive feedback loop for the filamentation instability.





END

FILMED

6-85

DTIC